



# University of HUDDERSFIELD

## University of Huddersfield Repository

Davison, Andrea Dianne

Synthesised Sulfonic Solid Acid Catalysts for Liquid Phase Reactions

### Original Citation

Davison, Andrea Dianne (2008) Synthesised Sulfonic Solid Acid Catalysts for Liquid Phase Reactions. Doctoral thesis, University of Huddersfield.

This version is available at <http://eprints.hud.ac.uk/id/eprint/5014/>

The University Repository is a digital collection of the research output of the University, available on Open Access. Copyright and Moral Rights for the items on this site are retained by the individual author and/or other copyright owners. Users may access full items free of charge; copies of full text items generally can be reproduced, displayed or performed and given to third parties in any format or medium for personal research or study, educational or not-for-profit purposes without prior permission or charge, provided:

- The authors, title and full bibliographic details is credited in any copy;
- A hyperlink and/or URL is included for the original metadata page; and
- The content is not changed in any way.

For more information, including our policy and submission procedure, please contact the Repository Team at: [E.mailbox@hud.ac.uk](mailto:E.mailbox@hud.ac.uk).

<http://eprints.hud.ac.uk/>

*Synthesised Sulfonic Solid  
Acid Catalysts for Liquid  
Phase Reactions*

*Andrea Dianne Davison  
B.Sc Hons*



*University of*  
**HUDDERSFIELD**

A thesis submitted to the University of Huddersfield  
In partial fulfilment of the requirements for  
The degree of Doctor of Philosophy

November 2008

## **Abstract**

The move to use heterogeneous solid acid catalysts as new, cleaner, renewable catalysts for liquid phase reactions is at the forefront of scientific research, with the focus on the ability to tailor and improve the physical and chemical properties of the catalysts in order to tailor their acidity to catalytic activity for specific liquid phase reactions.

The aim of this project was to determine the role of the support in imparting acidity and catalytic activity in liquid phase reactions to three different types of supported solid acid catalyst; polystyrene, silica and a fluorinated hydrocarbon polymer.

For the sulfonic acids supported on silica, two main synthesis routes (grafted and co-condensed) with the use of two alternative tethers (propyl, phenyl and also an additional non acidic tether) were compared.

Of the synthesised materials, structural properties were characterised and compared using several techniques. Nitrogen adsorption was used in order to ascertain the pore size and distribution, X-ray diffraction to determine the long range order, elemental analysis to determine the relative sulfur content and X-ray photoelectron spectroscopy to analyse the environment of the sulfur in order to establish successful acidification.

Surface acidities of all three supported sulfonic acids were better characterised and compared using ammonia adsorption calorimetry. The extent of the adsorption and molar enthalpies of ammonia adsorption ( $\Delta H_{\text{adsn}}$ ) were interpreted in terms of abundance, accessibility and strength of surface acid sites.

Catalytic activities were measured and compared using the isomerization of  $\alpha$ -pinene liquid phase reaction.

In brief, the main findings of this project indicate that the commercially available fluorinated polymer Nafion® resin demonstrated the highest acid strength and much higher specific catalytic activities compared to the other supported sulfonic acids. The acid strengths on polymeric and silica supports were similar, with poor catalytic activities. The routes used in order to synthesise, characterise and acidify the supported sulfonic acids were successful.

## Acknowledgements

*I would like to thank the University of Huddersfield for funding this research project.*

*I would like to thank Prof. Rob Brown for allowing me to take on this research project.*

*Further thanks to all the staff in the Centre for Applied Catalysis and technicians at the University for their invaluable help on the practical side of this research.*

*Last but by no means least, my heartfelt thanks and massive hugs goes to my friends and family who have stood by me, reassured me, picked me up and pushed me forward in times when I could not believe in myself. You have backed me up when I needed advice and kept me grounded. There have been tears, tantrums and laughter along the way, you have been there for all of it, and I thank you. There are too many of you to mention, and I mean no offence if your name is not written here in words, you are truly in my heart for your words and actions, you know who you are and how I could not have done this without you, I love you all.*

*But I must name a select few as without which this thesis would not exist.*

*Mum, Dad, Nicola and Aunt Di*

*Lee, Abbas and Rukhsana*

*Louise*

*Jenny*

*Jo (especially big thanks to you, words fail me when I think of everything you've done for me, tears do not, you're a star)*

*You have been there through it all with me, unwavering, my rocks, my lights in the dark when I could not find my way through, I cannot put into words how much you have helped me, I just hope I can make you proud.*

*Without you all (named and unnamed) I would not be the person I am today. Thank you.*

## List of Tables

<u>Table 2.1</u> : Microwave heating control vapour pressure parameters compared to the conventional heating synthesis route	...35
<u>Table 3.1</u> : Dependence of sulfonic acid loading of the propyl sulfonic acid functionalised silica gels on the pre-treatment of the silica support. The values are expressed as an average of triplicate data sources	...55
<u>Table 3.2</u> : Dependence of sulfonic acid loading ( $\text{mmol g}^{-1}$ acid sites) of propyl sulfonic acid silica gels. The values are expressed as averages of triplicate data sources	...56
<u>Table 3.3</u> : Sulfonic Acid Loading ( $\text{mmol g}^{-1}$ acid sites) of the silicas prepared by the Incipient wetness technique. The values are expressed as averages for triplicate data sources.	...57
<u>Table 3.4</u> : Sulfonic Acid Loading ( $\text{mmol g}^{-1}$ acid sites) of the propyl, phenyl and co-functionalised Sulfonated Silica Gels. The values are expressed as averages for triplicate data sources.	...58
<u>Table 3.5</u> : Physical properties of the Sulfonated Silica Gels.	...59
<u>Table 3.6</u> : Elemental analysis data of the Sulfonated Silica Gels.	...62
<u>Table 3.7</u> : Comparison of the data obtained of the Sulfonated Silica Gels derived from elemental analysis and XPS.	...63
<u>Table 3.8</u> : Physical properties of the selected co-condensed sulfonated mesoporous molecular sieve silicas.	...65
<u>Table 3.9</u> : Elemental analysis data of the Selected Sulfonated Mesoporous Molecular Sieve Silicas.	...67
<u>Table 3.10</u> : Comparison of the data obtained of the Selected Sulfonated Mesoporous Molecular Sieve Silicas derived from elemental analysis and XPS.	...67
<u>Table 3.11</u> : Overall comparison of the data obtained of the Selected Sulfonated Mesoporous Silicas and the Sulfonated Silicas derived from elemental analysis and XPS.	...68
<u>Table 4.1</u> : Commonly used Hammett Indicators.	...82
<u>Table 4.2</u> : Thermodynamics of a spontaneous system.	...90
<u>Table 4.3</u> : Method of correcting for the heat of base dilution as a blank run, for all the calorimetric systems investigated.	...93

<u>Table 4.4:</u> Method of correcting for the heat of interaction between solvent and catalyst as a blank run, for all the calorimetric systems investigated.	...93
<u>Table 4.5:</u> Experimental base adsorption calorimetry systems with varying solvents and titrants for use with the characterization of the solid acid catalysts in the liquid phase.	...100
<u>Table 4.6:</u> Average experimental enthalpy of neutralization HCl values compared to literature value before and after electrical calibration.	...103
<u>Table 4.7:</u> Chemical calibration of the calorimeter titrating 2ml 0.100M barium chloride into 2ml 0.01M 18 crown 6.	...104
<u>Table 4.8:</u> Experiments to detect heats of dilution during the planned titrations.	...104
<u>Table 4.9:</u> Experiments to detect heats due to interaction between solvent and solid acid catalysts.	...105
<u>Table 4.10:</u> $\Delta H^0_{\text{Neut}}$ value ( $\text{kJ mol}^{-1}$ ) from the 0.1M NaOH/H <sub>2</sub> O system for the Sulfonated Poly(styrene-co-divinylbenzene) Resins.	...107
<u>Table 4.11:</u> $\Delta H^0_{\text{Neut}}$ value ( $\text{kJ mol}^{-1}$ ) from the 0.1M NaOH/H <sub>2</sub> O system for the fluorinated sulfonated polymer resins.	...108
<u>Table 4.12:</u> $\Delta H^0_{\text{Neut}}$ value ( $\text{kJ mol}^{-1}$ ) from the 0.1M NaOH/H <sub>2</sub> O system for the Sulfonated Silica Gels.	...109
<u>Table 4.13:</u> $\Delta H^0_{\text{Neut}}$ value ( $\text{kJ mol}^{-1}$ ) from the 0.1M NaOH/H <sub>2</sub> O system for the Sulfonated Mesoporous Silicas.	...110
<u>Table 4.14:</u> $\Delta H^0_{\text{Neut}}$ value ( $\text{kJ mol}^{-1}$ ) from the 0.1M NaOH/MeOH system for the Sulfonated Poly(styrene-co-divinylbenzene) Resins.	...112
<u>Table 4.15:</u> $\Delta H^0_{\text{Neut}}$ value ( $\text{kJ mol}^{-1}$ ) from the 0.1M NBA/MeOH system for the Sulfonated Poly(styrene-co-divinylbenzene) Resins.	...113
<u>Table 4.16:</u> $\Delta H^0_{\text{Neut}}$ value ( $\text{kJ mol}^{-1}$ ) from the 0.05M NBA/CH system for the resins.	...115
<u>Table 4.17:</u> $\Delta H^0_{\text{Neut}}$ value ( $\text{kJ mol}^{-1}$ ) from the 0.05M NBA/CH system for the resins.	...116
<u>Table 4.18:</u> $\Delta H^0_{\text{Neut}}$ value ( $\text{kJ mol}^{-1}$ ) from the 0.05M NBA/CH system for the Sulfonated Silica Gels.	...116
<u>Table 4.19:</u> $\Delta H^0_{\text{Neut}}$ value ( $\text{kJ mol}^{-1}$ ) from the 0.05M NBA/CH system for the Sulfonated Mesoporous Silicas.	...117

Table 5.1: Catalytic activity in terms of percentage conversion of  $\alpha$ -pinene over a period of 4 hours, rate of conversion in  $\text{mol min}^{-1} \text{g}^{-1}$ , and reaction turn over number in  $\text{h}^{-1}$  of the sulfonated poly(styrene-co-divinylbenzene) resins and the fluorinated sulfonated polymer resins. ...136

Table 5.2: Catalytic activity in terms of percentage conversion of  $\alpha$ -Pinene over a period of 4 hours, and rate of conversion in  $\text{mol min}^{-1} \text{g}^{-1}$  and reaction turn over number in  $\text{h}^{-1}$  of the sulfonated silica gels and the sulfonated mesoporous materials. ...138

Appendix Tables: Complete results tables. ...150

## List of Figures

<u>Figure 1.1</u> : Schematic of the polymerization process during the formation of the polymeric resins.	...9
<u>Figure 1.2</u> : Schematic of sulfonation of the polymeric bead after treatment with concentrated sulphuric acid.	...9
<u>Figure 1.3</u> : Possible points of sulfonation of the polymeric resin beads.	...10
<u>Figure 1.4</u> : Structure of perfluorinated polymeric sulfonic acid Nafion®.	...11
<u>Figure 1.5</u> : Schematic of the crystalline cross linked silicon/oxygen chains that form the structure of the polysilicate gel (amorphous silica) generated by the two types of synthesis route.	...13
<u>Figure 1.6</u> : Schematic of 3-mercaptopropyltrimethoxysilane (MPTMS)	...14
<u>Figure 1.7</u> : Schematic of 2-(4-chlorosulfonylphenyl)trimethoxysilane (CSPTMS).	...14
<u>Figure 1.8</u> : Schematic of Phenyltriethoxysilane (PTES)	...14
<u>Figure 1.9</u> : Grafting and subsequent oxidation/acidification processes of the amorphous silica with MPTMS.	...14
<u>Figure 1.10</u> : Schematic of the possible functionalization of the hexagonal porous structure of the mesoporous sulfonated silica gel materials.	...16
<u>Figure 1.11</u> : Schematic of the formation of hexagonal mesoporous material MCM. With four distinctive steps a-d.	...17
<u>Figure 3.1</u> : IUPAC classification of adsorption isotherms.	...43
<u>Figure 3.2</u> : Schematic of X-ray electron diffraction on a crystal sample in XRD.	...50
<u>Figure 3.3</u> : Nitrogen adsorption/desorption isotherms for SiO <sub>2</sub> -propylSO <sub>3</sub> H.	...58
<u>Figure 3.4</u> : Nitrogen adsorption/desorption isotherms for phenyl-SiO <sub>2</sub> -propylSO <sub>3</sub> H.	...59
<u>Figure 3.5</u> : Nitrogen adsorption/desorption isotherms for SiO <sub>2</sub> -phenylSO <sub>3</sub> H.	...59
<u>Figure 3.6</u> : 3-Mercaptopropyltrimethoxysilane (MPTMS).	...60
<u>Figure 3.7</u> : Possible binding modes of MPTMS on silica.	...60
<u>Figure 3.8</u> : 2-(4-chlorosulfonylphenyl)ethyltrimethoxysilane (CSPTMS).	...61
<u>Figure 3.9</u> : Possible binding modes of CSPTMS on silica.	...62
<u>Figure 3.10</u> : X-ray diffraction pattern and Nitrogen adsorption/desorption isotherms for Pure MCM41.	...69
<u>Figure 3.11</u> : X-ray diffraction pattern and Nitrogen adsorption/desorption isotherms for MCM41-PhenylSO <sub>3</sub> H.	...71

<u>Figure 3.12</u> : X-ray diffraction pattern and Nitrogen adsorption/desorption isotherms for Pure SBA.	...72
<u>Figure 3.13</u> : X-Ray diffraction pattern and Nitrogen adsorption/desorption isotherms for SBA-PropylSO <sub>3</sub> H.	...73
<u>Figure 3.14</u> : X-Ray diffraction pattern for Microwave SBA-PropylSO <sub>3</sub> H (20 hours).	...74
<u>Figure 3.15</u> : X-Ray diffraction pattern and Nitrogen adsorption/desorption isotherms for SBA-PhenylSO <sub>3</sub> H.	...75
<u>Figure 4.1</u> : Thermochemical cycle for the adsorption of ammonia by a solid acid catalyst.	...84
<u>Figure 4.2</u> : Diagram of a Setaram Titrys Tain-Calvet Heat Flow Calorimeter.	...92
<u>Figure 4.3</u> : Sample heat output from the ITC.	...94
<u>Figure 4.4</u> : Typical plot of cumulative enthalpy versus amount of base added, for a titration of aqueous 0.1M NaOH solution against 0.1M HCl solution.	...95
<u>Figure 4.5</u> : Molar enthalpy of ammonia (irreversible) adsorption vs. surface coverage for the polystyrene sulfonic acid resins, Amberlyst 15, persulfonated CT275 (Amb 35) and the gel type C100H resin.	...120
<u>Figure 4.6</u> : Molar enthalpy of ammonia (irreversible) adsorption vs. surface coverage for the fluorinated sulfonated polymer resins, Nafion and the Nafion silica composite (SAC-13).	...122
<u>Figure 4.7</u> : Molar enthalpy of ammonia (irreversible) adsorption vs. surface coverage for the sulfonated silica gels, propyl and phenyl functionalised grafted silica materials.	...123
<u>Figure 4.8</u> : Molar enthalpy of ammonia (irreversible) adsorption vs. surface coverage for the selected sulfonated mesoporous silicas.	...124
<u>Figure 5.1</u> : Mechanism of formation of alpha pinene.	...131
<u>Figure 5.2</u> : Catalytic Activity activation setup.	...133
<u>Figure 5.3</u> : Catalytic Activity Reaction Setup.	...134
<u>Figure 5.4</u> : Catalytic activity data for the macroporous, stiochiometrically sulfonated Amberlyst 15, the persulfonated Amberlyst 35, the gel C100H poly(styrene-co-divinyl)benzene resins and the Fluorinated Nafion type resins.	...135
<u>Figure 5.5</u> : Catalytic activity data for the propyl and phenyl grafted silica gels, and the mesoporous sulfonated sulfonic acid materials.	...137

## **List of Abbreviations**

**MTBE:** Methyl-tert-butyl-ethyl

**AlCl<sub>3</sub>:** Aluminium chloride

**HF:** Hydrogen fluoride

**H<sub>2</sub>SO<sub>4</sub>:** Sulfuric acid

**HCl:** Hydrochloric acid

**Si:** Silica

**Al:** Aluminium

**MCM-41:** Mobil researchers, hexagonally ordered mesoporous oxide molecular sieve

**SBA-15:** Stucky et al, hexagonally ordered mesoporous material

**HMS:** Pinnavaia et al, hexagonally ordered mesoporous silicas

**DVB:** Divinylbenzene

**MPTMS:** 3-mercaptopropyltrimethoxysilane

**CSPTMS:** 2-(4-chlorosulfonylphenyl)trimethoxysilane

**PTES:** phenyltriethoxysilane

**TMAOH:** tetramethylammoniumhydroxide

**MTMS:** methyltrimethoxysilane

**TMOS:** tetramethoxysilane

**C<sub>16</sub>TAB:** hexadecyltrimethylammonium

**C<sub>12</sub>TAB:** dodecyltrimethylammonium

**TEOS:** tetraethoxysilane

**H<sub>2</sub>O<sub>2</sub>:** hydrogen peroxide

**MeOH:** methanol

**EtOH:** ethanol

**H<sub>2</sub>O:** water

**N<sub>2</sub>:** nitrogen

**NaCl:** sodium chloride

**NaOH:** sodium hydroxide

**H<sub>3</sub>O<sup>+</sup>:** hydronium ion

**CH:** cyclohexane

**NBA:** n-butylamine

**NH<sub>3</sub>:** ammonia

**SH:** silane

**C:** carbon

**S:** sulfur

**SO<sub>2</sub>Cl:** sulfonyl chloride

**XPS:** x-ray photoelectronspectroscopy

**EA:** elemental analysis

**SiO<sub>2</sub>-propylSO<sub>3</sub>H:** propyl sulfonic acid and phenyl functionalised silica gel

**SiO<sub>2</sub>-phenylSO<sub>3</sub>H:** phenyl sulfonic acid and phenyl functionalised silica gel

**Phenyl- SiO<sub>2</sub>-propylSO<sub>3</sub>H:** propyl sulfonic acid and phenyl functionalised silica gel

**Phenyl- SiO<sub>2</sub>-phenylSO<sub>3</sub>H:** phenyl sulfonic acid and phenyl functionalised silica gel

**MCM41-propylSO<sub>3</sub>H:** MCM-41 propyl sulfonic acid

**MCM41-phenylSO<sub>3</sub>H:** MCM-41 phenyl sulfonic acid

**Phenyl- MCM41-propylSO<sub>3</sub>H:** propyl sulfonic acid and phenyl functionalised MCM-41

**Phenyl- MCM41-phenylSO<sub>3</sub>H:** phenyl sulfonic acid and phenyl functionalised MCM-41

**SBA15-propylSO<sub>3</sub>H:** SBA-15 propyl sulfonic acid.

**SBA15-phenylSO<sub>3</sub>H:** SBA-15 phenyl sulfonic acid.

**Phenyl- SBA15-propylSO<sub>3</sub>H:** propyl sulfonic acid and phenyl functionalised SBA-15

**Phenyl- SBA15-phenylSO<sub>3</sub>H:** phenyl sulfonic acid and phenyl functionalised SBA-15

**HMS-propylSO<sub>3</sub>H:** HMS propyl sulfonic acid

**Contents**

<b>Abstract</b>	<b>...I</b>
<b>Acknowledgements</b>	<b>...II</b>
<b>List of Tables</b>	<b>...III-V</b>
<b>List of Figures</b>	<b>...VI-VII</b>
<b>List of Abbreviations</b>	<b>...VIII-IX</b>
<b>Contents</b>	<b>...X-XVI</b>
<b>Chapter 1: Introduction and Background</b>	<b>...1</b>
1.1 General Overview	...1
1.2 Overall Aim	...1
1.3 General Introduction	...1
1.4 Solid Acid Catalysts	...2
1.5 Specific Objectives	...7
1.6 Catalysts Studied	...7
1.6.1 Polymer Supported Sulfonic Acid Resins	...8
Sulfonated poly(styrene-co-divinylbenzene) ion exchange resins	...8
Sulfonated Fluorinated Polymer Resins	...11
1.6.2 Sulfonated Silica Gels (grafting route)	...12
1.6.3 Sulfonated Mesoporous Molecular Sieve Silicas (co-condensation route)	...15
MCM-41	...16
SBA-15	...17
HMS	...18
1.7 Summary	...18
References	...20
<b>Chapter 2: Catalyst Syntheses</b>	<b>...27</b>
2.1 General Overview	...27
2.2 Catalyst types, preparation and synthesis	...27
2.2.1 Polymer Supported Sulfonic Acid Resins	...28
2.2.1.1 Sulfonated poly(styrene-co-divinylbenzene) ion exchange resins	...28
2.2.1.2 Fluorinated Sulfonated Polymer Resins	...28

2.2.2 Sulfonated Silica Gels and Sulfonated Mesoporous Molecular Sieve Silicas	...28
2.2.2.1 Sulfonated Silica Gels (grafting route)	...29
2.2.2.1.a Propyl sulfonic acid functionalised silica gel	...30
2.2.2.1.b Oxidation	...30
2.2.2.1.c Acidification	...30
2.2.2.1.d Propyl sulfonic acid and phenyl functionalised silica gel	...30
2.2.2.1.e Phenyl sulfonic acid functionalised silica gel	...31
2.2.2.1.f Phenyl sulfonic acid and phenyl functionalised silica gel	...31
2.2.2.2 Sulfonated Silica Gels (grafting route) Incipient wetness technique	...31
2.2.2.2.a Propyl sulfonic acid functionalised silica gel (IW)	...31
2.2.2.2.b Propyl sulfonic acid and phenyl functionalised silica gel	...32
2.2.2.2.c Phenyl sulfonic acid functionalised silica gel	...32
2.2.2.2.d Phenyl sulfonic acid and phenyl functionalised silica gel	...32
2.2.2.3 Sulfonated Mesoporous Molecular Sieve Silicas (co-condensation route)	...32
MCM-41	...32
2.2.2.3.a Pure MCM-41	...33
2.2.2.3.b MCM-41 propyl sulfonic acid	...33
2.2.2.3.c MCM-41 propyl and phenyl functionalised sulfonic acid	...34
2.2.2.3.d MCM-41 phenyl sulfonic acid	...34
2.2.2.3.e MCM-41 phenyl and phenyl functionalised sulfonic acid	...34
2.2.2.4 Microwave heating synthesis route	...34
SBA-15	...36
2.2.2.5.a Pure SBA-15	...36
2.2.2.5.b SBA-15 propyl sulfonic acid	...36
2.2.2.5.c SBA-15 propyl and phenyl functionalised sulfonic acid	...37
2.2.2.5.d SBA-15 phenyl sulfonic acid	...37
2.2.2.5.e SBA-15 phenyl and phenyl functionalised sulfonic acid	...37
2.2.2.6 Co-condensed HMS propyl sulfonic acid	...37
2.3 Summary	...38
References	...39
<b>Chapter 3: Catalyst Structural Characterization</b>	<b>...42</b>
3.1 General Overview	...42

3.2 Catalyst Physical Characterization: Techniques and Background	...42
3.2.1 Nitrogen Adsorption	...42
Physisorption	...43
Chemisorption	...43
Adsorption isotherms	...43
Langmuir theory of adsorption	...44
BET theory of adsorption	...47
Pore size distribution and pore volume from nitrogen adsorption	...48
3.2.2 Powder X-Ray Diffraction	...49
3.2.3 Elemental Analysis	...51
3.2.4 X-Ray Photoelectron Spectroscopy (XPS)	...51
3.3 Catalyst Physical Characterization: Experimental	...52
3.3.1 Powder X-Ray Diffraction Measurements	...52
3.3.2 Porosity Measurements	...52
3.3.3 Elemental analysis characterization	...52
3.3.4 Concentration of acid groups by conventional titration	...52
3.4 Catalyst Physical Characterization: Results and Discussion	...53
3.4.1 Polymer Supported Sulfonic Acid Resins	...53
Sulfonated poly(styrene-co-divinylbenzene) ion exchange resins	...53
Fluorinated Sulfonated Polymer Resins	...53
3.4.2 Sulfonated Silica Gels. Grafting Route	...54
Pre-treated silica	...54
Propyl sulfonic acid functionalised silica gel, optimization of oxidation/acidification conditions	...55
Functionalised silica gel – Incipient Wetness Route	...56
Functionalised silica gel – Grafting Route	...57
3.4.3 Sulfonated Mesoporous Molecular Sieve Silicas (Co-condensed route)	...64
3.5 Summary	...74
References	...77
<b>Chapter 4: Acidity Measurements</b>	<b>...79</b>
4.1 General Overview	...79
4.2 Introduction and Background to Surface Acidity	...79

4.2.1 Surface Acidity	...79
Bronsted Acidity	...79
Lewis Acidity	...80
4.3 Methods of Characterization of Surface Acidity	...81
4.3.1 Titration Methods	...81
4.3.2 Thermal Characterization Methods	...82
Calorimetric Titration	...82
Temperature Programmed Desorption	...84
4.3.3 Vibration Spectroscopic Methods	...85
Infra-red and Raman Spectroscopy	...85
4.3.4 Nuclear Magnetic Resonance (NMR) Methods	...86
H <sup>1</sup> and <sup>13</sup> C NMR	...86
4.3.5 Conclusion	...86
4.4 Base Adsorption Calorimetry	...87
4.4.1 Surface Acidity	...87
4.4.2 Thermodynamics of Calorimetry	...88
4.4.3 Types of Calorimeter	...90
Heat Accumulation Calorimeter	...91
Heat Conduction Calorimeter	...91
4.4.5 Base Adsorption Calorimetry in the Liquid Phase	...92
Calibration of the Seteram Titrys Microcalorimeter	...92
Corrections for heats of addition/dilution	...93
Treatment of data	...94
4.4.6 Base Adsorption Calorimetry in the Gas Phase	...98
4.5 Base Adsorption Calorimetry: Experimental	...99
4.5.1 In the Liquid Phase: Base Adsorption Microcalorimetry	...99
4.5.2 In the Gas Phase: Flow Adsorption Calorimetry	...101
4.6 Base Adsorption Calorimetry: Results and discussion	...102
4.6.1 General Overview	...102
4.6.2 In the liquid phase; Isothermal Titration Microcalorimetry (Base adsorption calorimetry)	...103
4.6.2.1 Calibration of the seteram Titrys microcalorimeter	...103
4.6.2.2 Corrections for heats of addition/dilution	...104

4.6.3 In the liquid phase; Isothermal Titration Microcalorimetry (Base Adsorption Calorimetry) Solvent systems	...106
4.6.3.1 Water Solvent System	...106
0.1 M NaOH/H <sub>2</sub> O system	...106
Sulfonated polymer supported sulfonic resins	...107
Sulfonated poly(styrene-co-divinylbenzene) resins	...107
Fluorinated sulfonated polymer resins	...108
Sulfonated silica gels. Grafting route	...109
Sulfonated mesoporous molecular sieve silicas. Co-condensation route	...110
4.6.3.2 Methanol solvent system	...111
0.1 M NaOH/MeOH system	...111
Sulfonated poly(styrene-co-divinylbenzene) resins	...111
0.1 M n-butylamine/MeOH system	...113
Sulfonated poly(styrene-co-divinylbenzene) resins	...113
4.6.3.3 Cyclohexane solvent system	...114
0.05 M n-butylamine/cyclohexane system	...114
Sulfonated polymer supported sulfonic acid resins	...114
Sulfonated poly(styrene-co-divinylbenzene) resins	...115
Fluorinated sulfonated polymer resins	...115
Sulfonated silica gels. Grafting route	...116
Sulfonated mesoporous molecular sieve silica gels	...117
4.6.3.4 Summary	...117
4.6.4 In the gas phase; Flow Adsorption Calorimetry	...119
4.6.4.1 Sulfonated polymer supported sulfonic acid resins	...120
Sulfonated poly(styrene-co-divinylbenzene) resins	...120
Fluorinated sulfonated polymer resins	...122
4.6.4.2 Sulfonated silica gels. Grafting route	...123
4.6.4.3 Sulfonated mesoporous molecular sieve silica gels	...124
4.6.4.4 Summary	...125
References	...127
<b>Chapter 5 Catalytic Activity</b>	<b>...130</b>
5.1 General Overview	...130

5.2 Catalytic Activity Characterization: Introduction and Background	...130
5.2.1 Gas Chromatography	...131
5.3 Experimental	...132
Thermal Activation	...132
Reaction Vessel	...133
5.4 Summary	...134
5.5 Catalytic Activity Results and Discussion	...135
5.5.1 Sulfonated polymer supported sulfonic acid resins	...135
Sulfonated poly(styrene-co-divinylbenzene) resins and Fluorinated sulfonated polymer resins	...135
5.5.2 Sulfonated silica gels. Grafting route and Sulfonated mesoporous molecular sieve silica gels	...137
5.6 Summary	...138
References	...140
<b>Chapter 6: Conclusions and Future Work</b>	<b>...141</b>
6.1 General Overview	...141
6.2 Overall aim and specific objectives	...141
6.3 Structural analysis conclusions	...142
Sulfonated polymer supported sulfonic acid resins	...142
Sulfonated Silica Gels	...142
Sulfonated Mesoporous Molecular Sieve Silicas	...143
6.4 Base Adsorption Calorimetry Conclusions	...143
6.4.1 In the liquid phase: solvent systems	...143
0.1 M Sodium hydroxide /Methanol solvent system	...144
0.1 M N-butylamine/Methanol solvent system	...144
0.1 M Sodium hydroxide/Water solvent system	...144
0.05 M N-butylamine/Cyclohexane solvent system	...144
6.4.2 In the gas phase	...144
6.5 Catalytic Activity Conclusions	...145
6.6 Overall Conclusions	...145
6.7 Future Work	...147
6.7.1 Improvements of equipment	...147

6.7.2 Materials	...147
6.7.3 Further Experimentation	...148
<b>Appendix</b>	<b>...149</b>

# *Chapter One*

## *Introduction and Background*

## Chapter 1 Introduction and Background

### 1.1 General Overview

This chapter aims to give an overall view of the project, and to introduce the concepts and theories behind the fundamental aspects of the research that have been conducted.

### 1.2 Overall Aim

The Overall Aim of this project was to determine the role of the support in imparting acidity and catalytic activity in liquid phase reactions to three different types of supported solid acid catalyst.

### 1.3 General Introduction

Solid acid catalysts for use in gas phase reactions have been very successful, leading to the widespread use of zeolites, acid treated clays and other materials for industrial reactions such as methyl tert-butyl ethyl (MTBE) synthesis. In comparison the use of heterogenous solid acid catalysts for liquid phase reactions is less common, but crucial in industry today. Acid catalysed reactions for use in speciality liquid phase processes such as fine chemical synthesis and pharmaceutical manufacture are some of the most important in industry today. Typically homogenous catalysts such as  $\text{AlCl}_3$ , HF and  $\text{H}_2\text{SO}_4$  are mainly used. However the production of large volumes of toxic waste during the catalyst separation step is proving to be both highly environmentally unsound and cost inefficient. There is a drive towards greener chemistry due to public, legislative and corporate pressure which tackle the serious environmental, and health and safety implications involved in the use of such processes. The move to use heterogeneous solid acid catalysts as new, cleaner, renewable catalysts for liquid phase reactions is at the forefront of research, with the focus on the ability to tailor and improve the physical and chemical properties of the catalysts in order to tailor their acidity to catalytic activity for specific liquid phase reactions.<sup>[1-10]</sup>

## 1.4 Solid Acid Catalysts

In general terms, a solid acid catalyst is a solid porous support (either rigid or non-rigid) upon which active acid groups are grafted or otherwise incorporated. [Surface acidity and Bronsted acidity in particular is discussed later in Chapter Four].

The material's use as a solid acid catalyst is governed by the number, type and strength of acid sites present. The porosity of the solid limits the reaction systems the catalyst is suitable for, since the reactant molecules must first diffuse into the framework of the solid acid catalyst, enabling their attachment and subsequent reaction at the active sites. Therefore the size of the pore channels in the solid are crucial when considering its purpose. The selective action of the solid with regards to the reactive molecules shape and size is known as "shape selectivity", thus only molecules of suitable size to the solids pores can diffuse into and out of the solid, thereby the solid acts as a "molecular sieve", a term used to commonly describe these materials <sup>[1-10]</sup>.

According to the IUPAC classification, porous materials are grouped into three classes based on their pore diameter ( $d$ ), firstly microporous materials with  $d < 2$  nm, mesoporous materials with  $d = 2 - 50$  nm, and finally macroporous materials with  $d > 50$  nm. The most common group of ordered microporous molecular sieves are the zeolites, which have been found to be a particularly good catalyst in gas phase reactions and are widely used in the petrochemical industry <sup>[2/7]</sup>. Zeolites are oxides of silicon and aluminium which are typically structured around an organic template molecule in the form of a gel which later crystallises. The template is then removed via calcination leaving an ordered porous material. They are ideal for use with relatively small molecules because their design and structure can be tailored to match the dimensions of the molecules that must diffuse into the solid's and react. They are thermally stable, possess a high surface area, and possess a crystalline well defined ordered porous structure enabling favourable adsorption properties and the inclusion of active acid sites. Their "shape selectivity" allows the catalysts to be tailored to specific reaction requirements <sup>[2/7]</sup>. The total number of acid sites is controlled by the total number of Al ions in the framework. The acid strength of these sites is somewhat dependant on the Si:Al ratio of the zeolite.

However for use in liquid phase reactions, a microporous solid acid catalyst is undesirable as the molecules involved are often too large to diffuse through at an appreciable rate to the active acid sites. Therefore larger pore mesoporous materials would be the most logical choice.

A commonly used, commercially available solid acid catalyst for liquid phase reactions is the well established polystyrene supported sulfonic acids (cationic ion exchange resins). These non rigid resin catalysts are sometimes used as simple gel materials in which diffusion of the active site is through the solvated polymer gel. They are also prepared with permanent macroporosity for use in solvents that do not swell the polymer gel so effectively. They have been successfully utilised in various catalytic applications<sup>[13-20]</sup> and offer numerous advantages over other solid acid catalysts (high concentration of acid sites, uniform bead size, and very uniform structures), including the ability to allow reactions to be conducted in aqueous, non aqueous, polar and non-polar media. However despite these numerous advantages they are regarded as exhibiting relatively weak acid sites compared to those found on zeolitic and other solid acid catalysts and have been shown to be thermally unstable at temperatures exceeding 150°C<sup>[11/17]</sup>. Water has been found to have a levelling effect on the strength of the acid groups (the hydronium ion is thought to be stronger than the supported acid groups and thus level the strength of the acid to that of its own strength)<sup>[17]</sup> thus it is thought that controlling the amount of water within the resin could control the resultant strength of acidity, but low thermal stability limits the extent to which they can be dehydrated. Therefore producing acid catalysts on inorganic supports is expected to allow the water content to be reduced further<sup>[11/17]</sup>.

It is important to note at this point that interesting and novel work with the fluorinated polymer supported sulfonic acid Nafion® resin has observed this resin to have a high acid strength, and it is even regarded as “superacidic”, on account of the fluorine atoms close to the sulfonic acid groups<sup>[21-23]</sup>. In the work reported in this thesis, Nafion® has been tested and compared to other solid acid catalysts, and will be discussed in more detail later in this chapter.

In producing acid catalysts on inorganic supports, a Mobil research group were the first to discover a new family of mesoporous oxide molecular sieves known as the M41S

family in 1992 based on the zeolite templating model. Their pore sizes range from 1.5-10nm in size, and due to the order of the pores, three key members of the family exist, the most important of which is the hexagonally ordered MCM-41. These particular molecular sieves possess long range order and surface areas greater than  $700\text{m}^2\text{g}^{-1}$ . The materials are formed by what has become known as *Liquid Crystal Templating* (LCT), and now more commonly as *sol-gel synthesis*, where liquid crystal (highly ordered liquid structure) rod like micelles of cationically charged copolymer surfactant molecules serve as organic templates for the materials (in this case alkyltrimethyl ammonium salt surfactant) [7/ 24-28]. The surfactant molecules are further treated by oxidation and acidification in order to produce sulfonic acid groups.

Research by Corma, Diaz and co-workers has been carried out on these mesoporous oxide molecular sieves investigating their organic modification with methyl/propyl and phenyltrialkoxysilane groups to further tailor the solids pore size and shape. This modification occurs during the sol-gel synthesis but retains the use of the quaternary ammonium surfactant, followed by oxidation and acidification steps. This synthesis route will be discussed in more detail further on in this chapter [6-7/ 29-32].

Stucky and co-workers have developed an alternative model for sol gel synthesis, utilising different templates in order to modify the resultant gel. Giving distinct advantages over MCM-41 that the composition and gel crystallization variables could be extensively varied offering a wider variety of tailored porous materials with different properties dependant on the specific catalyst required [23]. The alkyl poly(ethylene oxide, propylene oxide) triblock copolymer surfactant was used, and generated a highly ordered hexagonal structured material named SBA-15 [7/33-35]. Further organic modification utilising both propyl/phenyltrialkoxysilane groups in order to see their effect on the resulting materials has also been investigated [36-38], and will be discussed in more detail further on in this chapter.

Using cationically charged surfactant template molecules, and triblock copolymer materials offer the distinct advantage of the ability to tailor the porous material by varying the concentration of the surfactant used, this in itself can be disadvantageous as when the concentration is too low, subsequent surfactant template removal leads to the collapse of the ordered structure. Therefore new synthesis routes which allow the surfactant template to be removed more easily are highly sought after.

To this end, utilising a neutral surfactant template during the sol-gel synthesis produced materials with weaker intermolecular bonding with respect to the neutral surfactant and neutral inorganic precursor interface. Pinnavaia, Clarke, Macquarrie and co-workers detail their synthesis of hexagonally ordered mesoporous silicas (HMS) utilising the neutral amine surfactant, and its subsequent organic modification with propyl/phenyl groups, and will be discussed in more detail later on in this chapter <sup>[1-5]</sup>.

These three inorganic mesoporous silicas have been the focus of various studies regarding synthesis and resulting pore size and distribution, and the effects on the subsequent physical properties of the catalyst. Altering the concentration of the precursors and the chain length of the surfactant used results in various pore channel sizes. Work has been completed on the use of alternative routes to synthesise a higher order of non-functionalised and functionalised mesoporous materials, including the use of alternative hydrophobic tethers (in this case phenyltriethoxysilane) in a bi-functionalisation process <sup>[32]</sup>, and the use microwave thermal technology <sup>[39-43]</sup>. Further organic modification resulted in the use of the more negatively charged phenyl functional groups, and more interestingly subsequent fluorination to determine the effect on the resultant activity of the acid catalyst <sup>[23/ 43-45]</sup>. As well as sulfonic acid supported catalysts, work has been completed with alternative acids, more recently with heteropolyacids supported on siliceous and other materials <sup>[46-47]</sup>. More recently Alazun and co-workers have used the sol-gel synthesis technique to further organically modify MCM type materials to allow them to possess antagonistic acidic and basic properties on the same material by the use of protection groups to ensure the functionality of the aminopropyl group is not effected during the chemical treatment. This is promising research in the new and upcoming field of bi-functional catalysis <sup>[48-49]</sup>.

Along side synthetic organic-inorganic mesoporous molecular sieve routes, attempts have also been made to synthesise catalytic materials based on amorphous silicas, due to their relatively low cost, again through organic modification with alternative surfactants <sup>[50-55]</sup>, silica supported heteropolyacid <sup>[45]</sup> and fluorinated or silica supported Nafion® <sup>[56]</sup>. Alternative functional group grafting techniques have been used in order to establish their effect on the catalytic activity of the resultant material. These include pre-activation of the silica support before synthesis <sup>[57-58]</sup>, grafting of the functional group through an incipient wetness technique <sup>[49]</sup>, as well as the subsequent

incorporation of metal ions into the amorphous structure. More recently research is underway into the synthesis of mesoporous molecular sieve silica containing aluminium and titanium ions, through the use of sol-gel synthesis, but without the expensive surfactant template, again highlighting the variability of these materials to be tailored<sup>[44]</sup>.

Aside from organic-inorganic supported solid acid catalysts, research has been completed on alternative non porous supports. In the early eighties some transition metal oxides were found to be highly acidic containing both Lewis and Bronsted acid sites, and like Nafion® today, were claimed to be “superacidic”. However, today it is more common practice to incorporate these transition metal oxides such as titanium, zirconium, zinc and aluminium into tailored sol-gel supports, thus increasing the surface area of the active acid catalyst. Yet in comparison to other solid acid catalysts sulfonated metal oxides have been found to deactivate quickly, and produce unwanted environmental waste (toxic metal solid deposits and noxious gases), thus limiting their use<sup>[6]</sup>.

There is a need for further study to characterise solid acid catalysts in order to relate physical and chemical properties to acidity and catalytic activity in liquid phase reactions. And also to investigate further the subsequent effect of the solvent used in these reactions on the materials.

The use of silica supported mesoporous molecular sieve materials for use as solid acid catalysts for liquid phase reactions is of high interest in current research. Many different types of solid acid catalyst exist and have been studied as demonstrated in the above text.

## 1.5 Specific Objectives

- ❖ To synthesise, functionalise and characterise a series of supported sulfonic acid catalysts in terms of structure, acidity and catalytic activity.

- ❖ To determine the role of the support in controlling acidity and activity of the catalysts based on chemically supported sulfonic acid, and the optimization of these materials as catalysts in liquid phase reactions.
- ❖ To determine the influence of the nature of the support and the sulfonic acid tether on the resultant properties of the supported acid catalyst.
- ❖ To evaluate the effect of the solvent used in catalytic reactions on the accessibilities and strengths of surface acid sites in the differing supports.
- ❖ To investigate the relationship between acidity measured by base adsorption calorimetry in the liquid phase and catalytic activity. To evaluate base adsorption calorimetry in the liquid phase to predict catalytic properties, and their relationship to the acidity of the solid acid catalyst in liquid phase reactions.

## 1.6 Catalysts Studied

In the course of this research, three separate types of solid acid catalyst support for sulfonic acid were studied and characterised in terms of acidity and catalytic activity.

Those catalysts were:

- a) **Polymer supported sulfonic acid resins.** These consisted of two types, the *sulfonated poly(styrene-co-divinylbenzene) ion exchange resins* with varying levels of sulfonation, and the Nafion® *sulfonated fluorinated polymer resins*.
- b) **Sulfonated silica gels.** Synthesised in house with both propyl and phenyl organic tethers for sulfonic acid, and the inclusion of a non acidic phenyl group.
- c) **Sulfonated mesoporous molecular sieve silica gels.** Synthesised in house with both propyl and phenyl organic tethers for sulfonic acid, and the inclusion of a non acidic phenyl group. Three types were synthesised, *MCM-41*, *SBA-15* and *HMS*.

All are discussed in detail below.

### 1.6.1 Polymer supported sulfonic acid resins

#### ❖ Sulfonated poly(styrene-co-divinylbenzene) ion exchange resins

Acidic cation exchange resin supported polymer materials are well established since 1935 and widely reported in literature for use in liquid phase reactions [12-16]. Commercially available resin catalysts are produced in the form of spherical beads with diameters of 0.5-1.0mm. In general ion exchange resins are based on addition copolymers prepared from the addition polymerisation of vinyl monomers in aqueous media [14]. Divinylbenzene is used as a cross linking agent to develop a semi-rigid structure which swells in the presence of organic solvents but has no ion exchange properties. Commercially produced ion exchange resins exist in two main forms, gel and macroporous. Gel type resins are polymerised as uniform beads with smooth external surfaces. Polymer beads swell in non porous organic solvents but not in water. Functional group acid sites are found only within the gel matrix, and a suitable organic solvent must be used in order to swell the matrix for the reactant molecules to access the sites. Gel type resins possess no overall degree of permanent porosity. Macroporous resins are polymerised as beads in the presence of additional compound known as porogens. The purpose of the porogen materials is to be trapped within the polystyrene and after polymerization is complete they are dissolved out leaving spherical beads with a degree of permanent porosity. Subsequently due to the presence of large pores, diffusion of reactant molecules occurs through the pores of the resin without swelling and not within the gel matrix, thereby allowing the resin to act as a catalyst in both polar and non polar solvents, including gaseous media [59].

Gel type resins despite their lower divinylbenzene concentration, generally possess a higher internal concentration of active acid groups than their macroporous counterparts (after functionalization with H<sub>2</sub>SO<sub>4</sub>). However solvent presence is required to swell the gel matrix in order to access the intrinsic acid sites, therefore these resins are unsuitable for use in non-polar solvents, and generally collapse when dry.

Macroporous resins possess a larger range of porosities and a greater surface area. Molecules are able to diffuse through the pores and not the gel matrix of the resin therefore allowing the resin to be more catalytically active in liquid phase media, both polar and non-polar, as well as gaseous media. Due to the larger concentration of cross

linking these macroporous resins have an increased thermal stability compared to the gel type [17-21].

Functionalization of the resins occurs through reaction of the already formed polymer (a schematic of which is shown in Figure 1.1 below) with concentrated sulphuric acid, a schematic of which is shown below in Figure 1.2. Commercially available resins are prepared and sulfonated at a stoichiometric level equivalent to one sulfonic acid group per styrene unit. This is an over simplification, sulfonation may not be uniform, resulting in disulfonation or the possible formation of sulfone bridges (Figure 1.3). Some resins have also been prepared with higher than stoichiometric levels of sulfonation. In theory these type of “persulfonated” resins contain stronger acid sites due to the interaction of the additional electron withdrawing sulfonic acid groups on disulfonated phenyl rings, thereby allowing easier donation of the proton.

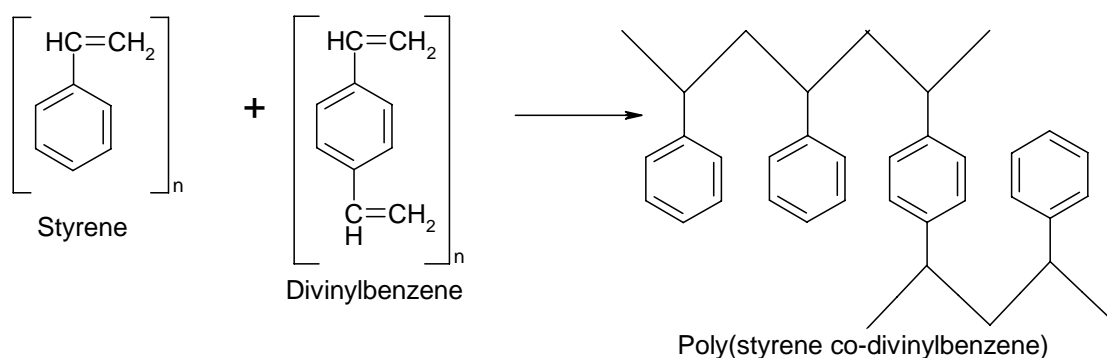


Figure 1.1 Schematic of the polymerization process during the formation of the polymeric resins.

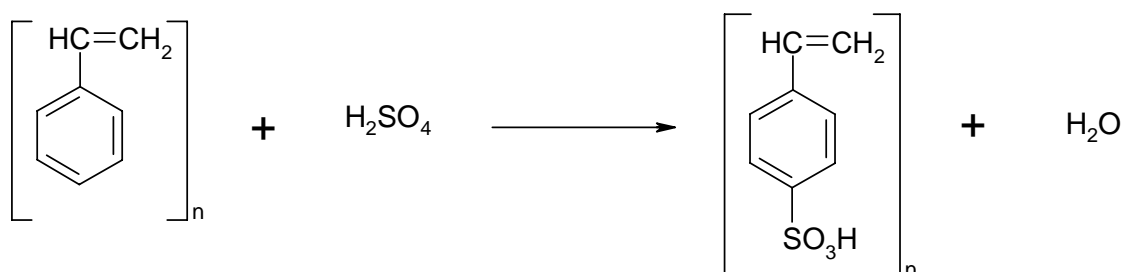


Figure 1.2 Schematic of sulfonation of the polymeric bead after treatment with concentrated sulphuric acid.

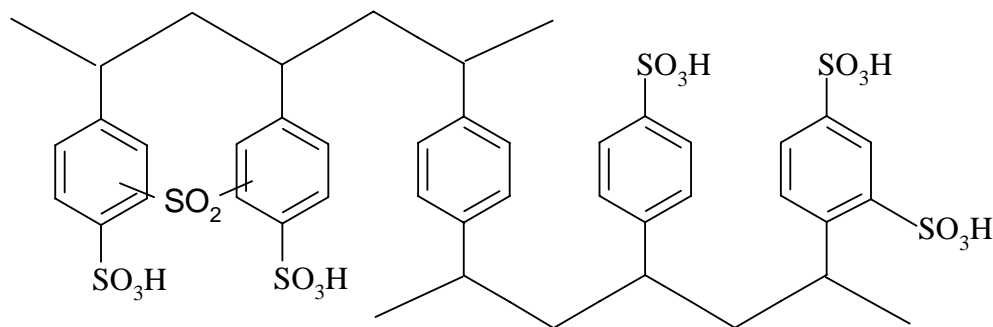


Figure 1.3 possible points of sulfonation of the polymeric resin beads.

The extent of the sulfonation increases the likelihood of interactions between neighbouring sulfonic acid groups which are believed to control the acid strength of the resin. A molecule's ability to diffuse into the polymer matrix is dependant on several factors including the level of sulfonation of the polymer thus its hydrophilicity, the polarity of the solvent used and so the extent to which it is able to swell the resin. The ability of the resin to swell is also dependant on its degree of crosslinking.

This ability to tailor the polymeric resins by controlling the degree of crosslinking and pore size through specific porogen compounds, degree of sulfonation and specific surface area is a distinct advantage over other solid acid catalysts. Other advantages include ease of handling, structural uniformity and a high abundance of acid sites. However they have been found to be thermally unstable at temperatures exceeding  $150^\circ\text{C}$ , and despite high levels of acid sites they have been found to be weaker than those found on zeolitic solid acid catalysts and clays <sup>[1]</sup>.

It has been reported in previous work that the relationship between the accessibility of the acid sites and the solvent type is critical in assessing the function of the catalysts and thus the possible reactions to which they would be most suited. One of the most important factors indicated in the previous research which affects the resulting catalytic activity of the incorporated sulfonic acid groups is the presence of water. Water has been found to have a levelling effect on the acid strength. The acid strength and catalytic activity of the resins has been found to decrease with increasing water content <sup>[18/20]</sup>. The most active sites are thought to be the undissociated sulfonic acid groups or their monohydrates <sup>[21]</sup>.

In this study the polymeric resins SP21/15, C100H, CT175, CT275 were provided by Purolite Ltd, Amberlyst 15 was provided by Rohm and Haas. After drying they were characterised in terms of acidity and catalytic activity as a benchmark comparison for the synthesised sulfonated inorganic supports. The resins possess a variety of levels of sulfonation. The macroporous SP21/15 resin is sulfonated to a level under that of stoichiometric sulfonation (less than one sulfonic acid group per styrene monomer unit). The gel type C100H resin, the macroporous CT175 and the Amberlyst15 resins are stoichiometrically sulfonated, and finally the macroporous CT275 resin is “persulfonated” to a level higher than normal stoichiometric sulfonation.

### ❖ Sulfonated Fluorinated Polymer Resins.

Perfluorinated sulfonic acid based ion exchange resins are currently of high interest when compared to the commercially available sulfonated polymeric supported resins. The comparatively higher acid strength is believed to be due to the presence of the highly electronegative fluorinated regions of the resin and the resultant ability of the attached sulfonic acid groups to donate protons is increased [23/56]. A cross linked perfluorinated polymeric sulfonic acid is commercially available under the name Nafion® from Dupont and the structure is shown below in Figure 1.4.

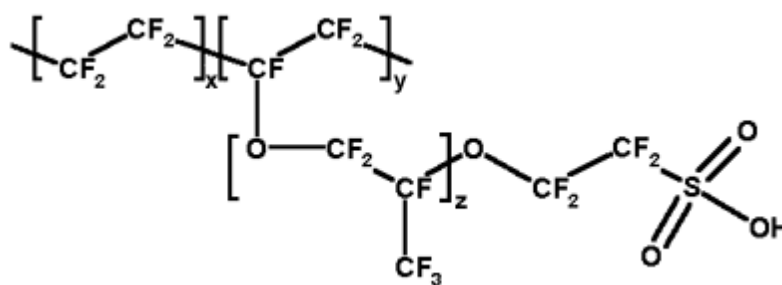


Figure 1.4 Structure of perfluorinated polymeric sulfonic acid Nafion®.

Nafion® is a copolymer of tetrafluoroethene and perfluoro-2-(fluorosulfonylethoxy)propyl vinyl ether. It has been found to increase many reaction rates when compared to traditional homogenous catalysts, including alkylations, acylations, isomerizations, esterifications, hydrations, dehydrations, nitrations and etherifications [23]. The resin is commercially available in bead form. Despite its

superacidic potential, the resin bead possesses only a small surface area of less than  $0.02\text{m}^2\text{g}^{-1}$ , and a concentration of only  $0.8\text{mmol g}^{-1}$  acid sites. The acid sites within the polymer bead are potentially difficult to access as the bead's structural matrix is not prone to swelling in most solvents. Hamer and Sun have reported the use of Nafion® catalyst supported on a silica framework SAC-13. The subsequent surface area of the catalyst was greatly increased, despite its much lower concentration of acid sites at  $0.1\text{mmol g}^{-1}$ , and yet there was an increased accessibility to the active acid sites due to the sol-gel synthesis of a porous material support <sup>[23]</sup>. The SAC-13 silica supported sulfonated Nafion® composite is also commercially available and was researched here as another benchmark comparison to not only the sulfonated polymeric resins, but also to the synthesised silica supported materials.

### 1.6.2 Sulfonated silica gels (grafting route)

Commercially available amorphous silica is prepared by a sol-gel technique using an aqueous silicate solution with subsequent acidification, neutralization and polymerization reactions to form the silica hydrogel, or from reaction of silicon alkoxides with water, and the subsequent hydrolysis and self condensation reactions to form the polysilicate <sup>[27]</sup>. The generalised structures of the resultant polysilicate gels are crystalline cross linked chains of alternate layered silicon and oxygen atoms in an  $\text{SiO}_4$  tetrahedral structure as shown in Figure 1.5 below <sup>[64]</sup>. These silica networks have however been found to possess relatively few acid sites, with source of acidity generated from the outside  $\text{SiO}_3(\text{OH})$  tetrahedral sites. Silicates with these structures are readily interdispersed with alternative metal atoms such as aluminium and subsequently  $\text{SiOHAl}$  bridges are formed, thus enabling an increased availability of readily donated protons thereby allowing the aluminosilicate material to act as a Bronsted acid. Thus man-made clays are synthesised, with an increasing number of acid sites dependant on the increasing Si:Al ratio.

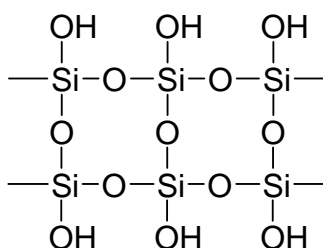


*Figure 1.5 Schematic of the crystalline cross linked silicon/oxygen chains that form the structure of the polysilicate gel (amorphous silica) generated by the two types of synthesis route.*

The term sol-gel synthesis comes from the two distinct steps in the synthesis: step one is the condensation polymerization of the formed silicic acids with other silicic acids or alkoxides to form high molecular weight polysilicate chains represent the formation of the “sol”. In step two the formed polysilicates then link together to form a three dimensional network, the pores of which are filled by solvent molecules forming a “gel”. The material is then dried, creating an amorphous, high surface area, porous solid.

Functionalization of the amorphous silica gel in this case can be achieved by grafting the desired functional groups to the silica surface. With work reported in literature and produced here, two types of organosilane functional group tethers were grafted; 3-mercaptopropyltrimethoxysilane (MPTMS) and 2-4chlorosulfonyltrimethoxysilane (CSPTMS), shown in Figures 1.6 and 1.7 below. The object of comparing the two tethering compounds was to ascertain the effect of the more electronegative phenyl group on the resultant acidity/catalytic activity of the material compared to its propyl functionalised counterpart. Bi-functionalization of the material was also achieved by the grafting of an additional phenyl group using phenyltriethoxysilane (PTES) shown in Figure 1.8 below. Oxidation and acidification of the thiol groups to sulfonic acid was achieved by oxidation with hydrogen peroxide and acidification with sulfuric acid, shown below in Figure 1.9. In the case of CSPTMS, there was no need for oxidation, only acidification to sulfonic acid, therefore only the MPTMS schematic is shown.

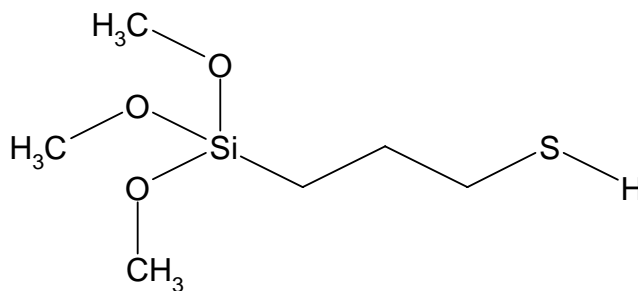


Figure 1.6 3-mercaptopropyltrimethoxysilane (MPTMS)

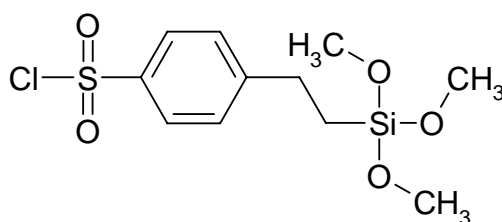


Figure 1.7 2-(4-chlorosulfonylphenyl)trimethoxysilane (CSPTMS)

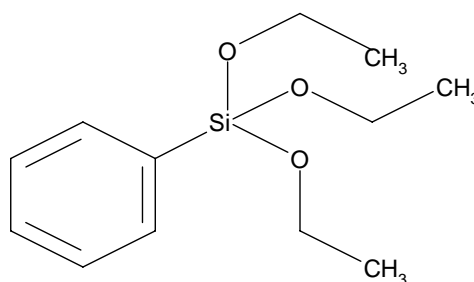


Figure 1.8 phenyltriethoxysilane (PTES)

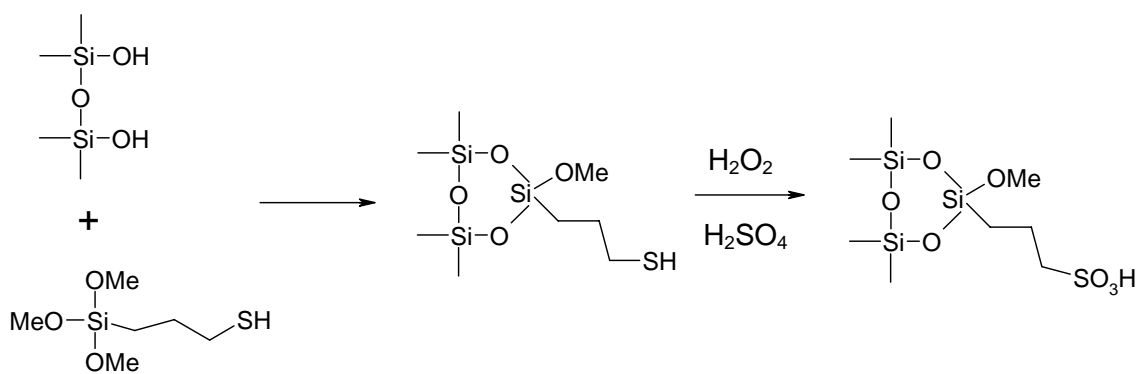


Figure 1.9 Grafting and subsequent oxidation/acidification processes of the amorphous silica with MPTMS.

With this form of sol gel derived amorphous silica structure, the pores are highly disordered in terms of shape and size. Order is obtained by heat treatment of the gel in the presence of a “structure directing” template species. Thus the synthesis of mesoporous molecular sieves produces non crystalline amorphous framework in which the pores are uniform and ordered.

### **1.6.3 Sulfonated Mesoporous molecular sieve silicas (co-condensation route)**

From the various syntheses reported by workers from Mobil group, Klinowski, Diaz, Stucky, Shanks, Cheng, Pinnavaia, Clarke, Macquarrie and co-workers [29-59] all of which are detailed further in Chapter Two, three main types of sulfonated mesoporous silica gels have been produced, one of which uses a *cationic surfactant template molecule (MCM-41)*, another an *amphiphilic polymer template surfactant molecule (SBA-15)*, and the remaining material utilises a *neutral surfactant template molecule (HMS)* in order to tailor the resultant pore size. These co-condensation sol gel synthesis routes enable the incorporation of the organic functional groups within the silica structure during synthesis with pore directing surfactant agents, resulting in the production of an ordered mesoporous material with functional groups within the pore structure as well as on the surface able to be further oxidised and acidified to yield sulfonic acid groups. In theory this tailoring of the pore size enables the material to be synthesised more specifically with regards its organic functionalization which allows the control of the materials surface properties, hydrophilicity/hydrophobicity modification and subsequent alteration of the surface reactivity of the material and therefore its use in specific catalytic reactions as a Bronsted acid. Figure 1.10 below shows a schematic of the MPTMS (in this instance) functionalised hexagonally structured mesoporous MCM-41 material. The MPTMS molecule is believed to be located within the pore.

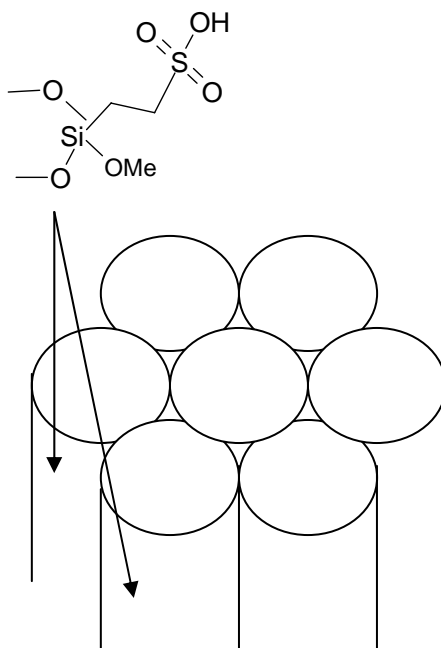


Figure 1.10 Schematic of the possible functionalization of the hexagonal porous structure of the mesoporous sulfonated silica gel materials.

#### ❖ MCM-41

The MCM-41 type mesoporous material is synthesised via a co-condensation of alkoxy silanes and 3-mercaptopropyltrimethoxysilane which is further oxidised and acidified to yield propylsulfonic acid groups anchored onto the silica framework <sup>[29]</sup>. This particular route uses alkyltrimethylammonium *cation surfactants*, and tetramethylammoniumhydroxide (TMAOH) as a co-structuring agent. The pore ordering of the final material depends on the hydrolysis and condensation kinetics of the alkoxy silane precursors used in the functionalization step of the synthesis, in this case 3-mercaptopropyltrimethoxysilane (MPTMS), or chlorosulfonylpropyltrimethoxysilane (CSPTMS), and phenyltriethoxysilane (PTES). The silica sources in this instance were methyltrimethoxysilane (MTMS) and tetramethoxysilane (TMOS). The surfactants used were hexadecyltrimethylammonium (C<sub>16</sub>TAB) and dodecyltrimethylammonium (C<sub>12</sub>TAB) bromides <sup>[30]</sup>.

### ❖ SBA-15

The SBA-15 type material is synthesised in the same manner but alternatively using an *amphiphilic block copolymer* as an organic structure directing agent (surfactant), in this case poly(ethyleneoxide, alkyene oxide) triblock copolymer “Pluronic®” 10400, and tetraethoxysilane as the silica source (TEOS)<sup>[35]</sup>. Again functionalization of the material occurs with the use of MPTMS, CSPTMS and PTES. SBA-15 has the larger pores compared to MCM-41 due to the Pluronic® 10400 copolymer.

In 1998 Stucky and co-workers proposed the surfactant-inorganic mechanism pathways for the synthesis of mesoporous materials utilising the electrostatic interactions between positively charged surfactant molecules ( $S^+$ ) and negatively charged inorganic species ( $I^-$ )<sup>[34]</sup>. The proposed schematic for hexagonal mesoporous MCM-41/SBA-15 material synthesis is shown in Figure 1.11, and is detailed in the paragraph below.

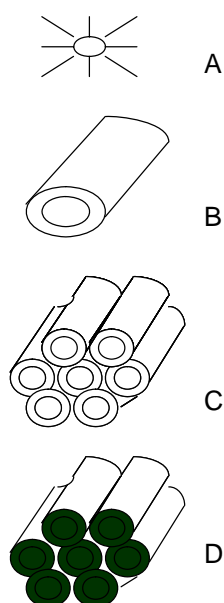


*Figure 1.11. Schematic of the formation of hexagonal mesoporous material MCM. With four distinctive steps a-d.*

The surfactants ( $S^+$ ) containing a polar head group and a non polar hydrocarbon tail form micelles in polar environments (A). The hydrophobic tails aggregate together in the centre of a sphere to avoid contact with the polar water solvent. The polar head groups form a layer on the surface of the sphere (charge dependant on the type of surfactant used). Silicate ( $I^-$ ) and organic precursor polymerisation now occurs around

the micelles forming a micellar rod (“Sol”) (**B**). The micellar rods aggregate together to form a hexagonal rod framework (“Gel”) (**C**), upon calcination the surfactant template is removed leaving a hexagonal mesoporous structure (**D**) (mesostructure).

### ❖ HMS

In comparison Pinnavaia and co-workers<sup>[60/65-66]</sup> researched into new synthetic routes to allow for easier removal of the surfactant molecules without the destruction of the pore walls. In this instance *neutral surfactant template* molecules were used, resulting in weaker hydrogen bonds at the surfactant-inorganic interface, and therefore making it easier to extract the surfactant template with solvent. In this case a neutral amine template was used (dodecylamine). The sol-gel synthesis routes remain the same, as did the functionalization, oxidation and acidification steps. These materials have been found to have a higher thermal stability compared to the MCM-41 materials due to their stronger bonding interactions.

## 1.7 Summary.

In this chapter the use of and the reasons behind the use of solid acid catalysts in liquid phase reactions have been discussed, with particular emphasis on mesoporous silica supported materials that have been synthesised, functionalised, acidified and characterised, and then compared to commercially available acidic ion exchange resin catalysts.

As stated previously, in the course of this research three separate types of solid acid catalyst support were studied and characterised in terms of acidity and catalytic activity.

Those catalysts were:

- I. **Polymer supported sulfonic acid resins.** These consisted of two types, the *sulfonated poly(styrene-co-divinylbenzene) ion exchange resins* with varying levels of sulfonation, and the *sulfonated fluorinated polymer resins*.
- II. **Sulfonated silica gels.** Synthesised in house with both propyl and phenyl organic tethers, and the inclusion of a non acidic phenyl group.
- III. **Sulfonated ordered mesoporous molecular sieve silicas.** Synthesised and functionalised in house with both propyl and phenyl organic tethers, and the

inclusion of a non acidic phenyl group. Three types were synthesised, *MCM-41*, *SBA-15* and *HMS*.

Techniques of synthesis and characterization of structure, surface acidity and catalytic activity are detailed and compared in the following chapters.

**References:****[1] Catalysis for green chemistry: ultrahigh loaded mesoporous solid acids.**

J. H. Clark, S. Elings and K. Wilson, *Comptes Rendus de l'Académie des Sciences - Series IIC – Chemistry*, 3, 6, (Nov 2000), 399-404.

**[2] Chemistry on the inside: green chemistry in mesoporous materials.**

D. J. Macquarrie. *Phil. Trans. R. Soc. Lond. A*, 358 (2000), 419-430.

**[3] Modified silicas for clean technology.**

P. M. Price, J. H. Clark, D. J. Macquarrie. *J. Chem. Soc. Dalton Trans.* (2000), 101-110.

**[4] Solid acids and their use as environmentally friendly catalysts in organic synthesis.**

K. Wilson, and J. H. Clark, *Pure Appl. Chem.* 72, 7, (2000), 1313-1319.

**[5] The application of modified mesoporous silicas in liquid phase catalysis.**

J. H. Clark, D. J. Macquarrie, S. J. Tavener. *Dalton Trans.* (2006), 4297-4309.

**[6] Solid acid catalysts,**

A. Corma, *Current Opinion in Solid State and Materials Science.* 2, 1, (Feb 1997), 63-75.

**[7] From Microporous to Mesoporous Molecular Sieve Materials and Their Use in Catalysis.**

A. Corma. *Chem. Rev.* 97, (1997), 2373-2419.

**[8] Inorganic Solid Acids and Their Use in Acid-Catalysed Hydrocarbon Reactions.**

A. Corma. *Chem. Rev.* 95, (1995), 559-614.

**[9] What do we know about the acidity of solid acids?**

R. J. Gorte. *Cat. Lett.* 62, (1999), 1-13.

**[10] Solid acids and bases as catalysts**

I. Arends, R. Sheldon, U. Hanefeld. *Green chemistry and catalysis.* Wiley-VCH, (2007), 49-90.

**[11] Supported sulfonic acid catalysts in aqueous reactions.**

S. Koujout, D. R. Brown. *Centre for applied catalysis, University of Huddersfield internal paper.*

**[12] Industrial application of solid acid-base catalysts.**

K. Tanabe, W. F. Holderich. *App. Catal A: Gen* 181, (1999), 399-434.

**[13] Some novel aspects of cationic ion-exchange resins as catalysts,**

M. M. Sharma, *Reactive and Functional Polymers*, 26, 1-3, (Sep 1995), 3-23.

**[14] Cationic ion exchange resins as catalysts,**

A. Chakrabarti and M. M. Sharma, *Reactive Polymers*, 20, (1993), 1-45.

**[15] Solid acid catalysts using ion-exchange resins.**

M. A. Harmer, Q. Sun. *App. Catal. A: General* 221, (2001), 45-62.

**[16] Acidic and basic ion exchange resins for industrial applications.**

M. Di. Girolamo, M. Marchionna. *J. Molec. Catal. A. Chem.* 177, (2001), 33-40.

**[17] Acidities and catalytic activities of persulfonated poly(styrene-co-divinylbenzene) ion-exchange resins.**

M. Hart, G. Fuller, C. Park, M. A. Keane, J. A. Dale, C. M. Fougret, R. W. Cockman. *Catal. Lett.* 72, (2001), 3-4.

**[18] Sulfonated poly(styrene-co-divinylbenzene) ion-exchange resins: acidities and catalytic activities in aqueous reactions.**

M. Hart, G. Fuller, D. R. Brown, J. A. Dale, S. Plant. *J. Molec. Catal. A. Chem.* 182-183, (2002), 439-445.

**[19] The nature of the internal acid solution in sulfonated poly(styrene-co-divinylbenzene) resins.**

S. Koujout, B. M. Kiernan, D. R. Brown, H. G. M. Edwards, J. A. Dale, S. Plant. *Catal. Lett.* 85, (Jan 2003), 1-2.

**[20] Sulphonated polystyrene resins: acidities and catalytic activities.**

C. N. Rhodes, D. R. Brown, S. Plant, J.A. Dale. *React and funct polym* 40, (1999), 187-193.

**[21] Acid strengths and catalytic activities of sulfonic acid on polymeric and silica supports.** P. F. Siril, A. D. Davison, J. K. Randhawa, D. R. Brown, *J. Molec. Catal A: Chem* 267, (2007), 72-78.**[22] Unique silane modified perfluorosulfonic acids as versatile reagents for new solid acid catalysts.**

M. A. Harmer, Q. Sun, M. J. Michalczyk and Z. Yang, *Chem. Commun.* (1997), 1803-1804.

**[23] High surface area Nafion® resin/silica nanocomposites: A new class of solid acid catalyst.**

M. A. Harmer, W. E. Farneth, Q. Sun. *J. Am. Chem. Soc.* 118, (1996), 7708-7715.

**[24] A New Family of Mesoporous Sieves Prepared with Liquid Crystal Templates.**

J.S. Beck, J.C. Vartuli, W.J. Roth, M.E Leonowicz, C.T. Kresge, K.D. Schmitt, C.T-W. Chu, D.H. Olson, E.W. Sheppard, S.B. McCullen, J.B. Higgins, and J.L. Schlenker. *J. Am. Chem. Soc.* 114, (1992), 10834-10843.

**[25] Recent advances in the synthesis, characterisation and applications of mesoporous molecular sieves.**

J. S. Beck and J. C Vartuli. *Curr Opp in solid state and materials sci. Elsevier*, 1, 1, (1996), 76-87.

**[26] Ordered mesoporous molecular sieves synthesised by a liquid crystal template mechanism.**

C. T. Kresge, M. E. Leonowicz, W. J. Roth, J. C. Vartuli, J. S. Beck. *Letters to nature.* 359, (1992), 710-712.

**[27] Tailored porous materials**

J. C. Vartuli et al. *Chem. Mater.* 11, (1999), 2633-2656.

**[28] Optimal parameters for the synthesis of the mesoporous molecular sieve [Si]-MCM-41.**

C. Cheng, D. H. Park and J. Klinowski, *J. Chem. Soc. Faraday Trans.* 93, 1, (1997), 193-197.

**[29] Combined alkyl and sulfonic acid functionalisation of MCM-41 type silica.****Part 1: synthesis and characterization**

I. Diaz, C. Marquez-Alvarez, F. Mohino, J. Perez-Pariente, E. Sastre. *J. Catal*, 193, (2000), 283-294.

**Combined alkyl and sulfonic acid functionalisation of MCM-41 type silica. Part 2: Esterification of Glycerol with Fatty Acids.**

I. Diaz, C. Marquez-Alvarez, F. Mohino, J. Perez-Pariente, E. Sastre. *J. Catal*, 193, (2000), 295-302.

**[30] Synthesis, characterisation and catalytic activity of MCM-41-type mesoporous silicas functionalised with sulfonic acid.**

I. Diaz, F. Mohino, J. Perez-Pariente, E. Sastre. *App. Catal A: Gen* 205, (2001), 19-30.

**A novel synthesis route of well ordered, sulphur-bearing MCM-41 catalysts involving mixtures of neutral and cationic surfactants.**

I. Diaz, C. Marquez-Alvarez, F. Mohino, J. Perez-Pariente, E. Sastre. *Microporous and mesoporous materials* 44-45, (2001), 295-302.

**[31] Synthesis of MCM-41 materials functionalised with dialkylsilane groups and their catalytic activity in the esterification of glycerol with fatty acids.**

I. Diaz, F. Mohino, J. Perez-Pariente, E. Sastre. *App. Catal A: Gen* 242, (2003), 161-169.

**[32] Template directed synthesis of bi-functionalised organo-MCM-41 and phenyl MCM-48 silica mesophases.**

S. R. Hall, C. E. Fowler, B. Lebeau, and S. Mann, *Chem. Commun.* (1999), 201-202.

**[33] Triblock Copolymer Syntheses of Mesoporous Silica with Periodic 50-300 Angstrom pores.**

D. Zhao, J. Feng, Q. Huo, N. Melosh, G. H. Fredrickson, B. D. Chmelka, G. D. Stucky, *www.sciencemag.org, science*, 279, (1998), 548-552.

**[34] Nonionic triblock and star diblock copolymer and oligomeric surfactant syntheses of highly ordered, hydrothermally stable, mesoporous silica structures.**

G. Stucky et al. *J. Am. Chem. Soc.* 120, (1998), 6024-6036.

**[35] Direct Syntheses of Ordered SBA-15 Mesoporous Silica Containing Sulfonic Acid Groups.**

D. Margolese, J. A. Melero, S. C. Christiansen, B. F. Chmelka, and G. D. Stucky. *Chem. Mater.* 12, (2000), 2448-2459.

**[36] Direct syntheses of ordered SBA-15 mesoporous materials containing arenesulfonic acid groups.**

J. A. Melero, G. D. Stucky, R. V. Grieken, G. Morales, *J. Mater. Chem.* 12, (2002), 1664-1670.

**[37] Organosulfonic acid-functionalised mesoporous silicas for the esterification of fatty acid.**

I.K. Mbaraka, D. R. Radu, V. S-Y. Lin, B. H. Shanks. *J. Catal.* 219, 2, (2003), 329-336.

**[38] Arenesulfonic acid functionalised mesoporous silica as a novel acid catalyst for the liquid phase Beckmann rearrangement of cyclohexanone oxime to  $\epsilon$ -caprolactam.**

X. Wang, C.C. Chen, S.Y. Chen, Y. Mou and S. Cheng. *Chem. Comm.* (2003), 124-131.

**[39] Microwave synthesis of molecular sieve MCM-41.**

C-G. Wu. T. Bein. *Chem. Commun.* (1996), 925-926.

**[40] Rapid synthesis of mesoporous SBA-15 molecular sieve by a microwave-hydrothermal process.**

B. L. Newalkar, S. Komarneni and H. Katsuki. *Chem. Commun.* (2000), 2389-2390.

**[41] Simplified synthesis of micropore-free mesoporous silica, SBA-15, under microwave-hydrothermal conditions.**

B. L. Newalkar, S. Komarneni. *Chem. Commun.* (2002), 1774-1775.

**[42] Microwave-hydrothermal synthesis and characterisation of microporous-mesoporous disordered silica using mixed-micellar templating approach.**

B. L. Newalkar, H. Katsuki, S. Komarneni. *Microporous and Mesoporous Materials* 73, (2004), 161-170.

**[43] A study into the use of microwaves and solid acid catalysts for friedel-crafts acetylations.**

D. J. Macquarrie et al. *J. Molec. Cat A: Chem* 231, (2005), 47-51.

**[44] Structure and reactivity of sol-gel sulphonic acid silicas.**

K. Wilson, A. F. Lee, D. J. Macquarrie, J. H. Clark. *App. Catal A: Gen* 228, (2002), 127-133.

**[45] Nafion® functionalised mesoporous mcm-41 silica shows high activity and selectivity for carboxylic acid esterification and friedel-crafts acylation reactions.**

M. Alvaro, A. Corma, D. Das, V. Fornes, H. Garcia. *J. Catal* 231, (2005), 48-58.

**[46] Preparation and characterisation of chemisorbents based on heteropolyacids supported on synthetic mesoporous carbons and silica.**

A. Lapkin et al, *Catalysis Today* 81, (2003), 611-621.

**[47] Synthesis, characterisation and catalytic applications of sol-gel derived silica-phosphotungstic acid composites.**

A. Kukovecz et al. *App. Catal A: Gen* 228, (2002), 83-94.

**[48] Organosilica the conciliator.**

M. Jaroniec, *Nature*, 442, (10 Aug 2006), 86-87.

**[49] Mesoporous materials with an acidic framework and basic pores. A successful co-habitation.**

Alazun, J. Mehdi, A. Reye, C & Corriu, R. J. P. *J. Am. Chem. Soc.* 128, (2006), 8718-8719.

**[50] Acid-functionalised amorphous silica by chemical grafting-quantitative oxidation of thiol groups.**

E. Cano-Serrano, G. Blanco-Brieva, J. M. Campos-Martin, and J. L. G. Fierro, *Langmuir* (2003), 7621-7627.

**[51] Fabrication of novel mesoporous dimethylsiloxane-incorporated silicas.**

J. Joo, T. Hyeon and J. Hyeon-Lee. *Chem. Commun.* (2000), 1487-1488.

**[52] Synthesis of mesoporous silica with tunable pore size from sodium silicate solutions and a polyethylene oxide surfactant.**

L. Sierra, J. L. Guth. *Microporous and Mesoporous Materials* 27, (1999), 243-253.

**[53] Non-ionic surfactant assembly of ordered, very large pore molecular sieve silicas from water soluble silicates.**

S. S. Kim, T. R. Pauly and T. J. Pinnavaia. *Chem. Commun.* (2000), 1661-1662.

**[54] Role of framework sodium versus local framework structure in determining the hydrothermal stability of mcm-41 mesostructures.**

T. J. Pinnavaia et al. *J. Am. Chem. Soc.* 124, (2002), 97-103.

**[55] A versatile pathway for the direct assembly of organo-functional mesostructures from sodium silicate.**

J. Shah, S. S. Kim and T. J. Pinnavaia. *Chem. Commun.* (2004), 572-573.

**[56] Acidity and Catalytic Activity of a Nafion®-H/Silica Nanocomposite Catalyst Compared with a Silica-Supported Nafion® Sample.**

B. Torok, I. Kiricsi, A. Molnar and G. A. Olah. *J. Catal.* 193, (2000), 132-138.

**[57] Silica functionalised sulphonic acid groups: synthesis, characterisation and catalytic activity in acetalization and acetylation reactions.**

S. Shylesh, S. Sharma, S. P. Mirajkar, A. P. Singh, *J. Molec. Cat A. chem.* 212, (2004), 219-228.

**[58] Solid silica-based sulfonic acid as an efficient and recoverable interphase catalyst for selective tetrahydropyranlation of alcohols and phenols.**

B. Karimi, M. Khalkhali, *J. Molec. Cat A. chem.* 232, (2005), 113-117.

**[59] Purolite ion exchange resins: CT series:** technical data sheets provided by Purolite International Ltd. [www.purolite.com](http://www.purolite.com)

**[60] Mesoporous Sulfonic Acids as Selective Heterogeneous Catalysts for the Synthesis of monoglycerides.**

W. D. Bossaert, D. E. De Vos, W. M. Van Rhijn, , J. Bullen, P. J. Grobet and P. A. Jacobs. *J. Catal.* 182, (1999), 156-164.

**[61] Organically modified hexagonal mesoporous silicas (HMS) remarkable effect of preparation solvent on physical and chemical properties.**

D. J. Macquarrie et al, *J. Mater. Chem.* 11, (2001), 1843-1849.

**[62] Pore size modification of mesoporous HMS molecular sieve silicas with wormhole framework structures.**

T. R. Pauly and T. J. Pinnavaia. *Chem. Mater.* 13, (2001), 987-993.

**[63] Single step preparation and catalytic activity of mesoporous MCM-41 and SBA-15 silicas functionalised with perfluoroalkylsulfonic acid groups analogous to Nafion®.**

M. Alvaro, A. Corma, D. Das, V. Fornes, H. Garcia, *Chem. Commun.* (2004), 956-957.

**[64] Comprehensive Inorganic Chemistry Volume 1; Chapter 4.4 Silicon Dioxide.**

J.C. Bailar, H. J. Emelius, R. Nyholm, A.F Trotman-Dickenson.

**[65] Templating of mesoporous molecular sieves by non-ionic polyethylene oxide surfactants.**

S. A. Bagshaw, E. Prouzet, T. J. Pinnavaia. *Science*, 269, (01 Sep1995), 1242-1244.

**[66] Organic reactions catalyzed over solid acids,**

A. Corma and H. Garcia, *Catalysis Today*, 38, 3, (17 Nov 1997), 257-308.

# ***Chapter Two***

## ***Catalyst Syntheses***

---

## Chapter 2 Catalyst Syntheses

### 2.1 General Overview

This chapter aims to introduce and detail the experimental pathways and instrumental parameters followed in the synthesis of the solid acid catalysts and their subsequent functionalization, acidification and characterization. This chapter also includes alternative synthesis routes in order to establish their effect on the resultant acidity/catalytic activities of the materials.

### 2.2 Catalyst Types, Preparation and Synthesis

The commercially available polymer-supported sulfonic ion exchange resins were provided by the manufacturers. The sulfonated mesoporous silica and sulfonated silica gels were synthesised in house using the techniques detailed below.

The nature of the three types of catalyst studied in this research have been detailed previously in Chapter 1.0 but below is a brief summary.

- **Polymer supported sulfonic acid resins.** Commercially available cationic ion exchange resins, macroporous and rigid in structure. These consisted of two types, the *sulfonated poly(styrene-co-divinylbenzene) ion exchange resins*, and the *sulfonated fluorinated polymer resins* with varying levels of sulfonation.
- **Sulfonated silica gels.** Post grafting functionalization of an amorphous silica gel surface, non-rigid in structure. These were synthesised in house with both propyl and phenyl organic tethers for acid groups, and the inclusion of a non acid bearing phenyl group.
- **Sulfonated mesoporous molecular sieve silica gels.** Sulfonated inorganic mesoporous materials, synthesised via sol-gel techniques with subsequent functionalization and acidification. Three types were synthesised, *MCM-41* (alkyltrimethylammonium cationic surfactant), *SBA-15* (amphiphilic triblock copolymer) and *HMS* (neutral amine surfactant). Again they were synthesised in house with both propyl and phenyl organic tethers for acid groups, and the inclusion of a non acid bearing phenyl group.

## 2.2.1 Polymer Supported Sulfonic Acid Resins

### ❖ 2.2.1.1 Sulfonated Poly(styrene-co-divinylbenzene) Resins

The sulfonated poly(styrene-co-divinylbenzene) resins were provided by Purolite International Ltd<sup>[1]</sup> and Amberlyst 15 was provided by Rohm and Haas Ltd<sup>[2]</sup>. All resins were used in their hydrogen ion ( $H^+$ ) form. Sulfonic acid group concentrations (are in the range of 2.97-5.33 meqg<sup>-1</sup>) and water concentrations were provided by the manufacturer<sup>[1-2]</sup>. The C100H resin is a gel resin, the CT175, CT275, Amberlyst 15 and SP21/15 are macroporous resins. The C100H gel resin, Amberlyst 15 and the CT175 macroporous resin contain approximately stoichiometric levels of sulfonation (one sulfonic acid group per DVB or styrene monomer unit) deemed normal sulfonation. The SP21/15 macroporous resin is partially sulfonated, to a level less than normal stoichiometric sulfonation. The CT275 macroporous resin is persulfonated to a level greater than normal stoichiometric sulfonation.

### ❖ 2.2.1.2 Fluorinated Sulfonated Polymer Resins

Nafion® resin beads were purchased from E. I. Du Pont de Nemours and Co. Inc. The sulfonic acid group concentration was determined by the manufacturer to be 0.8 meqg<sup>-1</sup>. Nafion® SAC-13, a Nafion polymer supported on amorphous silica was obtained from Sigma-Aldrich, but manufactured by DuPont and claimed to contain approximately 13 % w/w Nafion<sup>[3]</sup>.

Before characterization all resins were ground to fine powders (<125  $\mu\text{m}$ ), sieved and dried in a conventional oven at 373 K for 1 hour and when necessary saturated overnight in the appropriate solvent.

## 2.2.2 Sulfonated Silica Gels and Sulfonated Mesoporous Molecular Sieve Silicas.

The propyl/phenyl sulfonic acid functionalised mesoporous silicas were synthesised using procedures as detailed in the literature.<sup>[4-20]</sup>

All chemicals were obtained from Sigma-Aldrich unless otherwise stated.

The main silica sources for the synthesis of the supports were tetraethoxysilane 98 % (TEOS), tetramethoxysilane 98 % (TMOS) and silica gel (99.8 %) (EP-116 obtained from Ineos Chemicals Ltd). The silicas were functionalised in the various syntheses using the silane precursors: 3-mercaptopropyltrimethoxysilane 95 % (MPTMS) and 2-(4-chlorosulfonylphenyl)ethyltrimethoxysilane (CSPTMS). Further functionalization of the silicas to modify the hydrophobicity of the catalyst surface was achieved using phenyltriethoxysilane (PTES). For silicas prepared from TEOS and TMOS, the surfactant templates used denote the type of mesoporous molecular sieve silica produced. The neutral surfactant dodecylamine produced the silica **HMS**, the ionic surfactants cetyltrimethylammoniumbromide ( $C_{16}TAB$ ) and dodecyltrimethylammonium bromide ( $C_{12}TAB$ ) were used in the synthesis of **MCM-41**. Those synthesised using the poly(ethylene oxide, propylene oxide) triblock copolymer Pluronic PE 10400 (BASF), were denoted **SBA-15**.

In the syntheses of sulfonated mesoporous molecular sieve silicas, three types of support were used, MCM-41, SBA-15, HMS, and for the sulfonated amorphous silica gels, the silica gel EP-116 was used. Two common synthesis routes were utilised: firstly, the *grafting route* whereby functionalization, oxidation and acidification occur after the initial silica framework synthesis which is later described in section 2.2.2.1, and secondly, a “one-pot” *co-condensation route*, whereby the MPTMS or CSPTMS is incorporated in the silica synthesis mixture, oxidised and acidified in situ as later described in Section 2.2.2.3.

### 2.2.2.1 Sulfonated Silica Gels. Grafting route

The amorphous silica gel EP116 was chosen as a silica gel with a significant volume of pores of variable pore dimensions. It was decided to investigate the effect of pre-treatment of the silica on its subsequent ability to be functionalised.

There were two types of pre-treatment of the amorphous untreated silica gel (EP116) used.

- 1) Using conventional ovens, heated at a high temperature (423 K for 10 hours)<sup>[4]</sup>.
- 2) By refluxing in 6M HCl for 24 hours<sup>[5]</sup>.

The post-grafting functionalization and subsequent oxidation and acidification procedures were as detailed below. Organic modification of the silica gel support

occurred through functionalization with mercaptopropylthiol (MPTMS) and chlorosulfonylphenyl (CSPTMS) tethers, as well as the non acid bearing phenyl group (PTES).

#### ❖ 2.2.2.1.a Propyl sulfonic acid functionalised silica gel

In a typical synthesis 3.58 g 3-mercaptopropyltrimethoxysilane (MPTMS) was added to 1.50 g of dried silica gel EP116 in 50 ml toluene. This mixture was refluxed for 12 hours at 383 K. The resulting mixture was filtered and the solid washed with hot toluene, centrifuged with a 50/50 water/methanol mix, and air dried overnight at 373 K for initial experiments. The oxidation and acidification of the mercaptopropyl groups to sulfonic acid was achieved by treating 1 g of extracted sample with 16 ml H<sub>2</sub>O<sub>2</sub> (33 vol %) at room temperature overnight, followed by washing with deionised water and acidification with 16 ml 0.1 M H<sub>2</sub>SO<sub>4</sub> at room temperature overnight, with subsequent washing and drying at 333 K overnight.

The oxidation and acidification steps were further varied in an attempt to optimise conditions for maximising the sulfonic acid loading on the silica.

#### • 2.2.2.1.b Oxidation

As the H<sub>2</sub>O<sub>2</sub> solution used during synthesis was concentrated (33 vol %), it was decided to alter only the volume used. From the standard treatment of 16 ml to 1 g solid, the volume was altered to five times that at 80 ml to 1 g solid, left stirring at room temperature overnight.

#### • 2.2.2.1.c Acidification

The concentration of H<sub>2</sub>SO<sub>4</sub> was varied and samples were prepared using 0.1, 0.5, 1.0 and 2.0 M acid. Standard acidification treatment was carried out using 16 ml acid to 1 g of solid, left stirring overnight at room temperature.

#### ❖ 2.2.2.1.d Propyl sulfonic acid and phenyl functionalised silica gel

Further functionalization of the silica gel in attempts to render the surface more hydrophobic was achieved by functionalising some samples with simple non acid bearing phenyl groups in addition to the sulfonic acid propyl groups. The additional

groups were grafted onto the surface of the silica by adding phenyltriethoxysilane (PTES) at the same time as the MPTMS in equal amounts of 3.58 g.

#### ❖ 2.2.2.1.e *Phenyl sulfonic acid functionalised silica gel*

The phenyl sulfonic acid functionalised silica gel was synthesised using the same procedure as detailed above, but with the alternative 2-(4-chlorosulfonylphenyl)ethyltrimethoxysilane (CSPTMS) in place of MPTMS. No oxidation step was required, (as sulfonyl chloride does not require oxidation before acidification to sulfonic acid) and acidification was carried out using 16 ml 0.1 M H<sub>2</sub>SO<sub>4</sub> per 1 g solid sample. Further filtration and washing steps were as previously mentioned.

#### ❖ 2.2.2.1.f *Phenyl sulfonic acid and phenyl functionalised silica gel*

Further functionalization of the silica gel with additional non acid bearing phenyl groups was achieved in situ using equal amounts of PTES and CSPTMS at the point of organosilane addition.

### 2.2.2.2 Sulfonated Silica Gels. Grafting route: Incipient Wetness technique

Following an alternative method reported in the literature<sup>[6]</sup>, a comparison between the standard grafting technique and an incipient wetness technique was made, with the same variation of precursors.

#### ❖ 2.2.2.2.a *Propyl sulfonic acid functionalised silica gel (IW)*

Following the reported method of Cano-Serrano et al<sup>[6]</sup>, 0.68 g of MPTMS was added dropwise onto 2.0 g of dried amorphous silica until the entire volume was absorbed. To ensure complete absorption, the resulting mixture was left for 24 hours at room temperature. The thiol groups were then oxidised using 32 ml of 33 % H<sub>2</sub>O<sub>2</sub> at 333K stirring the mixture for 1 hour. The solid was then filtered and washed three times using 32 ml of deionised water. The solid was acidified by stirring with 32 ml of 10 wt % H<sub>2</sub>SO<sub>4</sub> solution at room temperature. The resulting solid was filtered, washed three times with 32 ml deionised water and dried at 333 K for 24 hours. Note, the oxidation step was carried out at a higher temperature than in the previous grafting process in line

with the published results of Canno-Serrano et al who claim that oxidation at 333 K was more effective than at 298 K.

❖ **2.2.2.2.b Propyl sulfonic acid and phenyl functionalised silica gel (IW)**

Functionalization of the silica gel was achieved with the simultaneous addition of 1.32 g of PTES again ensuring that both MPTMS and PTES were fully adsorbed.

❖ **2.2.2.2.c Phenyl sulfonic acid functionalised silica gel (IW)**

The phenyl sulfonic acid functionalised silica gel was synthesised with CSPTMS in place of MPTMS (0.68 g). No oxidation step was required. Acidification and post treatment were performed as above.

❖ **2.2.2.2.d Phenyl sulfonic acid and phenyl functionalised silica gel**

Simultaneous functionalization of the silica gel with phenyl silane groups was achieved with the addition of 1.32 g of PTES along with the CSPTMS.

### **2.2.2.3. Sulfonated Mesoporous Molecular Sieve Silicas. Co-condensation Route**

The sulfonated ordered mesoporous molecular sieve silica supports were synthesised and functionalised in-house using a range of methods reported in the literature<sup>[7-20]</sup>. Organic modification of the mesoporous supports occurred through functionalization with mercaptopropylthiol (MPTMS) and chlorosulfonylphenyl (CSPTMS) tethers, as well as the simple phenyl group (PTES), followed by oxidation and acidification steps. Three main mesoporous molecular sieve silica supports were synthesised and characterised, **MCM-41**, **SBA-15** and **HMS**.

#### **MCM-41**

This ionic surfactant based support was synthesised using procedures detailed in the literature<sup>[7-13]</sup>. Initially purely siliceous MCM-41 was synthesised following the method of Klinowski et al<sup>[7]</sup>, and Hall et al<sup>[8]</sup>. Synthesis of the pure unfunctionalised material was conducted in order to obtain a highly ordered material that could act as a

suitable comparison to the co-condensed materials during characterization. MCM-41 was then synthesised and functionalised in a co-condensation route following the method of Diaz et al<sup>[9-13]</sup>. Post-grafting functionalization of the pure material using the Klinowski method was found to be unsuccessful compared to the co-condensation method, in which the tether components were incorporated in the MCM-41 synthesis mixture.

#### ❖ 2.2.2.3.a *Pure MCM-41*<sup>[7]</sup>

In a typical synthesis procedure, 72 g of deionised water was added to a mixture of 1.73 g tetramethylammonium hydroxide (TMAOH) and 9.84 g cetyltrimethylammonium bromide (C<sub>16</sub>TAB). The resultant solution was stirred until clear at 303 K. To this solution, 6.00 g fumed silica was added and stirred for 30 minutes at 303 K. The subsequently formed gel was aged for 24 hours at 293 K, and a pH of 11.5 was maintained through adjustment with 0.1 M acid or base. The reaction mixture was then introduced to a 100 ml teflon lined stainless steel autoclave which was heated to 423 K for 48 hours without stirring. The solid products were recovered by filtration, washed with deionised water and dried at 333 K overnight, and lastly calcined in air at 823 K for 8 hours.

After synthesis of the pure material using the Klinowski<sup>[7]</sup> method, it was hoped to functionalise the material with propyl thiol groups via a grafting process, followed by subsequent acidification and oxidation steps. This grafting method of the pure material however resulted in very low levels of functionalization when compared to the direct functionalization of the material in situ during synthesis utilising the Diaz method.<sup>[9-13]</sup>

#### ❖ 2.2.2.3.b *MCM-41 propyl sulfonic acid*. One step, co-condensation synthesis<sup>[9-13]</sup>

In a typical synthesis 1.74 g of C<sub>16</sub>TAB and 0.61 g dodecyltrimethylammonium bromide (C<sub>12</sub>TAB) surfactants were dissolved in a mixture of 34 g MeOH and 74 g deionised water. To this solution, a mixture of 6.2 g tetramethoxysilane (TMOS), 2.87 g MPTMS and 0.23 g methyltrimethoxysilane (MTMS) was added. Finally 5.52 g of tetramethylammonium hydroxide (TMAOH) was added drop wise to the solution. The resultant gel was stirred at room temperature for 16 hours in order to evaporate the

methanol. The reaction mixture was then introduced to a sealed 100 ml teflon lined stainless steel autoclave which was heated to 368 K for 48 hours without stirring. The solid products were recovered by filtration, washed with deionised water and dried at 333 K overnight. The surfactant was removed by stirring 3.0 g of dried sample with a solution of 40 ml HCl (35 wt%) in 410 ml EtOH at 343 K for 24 hours. The solid products were recovered by filtration, washed with deionised water and dried at 333 K overnight. The oxidation of the mercaptopropyl groups was achieved by treating 1.0 g of extracted sample with 16 ml H<sub>2</sub>O<sub>2</sub> (33 vol %), followed by washing with deionised water and acidification with 0.1 M H<sub>2</sub>SO<sub>4</sub>, with subsequent washing and drying at 333 K overnight. These conditions were identified as optimal in the previous syntheses.

❖ **2.2.2.3.c MCM-41 propyl and phenyl functionalised sulfonic acid.**

One step, co-condensation synthesis

Functionalization of the MCM-41 was achieved in situ using an equal amount of PTES and MPTMS to the original solution described above, based as a direct comparison to the arene-functionalised SBA-15 cited in the literature by Stucky<sup>[23]</sup>

❖ **2.2.2.3.d MCM-41 phenyl sulfonic acid.** One step, co-condensation synthesis

The phenyl sulfonic acid functionalised MCM-41 was synthesised with CSPTMS in place of MPTMS in the method described in 3.1.2.3.b and omitting the oxidation step from the final treatment.

❖ **2.2.2.3.e MCM-41 phenyl sulfonic acid and phenyl functionalised.**

One step, co-condensation synthesis

Functionalization of the MCM-41 was achieved in situ using an equal amount of PTES and CSPTMS to the original solution in the method described in 3.1.2.3.b and omitting the oxidation from the final treatment.

**2.2.2.4 Microwave heating synthesis route**

Microwave heating as an alternative to conventional heating was investigated in an attempt to produce a more ordered and more acidic mesoporous inorganic silica as was

reported separately in the literature by Bein, Newalker and Macquarrie (the relative pressures generated from the microwave heating resulting in the higher order formation of the product materials<sup>[14-18]</sup>). From these methods it was decided a comprehensive study of the oven ageing step in the synthesis of **pure MCM-41**, **SBA-15**, and the **propyl sulfonic acid** functionalised co-condensed **MCM-41** and **SBA-15** silicas would be completed. The heating time was varied up to and including the same time used in the conventional oven synthesis route. Note that the details of the SBA-15 synthesis routes appear below in Section 2.2.2.5.

Syntheses were performed in a MARS<sub>X</sub> microwave digestion system by CEM technologies. The system was operated at 300W, control of the microwave power was via pressure monitoring in the sealed reaction vessels. (The oven can be controlled using a temperature probe, but the glass sheath around the probe cannot be used in alkaline solution). It was assumed that the vapour pressure of the synthesis solution was the same as pure water and the control pressure was set to the estimated vapour pressure of water at the temperature required. The same temperatures were used in the microwave experiments as in the conventional heating experiment.

The syntheses of the inorganic silicas were as stated in their synthesis routes, with the exception of the ageing step now taking place in the microwave digestion oven. Table 2.1 below indicates the various synthesised silicas and the relevant vapour pressure and times for the microwave heating experiment. The post treatment (oxidation and acidification) of the silicas was as stated in the synthesis notes.

Silica	Conventional heating route, temperature and duration.	Microwave heating route, control water vapour pressure and duration.
Pure MCM-41	423 K, 48 hrs	475.7 kPa, 1-48 hrs
Co-condensed MCM-41 propyl sulfonic acid	368 K, 48 hrs	84.5 kPa, 1-48 hrs
Pure SBA-15	363 K, 24 hrs	70.1 kPa, 1-24 hrs
Co-condensed SBA-15 propyl sulfonic acid	373 K, 24 hrs	101.3 kPa, 1-24 hrs

*Table 2.1 Microwave heating control vapour pressure parameters compared to the conventional heating synthesis route.*

### 2.2.2.5 SBA-15

This ethylene oxide, propylene oxide triblock copolymer surfactant based support was synthesised using procedures detailed in the literature<sup>[19-24]</sup>. Initially, purely siliceous (un-functionalised) SBA-15 was synthesised<sup>[19]</sup>. It is important to note here that the literature reported Pluronic P123 compound is not readily available in the U.K., therefore all syntheses took place using its nearest relative molecular weight counterpart Pluronic 10400.

#### ❖ 2.2.2.5.a *Pure SBA-15*<sup>[19/20]</sup>

In a typical synthesis procedure reported by Lapkin et al<sup>[19]</sup> 2.0 g Pluronic copolymer was dissolved in a mixture of 52.5 g H<sub>2</sub>O, and 12.0 g HCl (35 wt%) at 313 K. To this solution, 4.28 g tetraethoxysilane (TEOS) was added drop wise, and the resulting mixture stirred for 24 hours. The resulting mixture was introduced into a polypropylene bottle and aged for 24 hours at 363 K. The solid product was filtered, washed with deionised water and dried for 48 hours under atmospheric conditions, and finally calcined in air at 773 K for 6 hours to remove the Pluronic template.

Using a “one-pot” co-condensation synthesis method, it was possible to incorporate the copolymer and organic mercaptopropylthiol, chlorosulfonylphenyl functional groups into the silica framework during precipitation as reported by Stucky and Cheng<sup>[21-24]</sup>, rather than a secondary grafting step on the pure material.

#### ❖ 2.2.2.5.b *SBA-15 propyl sulfonic acid*. One step, co-condensation synthesis<sup>[20/21/23]</sup>

In a typical synthesis procedure 4.0 g of Pluronic copolymer was dissolved in a mixture of 125 g 1.9 M HCl and 120 g deionised H<sub>2</sub>O under stirring, at 313 K. To this solution 7.69 g TEOS was added, with a pre-hydrolysis time of 45 minutes before the subsequent addition of a mixture of 0.80 g of MPTMS and 1.25 g H<sub>2</sub>O<sub>2</sub> solution (30 vol %). The resulting solution was stirred for 24 hours at 313 K and aged for 24 hours at 373 K under static conditions. The solid product was recovered by filtration, washed with a 50/50 methanol/water mix and air dried at room temperature overnight. The copolymer template was removed by reflux in ethanol for 24 hours (1.50 g solid per 400

ml ethanol). The solid products were recovered by filtration, washed with deionised water and dried at 333 K overnight.

❖ **2.2.2.5.c SBA-15 propyl sulfonic acid and phenyl functionalised.**

One step, co-condensation synthesis

Functionalization of the mesoporous silica SBA-15 was achieved in situ using an equivalent amount of PTES and MPTMS as described in section 2.2.2.5b.

❖ **2.2.2.5.d SBA-15 phenyl sulfonic acid.** One step, co-condensation synthesis<sup>[23]</sup>

The phenyl sulfonic acid functionalised SBA-15 was synthesised using the same procedure as detailed above, but with CSPTMS in place of MPTMS, and omitting the oxidation step.

❖ **2.2.2.5.e SBA-15 phenyl sulfonic acid and phenyl functionalised.**

One step, co-condensation synthesis

Functionalization of the mesoporous silica SBA-15 was achieved in situ using a equivalent amount of PTES and CSPTMS following the method as described in 2.2.2.5.b.

### **2.2.2.6 Co-condensed HMS propyl sulfonic acid**

This neutral surfactant based support was synthesised using procedures detailed in the literature by Pinnavaia and Macquarrie<sup>[25-27]</sup>. In a typical synthesis procedure, 4.0 g dodecylamine was dissolved in a mixture of ratio 3:2 (10:15 ml) water and ethanol. To this mixture, 4.0 g TEOS and 0.94 g MPTMS was added drop wise. The resulting mixture was stirred at room temperature for 24 hours, and then filtered. The amine template was extracted from the as-synthesised material with boiling ethanol (1.50 g solid per 400 ml ethanol) at 343 K for 24 hours. The solid products were recovered by filtration, washed with a 50/50 methanol/water mix and dried at 333 K overnight. The oxidation of the mercaptopropyl group to sulfonic acid was achieved by treating 1.0 g of extracted sample with 16 ml H<sub>2</sub>O<sub>2</sub> solution (33 vol %), followed by washing and

acidification with 16 ml 0.10 M H<sub>2</sub>SO<sub>4</sub>, with subsequent washing with a 50/50 methanol/water mix and drying at 333 K overnight.

The chlorosulfonylphenyl functionalised HMS material was also synthesised using the same procedure as above with CSPTMS in place of MPTMS, however only a very small yield was obtained, and therefore no discernable characterization could be achieved.

The resulting materials were characterised in terms of structure, acid site concentration and catalytic activity.

### **2.3 Summary**

The experimental methods discussed in this chapter were the actual routes used for the synthesis, functionalization and characterization of the solid acid catalysts, the results of which are detailed in Chapters 3-5.

**References:**

- [1] **Purolite ion exchange resins: CT series:** technical data sheets provided by Purolite International Ltd. [www.purolite.com](http://www.purolite.com)
- [2] **Amberlyst cationic exchange resin data sheets** provided by Rohm and Haas Ltd. [www.rohmdhaas.com/ionexchange](http://www.rohmdhaas.com/ionexchange)
- [3] **High surface area nafion resin/silica nanocomposites: A new class of solid acid catalyst.** M. A. Harmer, W. E. Farneth, Q. Sun. *J. Am. Chem. Soc.* 118, (1996), 7708-7715.
- [4] **Silica functionalised sulphonic acid groups: synthesis, characterisation and catalytic activity in acetalization and acetylation reactions.**  
S. Shylesh, S. Sharma, S. P. Mirajkar, A. P. Singh, *J. Molec. Cat A. chem*, 212, (2004), 219-228.
- [5] **Solid silica-based sulfonic acid as an efficient and recoverable interphase catalyst for selective tetrahydropyranylation of alcohols and phenols.**  
B. Karimi, M. Khalkhali, *J. Molec. Cat A. chem.* 232, (2005), 113-117.
- [6] **Acid-functionalised amorphous silica by chemical grafting-quantitative oxidation of thiol groups.**  
E. Cano-Serrano, G. Blanco-Brieva, J. M. Campos-Martin, J. L. G. Fierro, *Langmuir.* 19, (2003), 7621-7627.
- [7] **Optimal parameters for the synthesis of the mesoporous molecular sieve [Si]-MCM-41.**  
C. Cheng, D. H. Park and J. Klinowski, *J. Chem. Soc., Faraday Trans.* 93, 1, (1997), 193-197.
- [8] **Template directed synthesis of bi-funcitonalised organo-MCM-41 and phenyl MCM-48 silica mesophases.**  
S. R. Hall, C. E. Fowler, B. Lebeau, and S. Mann, *Chem. Commun.* (1999), 201-202.
- [9] **Combined alkyl and sulfonic acid functionalisation of MCM-41 type silica.**  
**Part 1: synthesis and characterization**  
I. Diaz, C. Marquez-Alvarez, F. Mohino, J. Perez-Pariente, E. Sastre. *J. Catal*, 193, (2000), 283-294.

**[10] Combined alkyl and sulfonic acid functionalisation of MCM-41 type silica.****Part 2: Esterification of Glycerol with Fatty Acids.**

I. Diaz, C. Marquez-Alvarez, F. Mohino, J. Perez-Pariente, E. Sastre. *J. Catal*, 193, (2000), 295-302.

**[11] Synthesis, characterisation and catalytic activity of MCM-41-type mesoporous silicas functionalised with sulfonic acid.**

I. Diaz, F. Mohino, J. Perez-Pariente, E. Sastre. *App. Catal A: Gen* 205, (2001), 19-30.

**[12] Synthesis of MCM-41 materials functionalised with dialkylsilane groups and their catalytic activity in the esterification of glycerol with fatty acids.**

I. Diaz, F. Mohino, J. Perez-Pariente, E. Sastre. *App. Catal A: Gen* 242, (2003), 161-169.

**[13] A novel synthesis route of well ordered, sulphur-bearing MCM-41 catalysts involving mixtures of neutral and cationic surfactants.**

I. Diaz, C. Marquez-Alvarez, F. Mohino, J. Perez-Pariente, E. Sastre. *Microporous and mesoporous materials* 44-45, (2001), 295-302.

**[14] Microwave synthesis of molecular sieve MCM-41.**

C-G. Wu. T. Bein. *Chem. Commun.* (1996), 925-926.

**[15] Rapid synthesis of mesoporous SBA-15 molecular sieve by a microwave-hydrothermal process.**

B. L. Newalkar, S. Komarneni and H. Katsuki. *Chem. Commun.* (2000), 2389-2390.

**[16] Simplified synthesis of micropore-free mesoporous silica, SBA-15, under microwave-hydrothermal conditions.**

B. L. Newalkar, S. Komarneni. *Chem. Commun.* (2002), 1774-1775.

**[17] Microwave-hydrothermal synthesis and characterisation of microporous-mesoporous disordered silica using mixed-micellar templating approach.**

B. L. Newalkar, H. Katsuki, S. Komarneni. *Microporous and Mesoporous Materials* 73, (2004), 161-170.

**[18] A study into the use of microwaves and solid acid catalysts for friedel-crafts acetylations.**

D. J. Macquarrie et al. *J. Molec. Cat A: Chem* 231, (2005), 47-51.

**[19] Preparation and characterisation of chemisorbents based on heteropolyacids supported on synthetic mesoporous carbons and silica.**

A. Lapkin et al, *Catalysis Today* 81, (2003), 611-621.

**[20] Pluronic<sup>®</sup> PE Types.**

BASF Technical Information, T1/ES 1026 e, (Nov 2002), 1-16.

**[21] Direct Syntheses of Ordered SBA-15 Mesoporous Silica Containing Sulfonic Acid Groups.**

D. Margolese, J. A. Melero, S. C. Christiansen, B. F. Chmelka, and G. D. Stucky. *Chem. Mater.* 12, (2000), 2448-2459.

**[22] Arenesulfonic acid functionalised mesoporous silica as a novel acid catalyst for the liquid phase Beckmann rearrangement of cyclohexanone oxime to  $\epsilon$ -caprolactam.**

X. Wang, C-C. Chen, S-Y. Chen, Y. Mou and S. Cheng. *Chem. Comm*, (2003).

**[23] Direct syntheses of ordered SBA-15 mesoporous materials containing arenesulfonic acid groups.**

J. A. Melero, G. D. Stucky, R. V. Grieken, G. Morales. *J. Mater. Chem.* 12, (2002), 1664-1670.

**[24] Organosulfonic acid-functionalised mesoporous silicas for the esterification of fatty acid.**

I.K. Mbaraka, D. R. Radu, V. S-Y. Lin, B. H. Shanks. *J. Catal.* 219, 2, (2003), 329-336.

**[25] Pore size modification of mesoporous HMS molecular sieve silicas with wormhole framework structures.**

T. R. Pauly and T. J. Pinnavaia. *Chem. Mater.* 13, (2001), 987-993.

**[26] Organically modified hexagonal mesoporous silicas (HMS) remarkable effect of preparation solvent on physical and chemical properties.**

D. J. Macquarrie and J.H. Clark, *J. Mater. Chem.* 11, (2001), 1843-1849.

**[27] Structure and reactivity of sol-gel sulphonic acid silicas.**

K. Wilson, A. F. Lee, D. J. Macquarrie, J. H. Clark. *App. Catal A: Gen* 228, (2002), 127-133.

# ***Chapter Three***

## ***Structural Characterization: Results and Discussion***

## Chapter 3 Catalyst Structural Characterization

### 3.1 General Overview

This chapter aims to introduce the theory behind the techniques of characterization used, and to discuss the results of this research in order to determine the physical characteristics of the solid acid catalysts. The following physical characteristics of the catalysts were analysed and compared: surface area, average pore size and distribution, long range order, and the subsequent concentration and oxidation state of the sulfur atoms in order to confirm successful acidification. The techniques used in this instance were: nitrogen adsorption, x-ray diffraction, x-ray photoelectron spectroscopy and elemental analysis. A complete summary table of all results obtained is shown in the appendix of this thesis.

### 3.2 Catalyst Physical Characterization: Techniques and Background

#### 3.2.1 Nitrogen Adsorption

Nitrogen adsorption is one of the most commonly used techniques to ascertain the surface area and pore size distribution of solid materials <sup>[1-5]</sup>. Nitrogen adsorption is a process by which a known volume of gas (adsorbate) is physisorbed onto the surface of a solid sample (adsorbent) at 77 K. The adsorbate gas (nitrogen) is added in controlled doses to the previously degassed sample, adsorbing to its surface at increasing pressures until the saturated vapour pressure of the adsorbate gas is reached. Once the saturated vapour pressure is reached, the adsorbate gas fills the pores of the sample by capillary condensation. The pressures are then reduced to evacuate the pores. The pressures, volume of gas adsorbed and desorbed are monitored and measured. Analysis of the samples occurs at constant temperature which allows the adsorption/desorption isotherm to be generated. Thus through subsequent calculations <sup>[6-8]</sup>, the surface area and pore size distribution of the sample can be determined using the **BET** method, and **BJH** method respectively. As discussed in further detail later on in this chapter.

Adsorption of a gas to a solid surface can occur in different ways, physical and chemical adsorption <sup>[9-11]</sup>.

- ❖ **Physisorption** is the non specific bonding to the surface as a result of physical attraction between the adsorbate and adsorbent molecules. These attractive forces are usually weak Van der Waals and electrostatic. Physisorption is a readily reversible process at the temperature of adsorption. Multilayer adsorption is possible due to the electrostatic forces of interaction between adsorbate molecules.
- ❖ **Chemisorption** is the specific formation of chemical bonds between the adsorbent and adsorbate molecules, with much higher energies involved due to chemical bonding. It is therefore considered irreversible at the temperature of adsorption. Only monolayer formation is considered possible due to the specific nature of the chemical bond formations.

Solid/gas systems have been shown to exhibit characteristic adsorption isotherms, of which there are six main types, first classified in 1940 by Braunauer, Deming, Deming and Teller (BDDT) and then again in 1985 by IUPAC. Figure 3.1 below shows the six different types of adsorption isotherm.

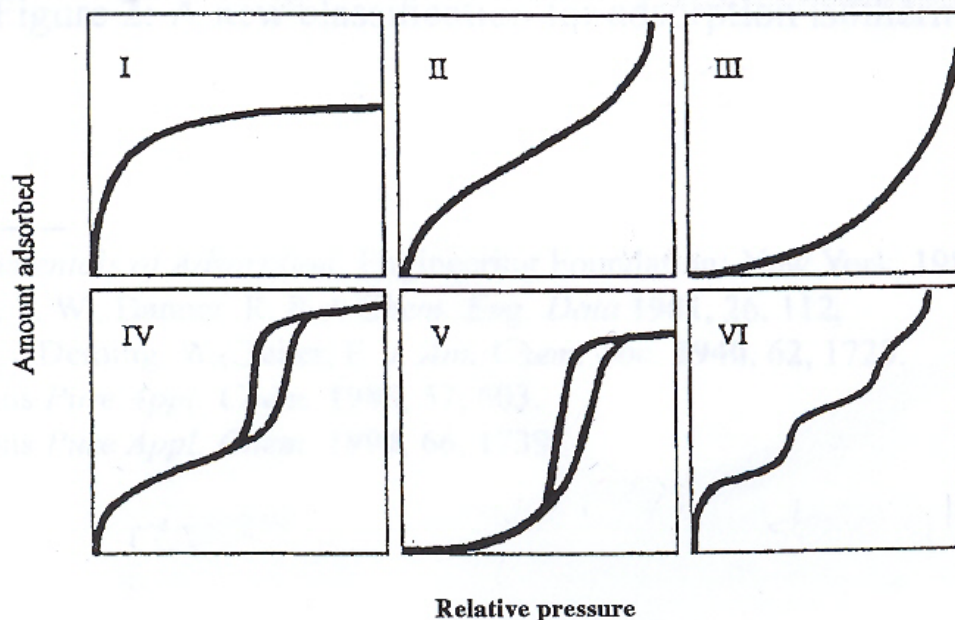


Figure 3.1 IUPAC classification of adsorption isotherms.

**Type I** adsorption isotherm is related to adsorption limited to one molecular layer. Most adsorption occurs at low pressure due to high adsorption in pores resulting from a strong interaction between pore walls and adsorbate. The plateau is due to monolayer formation from physisorption, no more adsorption is possible. This type of isotherm is most commonly observed with microporous solid materials.

**Type II** isotherm is related to multilayer adsorption most commonly observed with non porous solids. After the first monolayer is formed, increasing the pressure causes the second layer of molecules to adsorb to the first layer, until adsorption becomes complete.

**Type III** isotherm is again related to multilayer adsorption most commonly observed with non porous solids. Adsorption is difficult at low pressures with no initial uptake of gas, once the surface is filled adsorption onto monolayer to form multilayer is easier. (The adsorption interaction of adsorbate with adsorbate molecules is easier than the initial adsorbate to adsorbent).

**Type IV** isotherm is related multilayer formation with mesoporous materials. The slope increases at increasing pressure indicating an increase in the uptake of adsorbate as the pores are filled. Once the mesopores are filled, further adsorption occurs slowly on the surface.

**Type V** isotherms are uncommon yet related to type III. Adsorbent/adsorbate interactions are weak, and therefore adsorption is limited as the pores are filling.

**Type VI** isotherms are rare. The stepped isotherm represents monolayer capacity for each adsorbed layer.

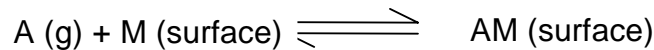
Adsorption isotherms are interpreted using two main theories, Langmuir and BET.

### ❖ **Langmuir Theory of Adsorption.**

Langmuir describes the simplest isotherm, the “Langmuir isotherm” (Type I) based on monolayer coverage using a derived equation based on the following assumptions.

- (1) Adsorption is a dynamic process.
- (2) Adsorption of gas molecules on a surface cannot exceed monolayer coverage.
- (3) All sites are equivalent and the surface is uniform.
- (4) The ability of a molecule to adsorb at a given site is independent of the surrounding sites, assuming no interactions between adsorbed molecules.

Adsorption is considered dynamic, so at equilibrium the rate of adsorption equals the rate of desorption.



When equilibrium is reached, only a fraction of the surface is considered covered by adsorbed molecules ( $\theta$ ), therefore a fraction of which is not covered is ( $1 - \theta$ ).

The rate of adsorption ( $R_a$ ) is proportional to the concentration of molecules in the gas ( $P_a$ ) and to the fraction of the surface that is vacant, where  $k_a$  is the rate constant for adsorption.

$$R_a = k_a P_a (1 - \theta)$$

The rate of desorption ( $R_d$ ) is proportional to the fraction of the surface that is covered. Where  $k_d$  is the rate constant for desorption.

$$R_d = k_d \theta$$

At equilibrium, the rate of adsorption is equal to the rate of desorption.

$$k_a P_a (1 - \theta) = k_d \theta$$

$$\left( \frac{\theta}{1 - \theta} \right) = \frac{k_a}{k_d} P_a$$

We can replace  $k_a/k_d$  with a constant **K**

Therefore

$$\frac{\theta}{1-\theta} = KP_a$$

and

$$\theta = \frac{KP_a}{1+KP_a}$$

Where coverage varies, the amount of gas adsorbed varies.  $\theta$  the fractional coverage of the gas adsorbed can be defined as

$$\theta = \frac{X}{X_m}$$

where  $X$  is the specific amount of gas adsorbed at equilibrium pressure, and  $X_m$  is the monolayer capacity.

Therefore

$$\frac{X}{X_m} = \frac{KP_a}{1+KP_a}$$

When rearranged:

$$\frac{P_a}{X} = \frac{1}{KX_m} + \frac{P_a}{X_m}$$

With a plot of  $P_a/X$  vs  $P_a$ , a straight line graph would give a gradient of  $1/X_m$ . The monolayer capacity value ( $X_m$ ) expressed in grams, can then be used to calculate the surface area of adsorbent using the known surface area occupied by a molecule of the adsorbate gas. Where  $mmm$  is the relative molecular mass of the adsorbate gas,  $N_A$  is Avagadros number, and  $A_M$  is the cross sectional area of the molecules.

$$SA = \frac{X_M}{rmm} \times N_A \times A_M$$

The Langmuir theory of adsorption has its disadvantages, one of which is that it only applies to monolayer formation and does not take into account adsorption past this level.

### ❖ BET Theory of Adsorption.

The BET theory is an extension of the Langmuir theory. BET theory extends the adsorption to multilayer adsorption, and is represented by the Type II isotherm. It is based on the following assumptions.

- (1) Enthalpy of adsorption and desorption in all layers beyond the monolayer are the same.
- (2) Rates of adsorption are the same in all layers above the monolayer and equal to the heat of condensation.
- (3) At the saturated vapour pressure, the adsorbate condenses into liquid where the number of adsorbed layers are infinite.

The derived BET equation is used to describe adsorption isotherms II and IV. Where ( $P$ ) is the vapour pressure in equilibrium, ( $P_0$ ) is the saturated vapour pressure, ( $X$ ) is the specific amount of gas adsorbed, ( $X_M$ ) is the monolayer capacity, and ( $C$ ) is a constant.

$$\frac{P}{X(P_0 - P)} = \frac{1}{X_M C} + \frac{(C - 1)}{X_M C} \times \frac{P}{P_0}$$

A plot of  $P/X(P_0 - P)$  vs  $P/P_0$  gives a straight line graph of gradient equal to  $C - 1/X_M C$  and an intercept of  $1/X_M C$ . The monolayer capacity can therefore be determined and used to calculate the BET surface area.

Nitrogen adsorption isotherms are commonly used to physically characterise mesoporous materials in terms of surface areas (via the adsorption curve of its

hysteresis loop and the calculations using the BET theory), from its desorption curve and the BJH method, it can also be used to determine pore size distributions and pore volumes of the solid materials [1-5].

### ❖ Pore Size Distribution and Pore Volume from Nitrogen Adsorption.

The effect of pores on the adsorption of the gas molecules is taken into account using the **Kelvin** equation and the **BJH** theory.

When a surface is flat, the liquid will condense when the vapour pressure of the adsorbate above the surface is equal to the saturation vapour pressure of adsorbate. Yet when the surface is porous, the liquid will condense at lower pressures because the liquid forms a curved surface within the pore.

The **Kelvin equation** relates the equilibrium vapour pressure of the adsorbate gas to the radius of curvature of the liquid surface in a cylindrical pore with which it is in equilibrium. Where  $\gamma$  is the surface tension of the condensed adsorbate,  $P_0$  is the saturated vapour pressure,  $P$  is the pressure of vapour in equilibrium with the adsorbate layer,  $r_K$  is the radius of curvature of the surface,  $V$  is the molar volume of the liquid adsorbate,  $R$  is the universal gas constant,  $T$  is the temperature and  $\theta$  is the contact angle between the adsorbate and the pore walls:

$$\ln \frac{P}{P_0} = -\frac{2V\gamma}{r_K RT} \times \cos \theta.$$

If the contact angle is zero, the radius of the liquid surface is equal to the radius of the pore.

$$\ln \frac{P}{P_0} = \frac{2V\gamma}{r_K RT}$$

Therefore vapour will condense in small pores at low pressures, and in large pores at higher pressures. By measuring the amount of liquid that condenses on the solid at a particular pressure, the Kelvin equation can be used to calculate the pore volume in pores of particular radii. However the radius of the condensed vapour meniscus is

smaller than the diameter of the pore wall as there is already a film of liquid present, and this is not taken into account using the Kelvin equation.

The **BJH** method is the most commonly used method for the determination of pore size distributions of mesoporous solids. This method uses the Kelvin equation to determine the distribution of mesopores in a solid, but allows for the pore being slightly larger than the meniscus due to the presence of the film of liquid. The desorption part of the hysteresis loop is used for this calculation.

### 3.2.2 Powder X-Ray Diffraction

Powder X-ray diffraction is a versatile, non destructive technique used to analyse the characteristic 3-dimensional structure of a solid crystalline sample <sup>[13]</sup>. The finely ground sample is placed onto a sample holder on a rotating platform. Both the X-ray generator and detector rotate around the plane of the sample. The generated X-rays hit the sample and diffract. The intensity of the reflected beam is measured as a function of incident (and reflected) angle, and recorded by the detector.

A crystalline solid consists of a repeating array of atoms. The distance (*d*) between the layers of atoms is characteristic of each individual solid, thus a distinctive XRD pattern is generated. When a monochromatic beam of X-rays (at an incident angle  $\theta$  to the solid) hits the sample, each atom diffracts the beam in different directions. If the solid consists of a regular repeating array of atoms, constructive interference of the X-ray beams occurs as shown in Figure 3.2. Constructive interference is detected at incident and reflected angles of  $\theta$  when the distance between scattering centres are of the same magnitude as the wavelength of radiation. Then the distance (*d*) between the reflecting plane of atoms can be determined using Bragg's equation where  $\theta$  is the angle of diffraction,  $\lambda$  is the wavelength of the incident beam, and *n* is the number of beams diffracted. The most intense reflection is when  $n=1$ .

$$n\lambda = 2d \sin \theta$$

*The Bragg's Law Equation*

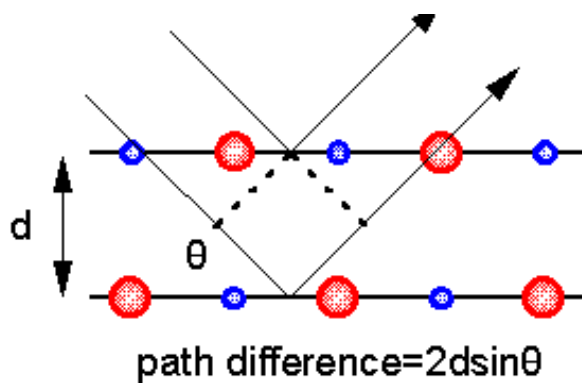


Figure 3.2 Schematic of X-ray electron diffraction on a crystal sample in XRD

For each crystal structure there is a number of sets of planes from which diffraction of the x-ray beam can occur. Each set of planes reflects at a characteristic angle. The generated x-ray diffraction plot of intensity of reflection vs  $2\theta$  gives a characteristic diffraction pattern for each crystalline structure.

Each set of planes in an ordered crystalline material is described by a set of Miller indices ( $h, k, l$ ). These refer to the frequency with which the planes intercept the  $x, y,$  and  $z$  axes relative to the dimension of the unit cell. The strongest reflection in a powder X-ray diffraction patterns tends to be “low angle reflection” from planes with low or zero values for  $h, k$  and  $l$  [14].

Powder X-ray diffraction is the most common method used to characterise the long range order of the ordered materials for example MCM-41 and SBA-15 [1-5]. Their regular repeating hexagonal framework is shown by the presence of characteristic reflections from 100, 110, 200, and 210 planes. A decrease in the long range order of the structure is indicated by the broadening of the 100 reflections, the minor reflections at 110, 200 and 210 planes may well disappear altogether. It is important to note here that the value of  $d$  determined using Bragg's equation from the 100 reflections is directly related to the size of the unit cell and hence is related to the pore size in the mesoporous molecular sieves.

### 3.2.3 Elemental Analysis

The percentage hydrogen, carbon, nitrogen and sulfur content were established using elemental analysis by Medac Ltd. In elemental analysis, the percentage C, H, N and S content are obtained by combustion analysis, whereby the organic sample is combusted in a flow of pure oxygen, the resultant gases all trapped separately and analysed. This was performed by Medac Ltd using a CE-440 and Carlo Erba elemental analysers. In the case of mesoporous materials, this technique was used to analyse the elemental composition of the samples in order to determine how the surface groups were bound, and thus help theorise on the resultant acidity and catalytic activity of the materials.

### 3.2.4 X-Ray Photoelectron Spectroscopy (XPS)

Further sulfur analysis on some samples was completed by Dr Karen Wilson using a KRATOS AXIS HSi XPS instrument at the University of York.

XPS is a spectroscopic surface science technique that characterises the chemical and electronic state of each of the elements on the surface of the sample, as well as the uniformity of its surface chemical composition.

The instrumentation consists of an x-ray source for the monochromatic x-rays, an electron collection lens, and an electron detector which measures the kinetic energy of the excited electrons. The process is conducted under ultra high vacuum conditions. The x-ray beam is generated by diffracting and focussing a beam of non monochromatic x-rays off a crystalline quartz disc. The x-ray beam irradiates and excites the electrons in the inner shells of the atoms on the surface of the sample. This irradiation provides the electron with the energy required to escape from its orbital, otherwise known as the binding energy, any excess energy appears as kinetic energy. The kinetic energy is measured by the detector and the binding energy calculated. An XPS spectrum plots the number of electrons detected against the binding energies. Each element on the surface produces a characteristic plot of XPS peaks at characteristic binding energy values, therefore enabling the direct identification of each element.

The binding energies are unique to the chemical environment of the atom, and therefore XPS is very useful in identifying the oxidation state of an atom on the surface. In the case of mesoporous materials, this technique was used to analyse the environment of the

sulfur atoms present, in particular to differentiate between sulfur as SO<sub>3</sub>H and as thiol (SH).

### **3.3 Catalyst Physical Characterization: Experimental**

#### **3.3.1 Powder X-Ray Diffraction measurements**

The X-Ray diffraction patterns of the ordered mesoporous molecular sieve materials were obtained with a BRUKER AXS D8 ADVANCE instrument, using CuK $\alpha$  ( $\lambda=1.5452\text{\AA}$ ) radiation. The finely ground powders were scanned over a  $2\theta$  range =  $0.70^\circ$  to  $10.0^\circ$  in  $0.020^\circ$  steps. The diffraction patterns were recorded and plotted as peak height vs  $2\theta$  scale using the DIFFRAC<sup>plus</sup> software package.

#### **3.3.2 Porosity Measurements**

The surface areas, and pore size distributions of all samples were characterised using nitrogen adsorption at 77 K using a COULTER OMNISOORB SA3100 instrument. The silicas were degassed for two hours at 423 K. The subsequently generated adsorption isotherm was used to calculate the BET surface area, and using the BJH method from the desorption isotherm the pore size distribution was determined.

#### **3.3.3 Elemental analysis characterization**

Both standard elemental analysis and X-ray photoelectron spectroscopy (XPS) were conducted on the samples. The percentage hydrogen, carbon, nitrogen and sulfur content were established using elemental analysis by Medac Ltd. Further data on sulfur content on some samples was completed by Dr Karen Wilson using a KRATOS AXIS HSi XPS instrument at the University of York.

#### **3.3.4 Concentration of acid groups, by conventional titration**

General purpose laboratory equipment was used for these experiments. In a typical experiment, 0.05 g of catalyst (resin, or the as-synthesised inorganic silicas and functionalised silicas) was suspended in water, excess NaCl was added. Using phenolphthalein indicator, standardised 0.005M NaOH solution was titrated into the acidic solution with vigorous stirring. From the equivalence point the concentration of the acid on each catalyst was determined (in  $\text{mmol g}^{-1}$ ).

### 3.4 Catalyst Physical Characterization Results and Discussion

This section aims to show the results obtained from the structural characterization of the synthesised materials

#### 3.4.1 Polymer Supported Sulfonic Acid Resins

##### ❖ Sulfonated Poly(styrene-co-divinylbenzene) Resins

This type of polymeric supported acid exists in the form of small uniformly sized beads, and can be sulfonated to give concentrations of acid sites (up to 5.33 mequiv g<sup>-1</sup>). The resin beads (provided by Purolite International Ltd) used in this study were of the gel type (C100H) and the macroporous type (SP 21/15, Amberlyst 15 [provided by Rohm and Haas Ltd], CT175, CT275) in nature. The C100H gel resin and the CT175 macroporous resin contain approximately stoichiometric levels of sulfonation (one sulfonic acid group per DVB or styrene monomer unit). The SP21/15 macroporous resin is partially sulfonated, to a level less than normal stoichiometric sulfonation. The CT275 macroporous resin is sulfonated to a level greater than normal stoichiometric sulfonation (known as “persulfonated”).

##### ❖ Fluorinated Sulfonated Polymer Resins

The fluorinated polymer resin sulfonic acid Nafion (provided by E. I. Du Pont de Nemours and Co. Inc) exists in the form of small uniformly sized polymer beads and has been sulfonated to give an acid site concentration of 0.8 mequiv g<sup>-1</sup>. In the commercially available Nafion silica composite (SAC-13), the Nafion polymer (obtained from Sigma-Aldrich) is supported on amorphous silica gel, and is 13% w/w Nafion. The fluorinated Nafion resin is regarded to possess a high acid strength, being referred to as possibly “superacidic”.

Acid site concentration data were provided by the manufacturers. Nitrogen adsorption experiments were not carried out on these materials because they are known to possess relatively low surface areas (at less than 40 m<sup>2</sup> g<sup>-1</sup>). The resins were characterised in terms of acidity and catalytic activity (detailed later in chapters 4 and 5).

### 3.4.2 Sulfonated Silica Gels. Grafting route

These silica gel supports were functionalised by the grafting route, whereby functionalization, oxidation and acidification of the supported thiol groups are performed on a porous silica support. The silica was functionalised with both propyl (3-mercaptopropyltrimethoxysilane MPTMS) sulfonic acid and phenyl (2-(4-chlorosulfonylphenyl)ethyltrimethoxysilane CSPTMS) sulfonic acid precursor tethers and also an additional non acidic hydrophobic group (phenyltriethoxysilane PTES). The oxidation of the starting thiol groups and subsequent acidification steps were varied, along with initial pre-treatment of the silica support. The silica supported sulfonic acids were characterised using nitrogen adsorption, elemental analysis and by manual titration. The results were as follows.

#### ❖ Pre-treated silica

The as-supplied silica support (EP116 provided by Ineos Chemicals Ltd) after drying was subjected to pre-treatments in the hope that they would activate the surface towards functionalization reaction with methoxy groups, and so yield higher ultimate acid loadings. The silica was kept in a dessicator at all times to keep it dry. As detailed in Chapter Two, there were two types of pre-treatment applied to the silica supports in an effort to enhance susceptibility to functionalization. In the first the silica was dehydrated for 10 hours in an oven at 423K and then added to the toluene solution without exposure to moisture. In the second the silica was refluxed in 6M HCl for 24 hours, and then dried in an oven at 333K overnight. In a typical synthesis, (after pre-treatment if it was applied) the amorphous silica was refluxed in toluene with the 3-mercaptopropyltrimethoxysilane sulfonic acid precursor. The materials were then oxidised with hydrogen peroxide solution and acidified with 0.10M sulfuric acid. Following functionalization and conversion of thiol and acid chloride groups to sulfonic acid, [the acid site concentrations were measured by titration with 0.005M NaOH in water with phenolphthalein indicator and the results are shown below in Table 3.1].

Pre-treatment	Sulfonic acid loading (mmolg <sup>-1</sup> ) acid sites
Drying for 10 hours at 423K	0.36 ± 0.02
6M HCl for 24 hours at room temperature	0.38 ± 0.02
Normal synthesis (no pre-treatment)	0.36 ± 0.02

*Table 3.1 Dependence of sulfonic acid loading of the propyl sulfonic acid functionalised silica gels on the pre-treatment of the silica support. The values are expressed as an average of triplicate data sources.*

It appears that the pre-treatments of the silica had no significant effect on the sulfonic acid loading, the materials surface susceptibility to functionalization has not been increased. This may be due to the action of a pre-treatment, and not in-situ when the material is functionalised. Or that the silane functional groups remain partially resistant to oxidation and acidification through inaccessibility, and thus yield a comparable sulfonic acid loading to the non pre-treated materials.

Therefore for the remaining syntheses, no pre-treatment was used.

### ❖ Propyl sulfonic acid functionalised silica gel, optimisation of oxidation/acidification conditions

Based on standard synthesis conditions as noted in Chapter Two, a typical synthesis consisted of 1.5g of the amorphous silica and 3.58g of the 3-mercaptopropyltrimethoxysilane. In attempts to refine the synthesis procedure, both oxidation and acidification steps were varied, and the resultant acid site concentrations analysed by manual titration. The standard synthesis volume of 33% hydrogen peroxide, and the 0.1 M concentration of sulfuric acid used was varied as recommended in the published method being followed. The results are shown in Table 3.2 below, indicating the various synthesis conditions.

H <sub>2</sub> O <sub>2</sub> Solution (33%). Volume used (ml)	H <sub>2</sub> SO <sub>4</sub> solution. Concentration used (M)	Sulfonic acid loading (mmolg <sup>-1</sup> ) acid sites
16	0.1	0.36 ± 0.02
80	0.1	0.25 ± 0.02
16	0.5	0.32 ± 0.02
16	1.0	0.25 ± 0.02
16	2.0	0.35 ± 0.02

*Table 3.2 Dependence of sulfonic acid loading (mmolg<sup>-1</sup> acid sites) of propyl sulfonic acid silica gels. The values are expressed as averages of triplicate data sources.*

From the Table 3.2, increasing the volume of hydrogen peroxide solution used in the oxidation step had no positive effect on the resulting sulfonic acid loading of the sample. Therefore the volume of the hydrogen peroxide solution used was maintained at 16 ml for further synthesis procedures. Increasing the concentration of sulfuric acid did not increase the observed acid loadings significantly. Therefore the initial 0.1 M acidification step was maintained for all further syntheses.

As an alternative method for functionalising the silica, a comparison between the standard grafting technique and another published method which relied on establishing incipient wetness when treating the silica with the solution of grafting agent.

### ❖ Functionalised silica gel – Incipient wetness route

Based on standard synthesis conditions as noted in Chapter Two, a typical synthesis of the propyl functionalised material consisted of 1.5 g of the amorphous silica and 3.58 g of the 3-mercaptopropyltrimethoxysilane sulfonic acid tether. These solutions were added until incipient wetness was observed. After subsequent oxidation with hydrogen peroxide at both room temperature and 100°C, and acidification with 0.1M sulfuric acid at room temperature, followed by washing and drying, the material was ready for analysis. The higher temperature is thought to increase the effectiveness of the oxidation step. The results appear in Table 3.3 below.

Sample	Sulfonic Acid Loading (mmol <sup>g</sup> <sup>-1</sup> acid sites)
SiO <sub>2</sub> -propylSO <sub>3</sub> H (Room temp oxidation)	0.17 ± 0.03
SiO <sub>2</sub> -propylSO <sub>3</sub> H (100°C oxidation)	0.35 ± 0.03
Normal synthesis (no pre-treatment, room temp oxidation)	0.36 ± 0.02

*Table 3.3 Sulfonic Acid Loading (mmol<sup>g</sup><sup>-1</sup> acid sites) of the silicas prepared by the Incipient wetness technique. The values are expressed as averages for triplicate data sources.*

As demonstrated when comparing the values in Table 3.3, the incipient wetness technique does not significantly increase the sulfonic acid loading of the solid acid catalysts when compared to the standard grafting synthesis route at room temperature. Increasing the oxidation temperature during the incipient wetness synthesis route also has no discernable effect on the sulfonic acid loadings of the samples when compared to the standard synthesis route at room temperature. However using the incipient wetness technique the sulfonic acid loadings of the samples oxidised at room temperature were much less when compared to the standard grafting synthesis, yet increasing the temperature doubled the loadings. The question remains as to whether oxidising at 100°C would affect the standard grafting synthesis route in the same way.

Therefore for the standard syntheses the method as described below was used for all further syntheses.

With the optimum synthesis conditions now established for the standard grafting route, it was necessary to reproduce and structurally characterise the functionalised silica gels in terms of sulfonic acid loading, surface area, pore size and distribution. The results were as follows.

#### ❖ Functionalised silica gel – grafting route

In Table 3.4 below, the acid loadings for the three types of functionalised silica gel which were used for this study are shown. The first, SiO<sub>2</sub>-propylSO<sub>3</sub>H was prepared using optimised conditions with the MPTMS propyl thiol tether. The second, phenyl-SiO<sub>2</sub>-propylSO<sub>3</sub>H, was prepared by grafting with MPTMS propyl thiol and, at the same time, the non acidic hydrophobic phenyl group PTES tether. The third, SiO<sub>2</sub>-

phenylSO<sub>3</sub>H, was prepared by grafting with the CSPTMS phenyl tether. The fourth material planned for this study, with phenyl sulfonic acid functionalised plus phenyl functional groups, was made but yields were low and insufficient for effective characterization and catalytic testing.

Sample	Sulfonic Acid Loading (mmolg <sup>-1</sup> acid sites)
SiO <sub>2</sub> -propylSO <sub>3</sub> H	0.36 ± 0.02
phenyl-SiO <sub>2</sub> -propylSO <sub>3</sub> H	0.52 ± 0.02
SiO <sub>2</sub> -phenylSO <sub>3</sub> H	0.72 ± 0.03

*Table 3.4 Sulfonic Acid Loading (mmolg<sup>-1</sup> acid sites) of the propyl, phenyl and co-functionalised Sulfonated Silica Gels. The values are expressed as averages for triplicate data sources.*

It is worth noting that these grafting experiments were performed a number of times and the samples with which this data is associated were the best produced in reasonable yields. Subsequent experiments were based on these optimal samples of sulfonic acid functionalised silicas. This approach of “picking the best” was not adopted earlier when optimising synthesis conditions, so acid loadings quoted for those experiments tend to be lower.

Figures 3.3-3.5 below show the nitrogen adsorption/desorption isotherms at 77 K for the three materials. The generated data was used to calculate the BET surface areas from the adsorption isotherms and, from the BJH method, the pore size distributions from the desorption isotherms. The results summary is shown in Table 3.5 below.

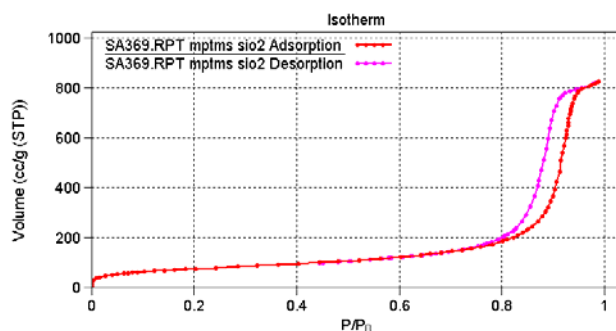


*Figure 3.3 Nitrogen adsorption/desorption isotherms for SiO<sub>2</sub>-propylSO<sub>3</sub>H*

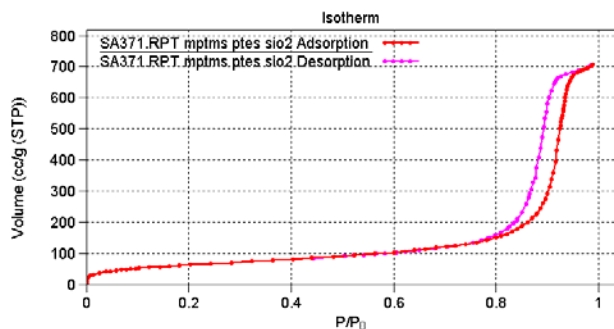


Figure 3.4 Nitrogen adsorption/desorption isotherms for phenyl-SiO<sub>2</sub>-propylSO<sub>3</sub>H

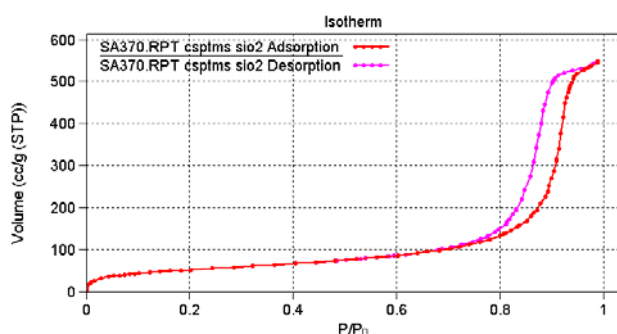


Figure 3.5 Nitrogen adsorption/desorption isotherms for SiO<sub>2</sub>-phenylSO<sub>3</sub>H

Sample	Sulfonic Acid Loading (mmol g <sup>-1</sup> acid sites)	BET Surface Area (m <sup>2</sup> g <sup>-1</sup> )	Average Pore Diameter (nm)	Pore Volume (cm <sup>3</sup> g <sup>-1</sup> )
Unfunctionalised SiO <sub>2</sub>	0.0	324	19.9	2.01
SiO <sub>2</sub> -propylSO <sub>3</sub> H	0.36 ± 0.02	271	16.8	1.39
phenyl-SiO <sub>2</sub> -propylSO <sub>3</sub> H	0.52 ± 0.02	232	17.6	1.19
SiO <sub>2</sub> -phenylSO <sub>3</sub> H	0.72 ± 0.03	191	15.4	0.95

Table 3.5 Physical properties of the Sulfonated Silica Gels.

From Figures 3.3-3.5 the isotherms all possess the ‘S’ shape indicative of a mesoporous material. From Table 3.5, it is evident that functionalization of the material decreases surface area and pore volume which is consistent with the idea that a bulky functional group reduces pore size upon inclusion. Furthermore the average pore diameters are lower for the functionalised materials.

After the sulfonic acid loading of the material and its porosity were determined, elemental analysis was performed to ascertain how the tether was bound within the bulk of the material and, later, XPS to determine the amount of sulfonic acid present on the external surface of the silica support, and to further confirm the sulfonic acid loading data.

Table 3.6 shows the results obtained from elemental analysis of the sulfonated silica gels. The carbon to sulfur molar ratios were determined. This ratio gives an indication of the binding mode of the tether to the silica support. There are three ways in which the silane could be bound to the SiO<sub>2</sub> surface, through condensation of one, two or all three methoxy groups with surface silanol groups. As shown in Figures 3.6 – 3.9 below the carbon/sulfur molar ratios would be 5/1, 4/1 and 3/1 for the mercaptopropyltrimethoxysilane tether, and 10/1, 9/1 and 8/1 for the chlorosulfonylphenyltrimethoxysilane tether for the three binding modes.

Further analysis of the samples using XPS to determine the oxidation state of the sulfur and hence gives an indication to the extent of which it is converted to sulfonic acid. Separate signals for sulfur as thiol (SH) and sulfur as sulfonic acid (SO<sub>3</sub>H) can be integrated to give its relative concentration of the two forms.

### MPTMS

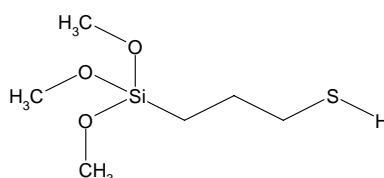
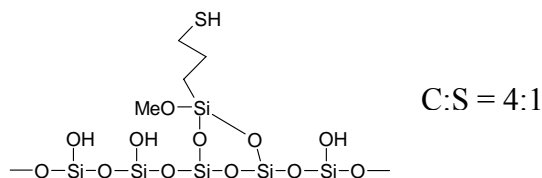
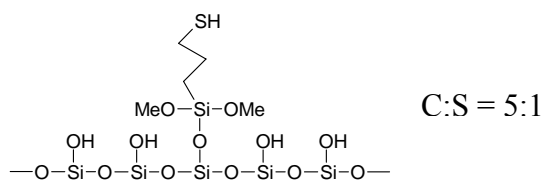


Figure 3.6 3-Mercaptopropyltrimethoxysilane (MPTMS)



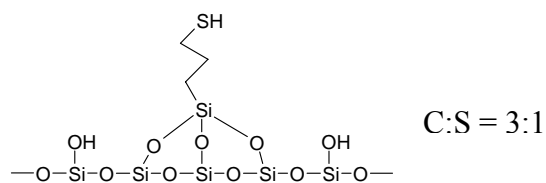


Figure 3.7 Possible binding modes of MPTMS on silica.

### CSPTMS

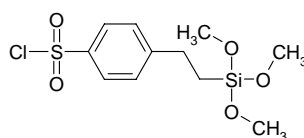
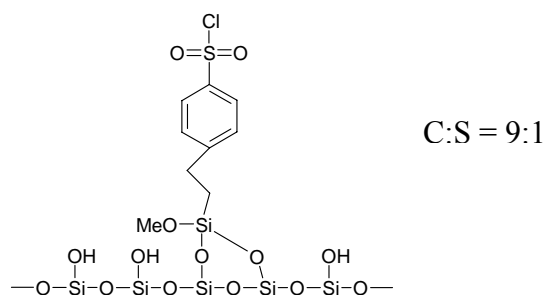
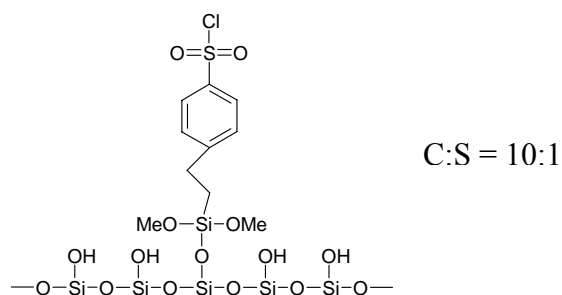


Figure 3.8 2-(4-chlorosulfonylphenyl)ethyltrimethoxysilane (CSPTMS)



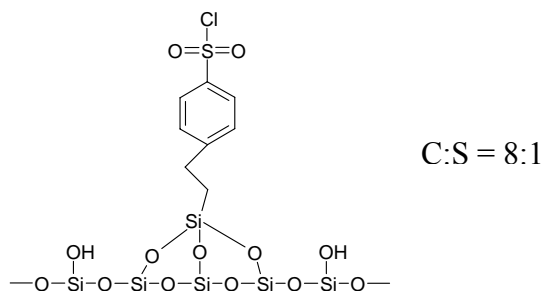


Figure 3.9 Possible binding modes of CSPTMS on silica.

It is worth noting at this point, that the bi-functionalised (with additional non acidic phenyl group) materials were analysed by elemental analysis, but due to the nature of the two tethers present it is impossible to assume how each is bound due to the possible variations, and therefore how many carbon atoms are detected. It is also worth noting that the phenyl functionalised materials were not analysed using XPS, because the technique would not be able to distinguish between the sulfur atom present in the sulfonyl chloride ( $\text{SO}_2\text{Cl}$ ) and the sulfonic acid ( $\text{SO}_3\text{H}$ ) forms, giving a resolved band for one, not two as the oxidation state of the sulfur atom is the same.

Tables 3.6 below shows the results obtained from sulfur and carbon analysis of the sulfonated silica gels, by comparing with the acid site concentration data by titration, the overall the percentage Sulfur in  $\text{SO}_3\text{H}$  form in the bulk of the material is given.

Sample	Sulfonic Acid Loading ( $\text{mmol g}^{-1}$ acid sites)	% S in $\text{SO}_3\text{H}$ form in the bulk	Molar C:S ratio
$\text{SiO}_2$ -propyl $\text{SO}_3\text{H}$	$0.36 \pm 0.02$	48	4.01 : 1
phenyl- $\text{SiO}_2$ -propyl $\text{SO}_3\text{H}$	$0.52 \pm 0.02$	56	N/A
$\text{SiO}_2$ -phenyl $\text{SO}_3\text{H}$	$0.72 \pm 0.03$	69	7.57 : 1

Table 3.6 Elemental analysis data of the Sulfonated Silica Gels.

In the three materials prepared for this study, the acid sites for the propyl functionalised materials (presumably sulfuric acid sites) account for 48 and 56 % of the total sulfur

added as tethered thiol groups. Therefore 52 and 44 % of the then thiol groups have resisted either oxidation or acidification. The most obvious explanation for this surprisingly high concentration of residual thiol groups may be linked to limited accessibility of the groups to peroxide and acid, possibly due to restricted access within the pores from the molecule itself, or from synthesis the functional group becomes inaccessible as is buried within the bulk of the material. However, it was anticipated that a possible advantage of the grafting route might be that surface thiol groups would virtually all, by definition, be accessible for further reaction. This was confirmed by XPS data (shown in Table 3.7 below) where 74 and 84 % of the sulfur was converted on the surface of the particles. This result and relatively poor conversion of thiol to acid within the bulk of the material was disappointing.

For the material prepared from the thionyl chloride precursor (CSPTMS), the percentage of sulfur eventually converted to sulfonic acid is much higher at almost 70 %. The hydrolysis reaction converting the chloride to acid is clearly more facile than that required for thiol conversion. It seems likely that it is this difference in reactivity of the thionyl chloride compared to the thiol that explains the different conversions and that is less to do with functional group accessibility. If this is the case then it would be worth investigating other, more effective ways of converting tethered thiol groups to sulfonic acid for future work.

With XPS measurements it was possible determine the percentage of sulfur in sulfonic acid form on the surface of the material, thus making a suitable comparison against that observed in the bulk of the material from elemental analysis. Table 3.7 below compares the results obtained.

Sample	Sulfonic Acid Loading (mmolg <sup>-1</sup> acid sites)	% S in SO <sub>3</sub> H form in the bulk (E.A)	% S in SO <sub>3</sub> H form on surface (XPS)
SiO <sub>2</sub> -propylSO <sub>3</sub> H	0.36 ± 0.02	48	74
phenyl-SiO <sub>2</sub> -propylSO <sub>3</sub> H	0.51 ± 0.02	56	84

*Table 3.7 Comparison of the data obtained of the Sulfonated Silica Gels derived from elemental analysis and XPS.*

The phenyl functionalised material demonstrates the higher percentage of sulfur in sulfonic acid form on the surface and within the bulk of the material in comparison to its propyl counterpart. The percentage of sulfur in sulfonic acid form is greater on the surface than within the bulk in both of the materials highlighted above, which was to be expected as the materials were oxidised and acidified after the fact.

In summary from the structural data obtained for the **sulfonated silica gels**, it seems by using the grafting method, the silica support has been successfully functionalised with the MPTMS, CSPTMS and the additional non acidic PTES tethers, and furthermore, successfully converted to sulfonic acid with loadings in the region of 0.36-0.71mmolg<sup>-1</sup>, and sulfur present in the form of sulfonic acid on the surface in the high percentiles. It is worth noting that when compared to the sulfonated polystyrene resins, this sulfonic acid loading is low (as they demonstrate an average 4.9mmolg<sup>-1</sup> acid loading).

However, as the objective of this research was to compare the observed structural characteristics, acidities / catalytic activities of sulfonic acid functionalised on different supports, the sulfonated silica gels made by the grafting method offered a suitable basis for comparison with the next type of supported sulfonic acid.

### **3.4.3 Sulfonated Mesoporous Molecular Sieve Silicas (Co-condensation route)**

The sulfonated mesoporous molecular sieve silicas were synthesised utilising the “one pot” co-condensation route, whereby the sulfonic acid precursor thiol groups are incorporated into the solid matrix. The mesoporous silicas were functionalised with both MPTMS, CSPTMS tethers, and an additional phenyl group tether (PTES).

The surfactant templates used control the type of mesoporous silica produced. The neutral surfactant dodecylamine 98% produced the silica **HMS**, and the ionic surfactants cetyltrimethylammonium bromide (C<sub>16</sub>TAB) and dodecyltrimethylammonium bromide (C<sub>12</sub>TAB) were used in the synthesis of **MCM-41**. Those synthesised using the poly(ethylene oxide, propylene oxide) triblock

copolymer Pluronic PE 10400 (BASF), were denoted **SBA-15**. (The typical syntheses of these materials are described in chapter two).

Of the samples produced, each of the three different types MCM-41, SBA-15 and HMS with their corresponding different tethers were synthesised many times and the best of which (highest acid loading) were selected for complete characterization.

These selected co-condensed sulfonated mesoporous silicas were characterised in terms of structure, using X-ray diffraction, nitrogen adsorption, elemental analysis, XPS and by manual titration. Each sample was tested in triplicate (in the cases where there was not an ample amount to test thoroughly, the samples were pooled).

Of these materials a *selected few* were chosen (shown in Table 3.8 below) as a typical illustration of functionalization of this type of support. The characterization results of which are shown later in this section.

Table 3.8 below shows the sulfonic acid loadings of the functionalised mesoporous silicas determined by titration with 0.005M sodium hydroxide solution, and nitrogen adsorption data indicating the physical properties of the materials.

The nitrogen adsorption isotherms from which this data was derived appear later in this chapter.

Sample	Sulfonic Acid Loading (mmol g <sup>-1</sup> acid sites)	BET Surface Area (m <sup>2</sup> g <sup>-1</sup> )	Average Pore Diameter (nm)	Pore Volume (cm <sup>3</sup> g <sup>-1</sup> )
Pure MCM-41	0	638	3.42	0.69
MCM41-propylSO <sub>3</sub> H	1.09 ± 0.05	301	-	-
MCM41-phenylSO <sub>3</sub> H	0.40 ± 0.03	301.7	3.63	0.176
Pure SBA-15	0	612	8.59	0.38
SBA-propylSO <sub>3</sub> H	0.56 ± 0.01	438.5	10.33	0.56
SBA-phenylSO <sub>3</sub> H	0.67 ± 0.01	385	15.78	0.94

*Table 3.8 Physical properties of the selected co-condensed sulfonated mesoporous molecular sieve silicas.*

In a general trend, for the sulfonated mesoporous molecular sieve silicas, the surface areas decrease with the level of functionalization of the materials. The pore volume also decreases as expected with functionalization, and the pore diameter increases as expected which is consistent with the idea that a bulky functional group reduces pore volume upon inclusion. There appears to be no real difference in the difference in physical properties between the propyl and phenyl functional group tethers. The selected materials demonstrated a mesoporous pore size based on the “S” shape of the resultant nitrogen isotherms.

Specifically the propylSO<sub>3</sub>H functionalised **MCM-41** demonstrated the highest sulfonic acid loading of all the synthesised materials, prepared both by grafting and by the co-condensation routes. The addition of the non acidic phenyl group along with the propyl sulfonic acid group (in order to increase the hydrophobicity of the synthesised material) appears to decrease the overall concentration of acid sites and an increase in surface area when compared to the propyl/phenyl alone functionalised materials.

The PhenylSO<sub>3</sub>H functionalised **SBA-15** material demonstrated the slightly highest sulfonic acid loading of its group, with the addition of the non acidic phenyl group again causing a decrease in sulfonic acid loading but an increase in overall surface area when compared to the propyl or phenyl functionalised materials.

The propylSO<sub>3</sub>H functionalised **HMS** only demonstrated an average value for sulfonic acid loading and surface area when compared to its counterparts and was discounted from further characterization due to lack of reproducibility during synthesis.

With the exception of propyl-MCM41, the acid loadings of the co-condensed mesoporous materials are comparable to the grafted silicas.

Bulk elemental analysis of the co-condensed materials for carbon and sulfur yielded the results shown in Table 3.9 below.

The elemental analysis data in Table 3.9 below also gives an indication to the amount of SO<sub>3</sub>H present within the bulk of the material. Further analysis of the samples using XPS determines which form the sulfur atom has adopted and gives an indication of the amount of SO<sub>3</sub>H present on the external surface of the material, thereby allowing a

comparison of support, tether and bulk/surface SO<sub>3</sub>H presence. Table 3.10 below shows the XPS results obtained.

It is important to note that only a select few were chosen to illustrate the results observed of the differing supports.

Sample	Sulfonic Acid Loading (mmolg <sup>-1</sup> acid sites)	% S in SO <sub>3</sub> H form in the bulk (E.A)	Molar C:S ratio
MCM41-propylSO <sub>3</sub> H	1.09 ± 0.05	47.4	4.31 : 1
MCM41-phenylSO <sub>3</sub> H	0.40 ± 0.03	35.5	10.48 : 1
SBA-propylSO <sub>3</sub> H	0.53 ± 0.01	51.4	9.05 : 1
SBA-phenylSO <sub>3</sub> H	0.67 ± 0.01	85.9	13.39 : 1

*Table 3.9 Elemental analysis data of the Selected Sulfonated Mesoporous Molecular Sieve Silicas.*

Sample	Sulfonic Acid Loading (mmolg <sup>-1</sup> acid sites)	% S in SO <sub>3</sub> H form in the bulk (E.A)	% S in SO <sub>3</sub> H form on surface (XPS)
MCM41-propylSO <sub>3</sub> H	1.09 ± 0.05	47.4	75.0
SBA-propylSO <sub>3</sub> H	0.53 ± 0.01	51.4	53.6

*Table 3.10 Comparison of the data obtained of the Selected Sulfonated Mesoporous Molecular Sieve Silicas derived from elemental analysis and XPS.*

With the propyl functionalised MCM-41 and SBA-15, acid sites within the bulk account for 47 and 51 % of the total sulfur added indicating 53 and 49 % remains resistant to conversion to sulfonic acid. These co-condensed materials with a high percentage of sulfur still remaining resistant to conversion, as with sulfonated silicas it must again be assumed there is limited accessibility to the thiol groups or they are simply more

awkward to convert. As the material is co-condensed it is assumed the thiol groups would be dispersed relatively uniformly throughout the material, yet the data from XPS (shown in Table 3.11 below) demonstrates a higher percentage of sulfur in sulfonic acid form on the surface, indicating when synthesised the functional group tethers must align with the surface of the material.

With the phenyl functionalised MCM-41 and SBA-15, acid sites within the bulk account for surprisingly 35 and 86 % of the total sulfur added, a much lower and also much higher amount than their propyl functionalised counterparts. With the higher percentage conversion to sulfonic acid within the bulk, it must be assumed the larger phenyl tether is more accessible or its thionyl chloride group is more readily converted.

In comparison to the grafted propyl-silica samples, the co-condensed propyl-materials show a slightly decreased percentage of sulfonic acid on the surface but comparable amounts within the bulk which was unexpected, as co-condensed would imply functionalization would occur within the material as oppose to its surface. The exact results of which are shown in Table 3.11 below.

Sample	Sulfonic Acid Loading (mmolg <sup>-1</sup> acid sites)	% S in SO <sub>3</sub> H form in the bulk	% S in SO <sub>3</sub> H form on surface
MCM41-propylSO <sub>3</sub> H	1.09 ± 0.05	47.4	75.0
SBA-propylSO <sub>3</sub> H	0.53 ± 0.01	51.4	53.6
SiO <sub>2</sub> -propylSO <sub>3</sub> H	0.36 ± 0.02	48.0	74.0
phenyl-SiO <sub>2</sub> -propylSO <sub>3</sub> H	0.51 ± 0.02	56.0	84.0

*Table 3.11 Overall comparison of the data obtained of the Selected Sulfonated Mesoporous Silicas and the Sulfonated Silicas derived from elemental analysis and XPS.*

The powder X-ray diffraction patterns obtained from the selected synthesised mesoporous materials are shown below; accompanied with nitrogen adsorption/desorption isotherms.

Figure 3.10 below shows the powder XRD pattern recorded for a siliceous un-functionalised MCM-41 sample prepared by the synthesis route described earlier in this chapter. It shows intense and well resolved reflections assigned to the 100, 110 and 210 planes. This pattern is typical of MCM-41 made in this way and indicates the structure has good long range order. The 100 reflection at  $1.00^\circ$  corresponds to a  $d_{100}$  of 4.78nm. The nitrogen adsorption isotherm shows a sharp rise at  $P/P^0$  between 0.4 and 0.5 in both adsorption and desorption, with some hysteresis. Note that there is a discontinuity in the desorption isotherm at about  $P/P^0$  of 0.4 but this is due to an instrumental artefact and can be ignored. The surface area (BET) calculated from the adsorption branch is  $638 \text{ m}^2 \text{ g}^{-1}$ , again typical of MCM-41. The pore size distribution calculated using the BJH method, while not shown, gives a well defined maximum in pore size at pore diameter of 3.42 nm, with an overall pore volume (in pores of diameter greater than 0.2 nm) of  $0.69 \text{ cm}^3 \text{ g}^{-1}$ . This again is typical. The difference between the 100 spacing and the pore diameter gives an indication of the pore wall thickness. This XRD and the  $\text{N}_2$  data will be used as a baseline with which equivalent data collected on the sulfonic acid functionalised MCM-41 materials will be compared.

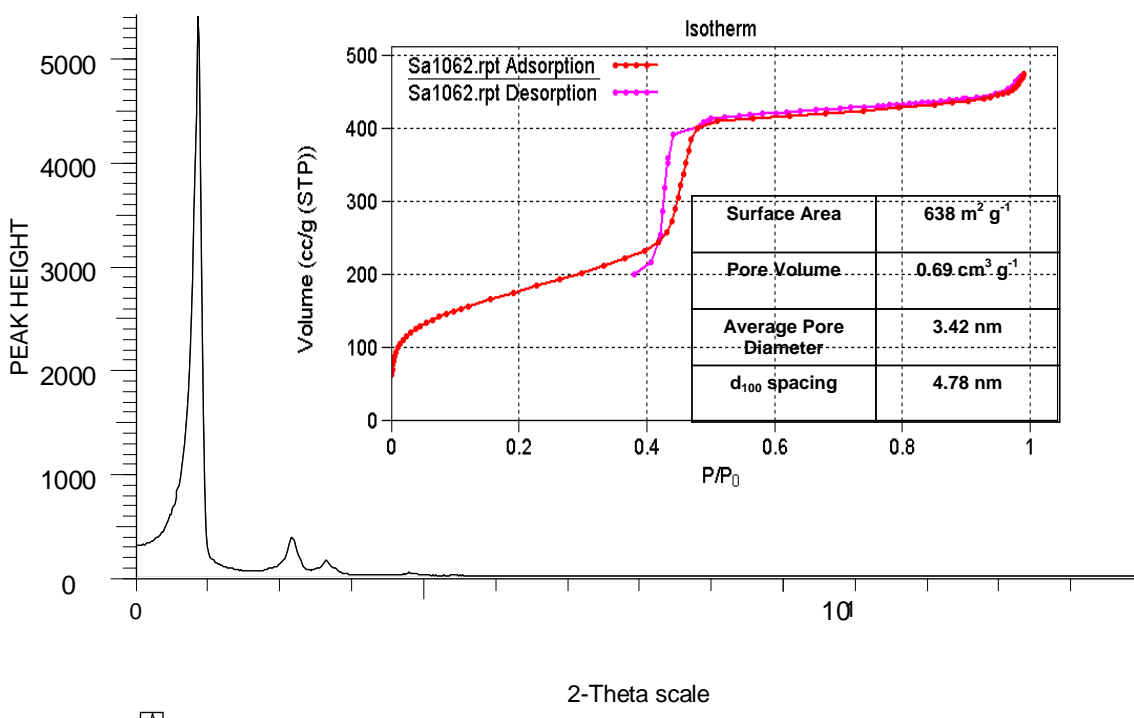


Figure 3.10 X-ray diffraction pattern and Nitrogen adsorption/desorption isotherms for Pure MCM41

Attempts to synthesise the same materials were made using microwave, rather than conventional heating, on the basis that this might be beneficial when preparing functionalised MCM-41 as has been reported in the literature. Details were given in chapter 2. In fact, even though several attempts using various heating times were made, the XRD patterns of the co-condensed MCM-41 products were invariably poor, suggesting that little if any of the required ordered materials were produced. This could be attributed to problems during synthesis or to characterisation equipment error.

Sulfonic acid functionalization of MCM-41 was carried out by the co-condensation route, incorporating tethered propylthiol MPTMS (which then required oxidation and acidification) and tethered phenylsulfonylchloride CSPTMS (which then required hydrolysis to the acid form).

A typical powder XRD and N<sub>2</sub> adsorption/desorption isotherm for nominally MCM-41-propylSO<sub>3</sub>H is not shown as no reasonable visual data was obtained despite several attempts, indicating it may be amorphous in nature.

When attempts to prepare the same MCM41-propylSO<sub>3</sub>H using microwave heating were tried, similar results were obtained, producing even weaker powder XRD patterns.

After functionalization with the phenyl propyl tether CSPTMS, and subsequent acidification, a typical powder XRD and N<sub>2</sub> adsorption/desorption isotherms are shown in Figure 3.11 for MCM-41-phenylSO<sub>3</sub>H. The XRD shows an intense reflection at low angle (less than 1.00°) assigned to the 100 planes, but no further peaks as seen with pure MCM material. The XRD pattern indicates a reasonable long range order and the isotherms give a surface area of 301.7 m<sup>2</sup> g<sup>-1</sup> and a pore size maximum at diameter 3.63 nm with a pore volume of 0.176 cm<sup>3</sup> g<sup>-1</sup>. The resultant shape of the isotherm is not indicative however of a mesoporous material, despite the pore volume demonstrating a mesoporous size.

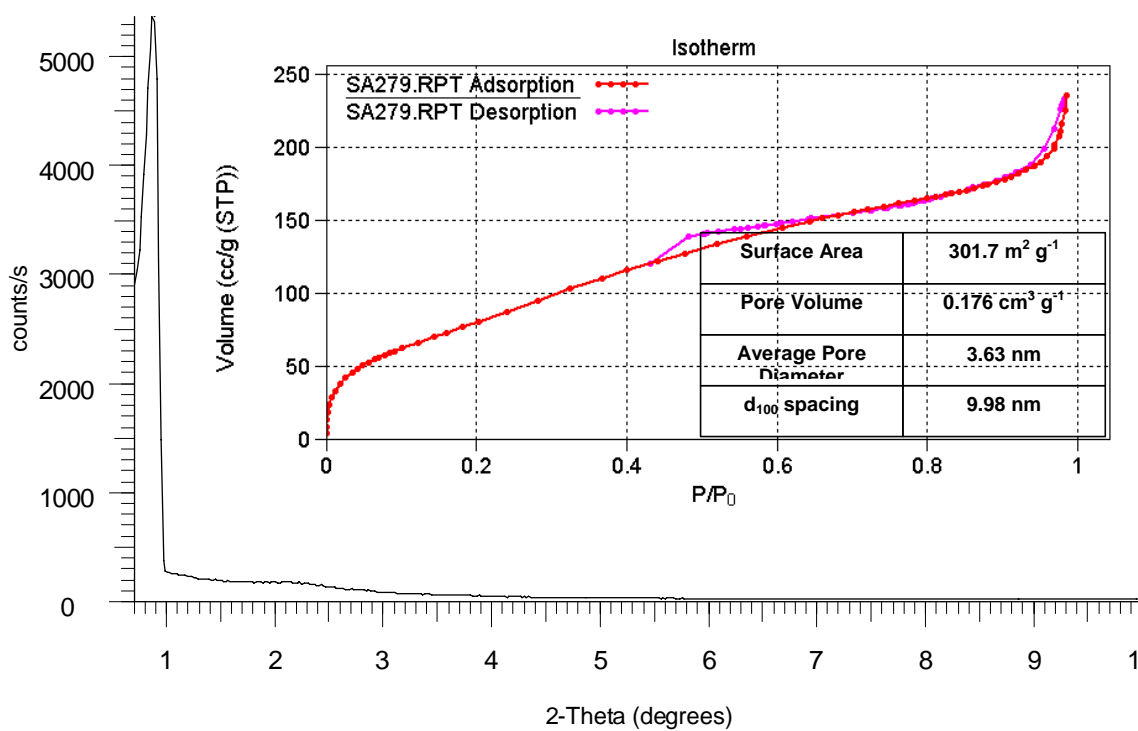


Figure 3.11 X-ray diffraction pattern and Nitrogen adsorption/desorption isotherms for MCM41-PhenylSO<sub>3</sub>H

The other ordered mesoporous molecular sieve material on which this study has been based is SBA-15. As above, the first data to show is that for the siliceous SBA-15 prepared using the published method and with no added functional groups. Figure 3.12 shows the powder XRD pattern and N<sub>2</sub> adsorption/desorption isotherms for this material.

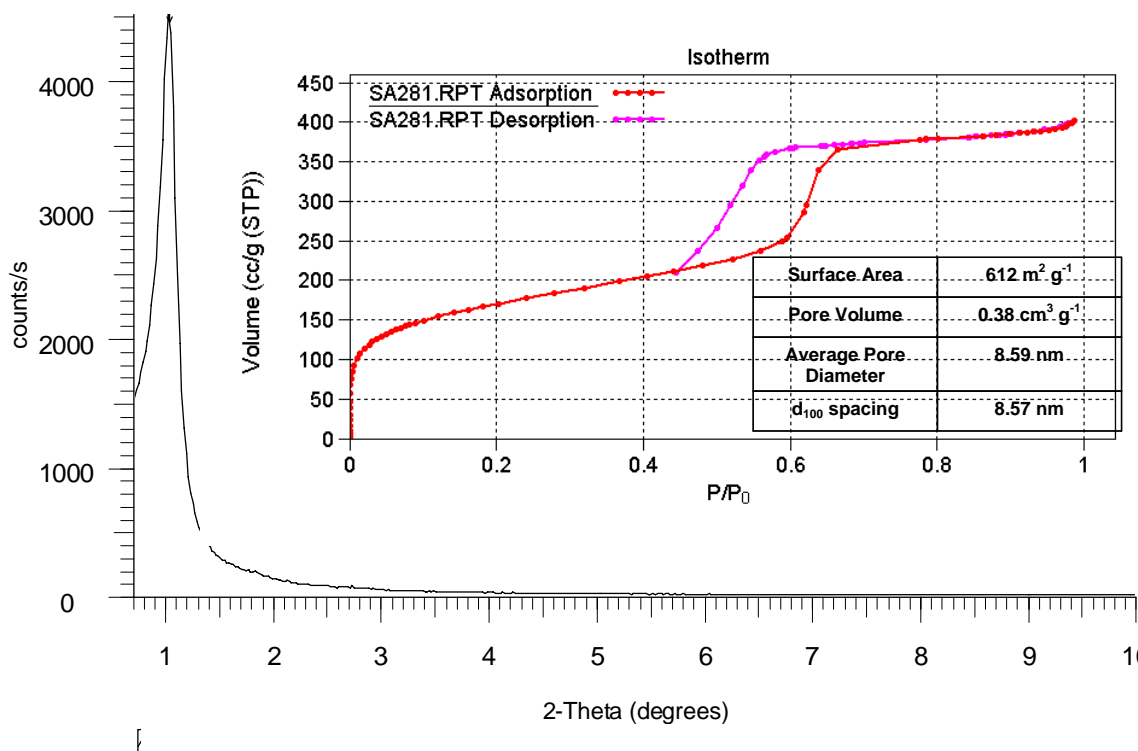


Figure 3.12 X-ray diffraction pattern and Nitrogen adsorption/desorption isotherms for Pure SBA

The isotherms show steps at around  $P/P^0$  of 0.6 indicative of larger pores than MCM-41 and the XRD pattern shows an intense reflection at low angle (less than  $1.00^\circ$ ) assigned to the 100 plane. This data is all typical of that published for SBA-15. The XRD pattern indicates good long range order and the isotherms give a surface area of  $612 \text{ m}^2 \text{ g}^{-1}$  and a pore size maximum at diameter 8.59 nm with a pore volume of  $0.38 \text{ cm}^3 \text{ g}^{-1}$ .

Attempts to synthesise siliceous SBA-15 using microwave heating was unsuccessful, yielding an XRD pattern with no identifiable reflections.

Combining mercaptopropyltrimethoxysilane (MPTMS) in a co-condensation synthesis, oxidising and acidifying, gave materials with equally good XRD patterns (a typical pattern is shown in Figure 3.13).

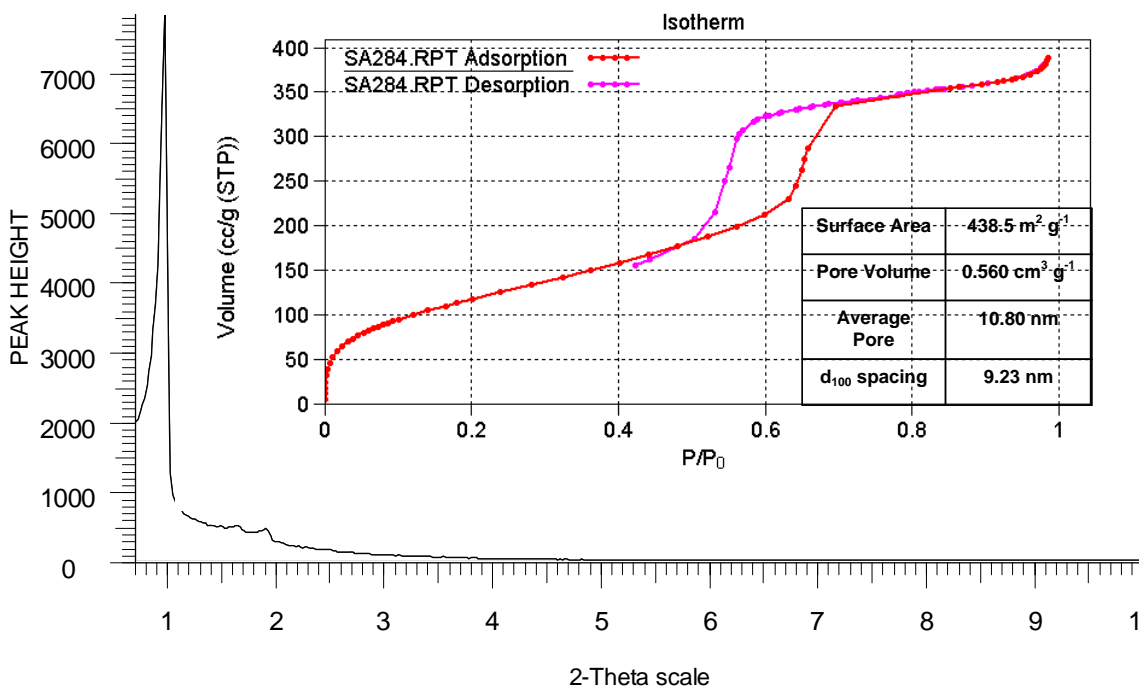


Figure 3.13 X-Ray diffraction pattern and Nitrogen adsorption/desorption isotherms for SBA-PropylSO<sub>3</sub>H

The N<sub>2</sub> adsorption/desorption isotherm shows a step corresponding to adsorption in/desorption from mesopores. This SBA-15-propylSO<sub>3</sub>H has a surface area of 438.5 m<sup>2</sup> g<sup>-1</sup>, a pore volume of 0.56 cm<sup>3</sup> g<sup>-1</sup>, and a pore size distribution with a maximum at pore diameter of 10.80 nm. This is consistent with an SBA-15 silica structure in which pore volume and pore size is reduced by the presence of functional sulfonic acid groups, tethered to the surface by alkyl chains.

It is worth noting here that performing the same co-condensation synthesis of SBA-15-propylSO<sub>3</sub>H using microwave rather than conventional heating surprisingly resulted in a material with a stronger and better defined powder XRD pattern (Figure 3.14).

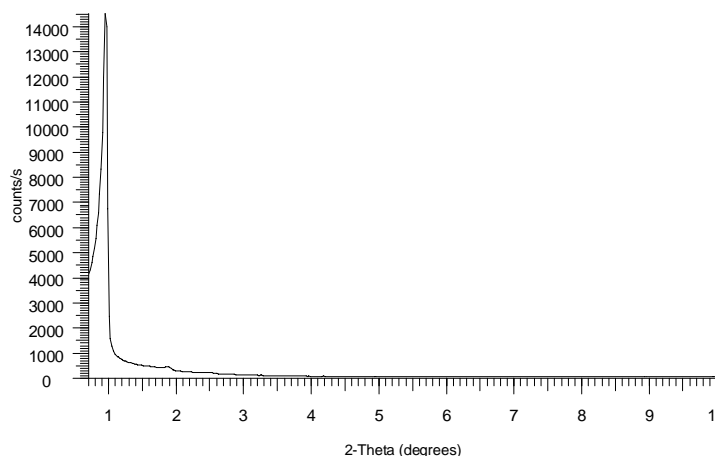


Figure 3.14 X-Ray diffraction pattern for Microwave SBA-PropylSO<sub>3</sub>H (20 hours)

Despite this “one-off” material that seemed to benefit from microwave heating, all other materials for which microwave and conventional heating were compared showed conventional heating to lead to more highly ordered materials. For this reason syntheses reported from here on have used conventional heating.

Upon functionalization with the phenyl sulfonic acid group, as demonstrated in Figure 3.15 below, the SBA-15 material is ordered, demonstrating a reasonably sharp, intense peak at the 100 plane, and two weak reflections at the 100 and 200 peak locations. Its adsorption/desorption isotherm resembles the Type IV “S” shape which is indicative of a mesoporous material. Again the pore size distribution data obtained defines this material as mesoporous in nature with an average pore diameter of 7.01 nm.

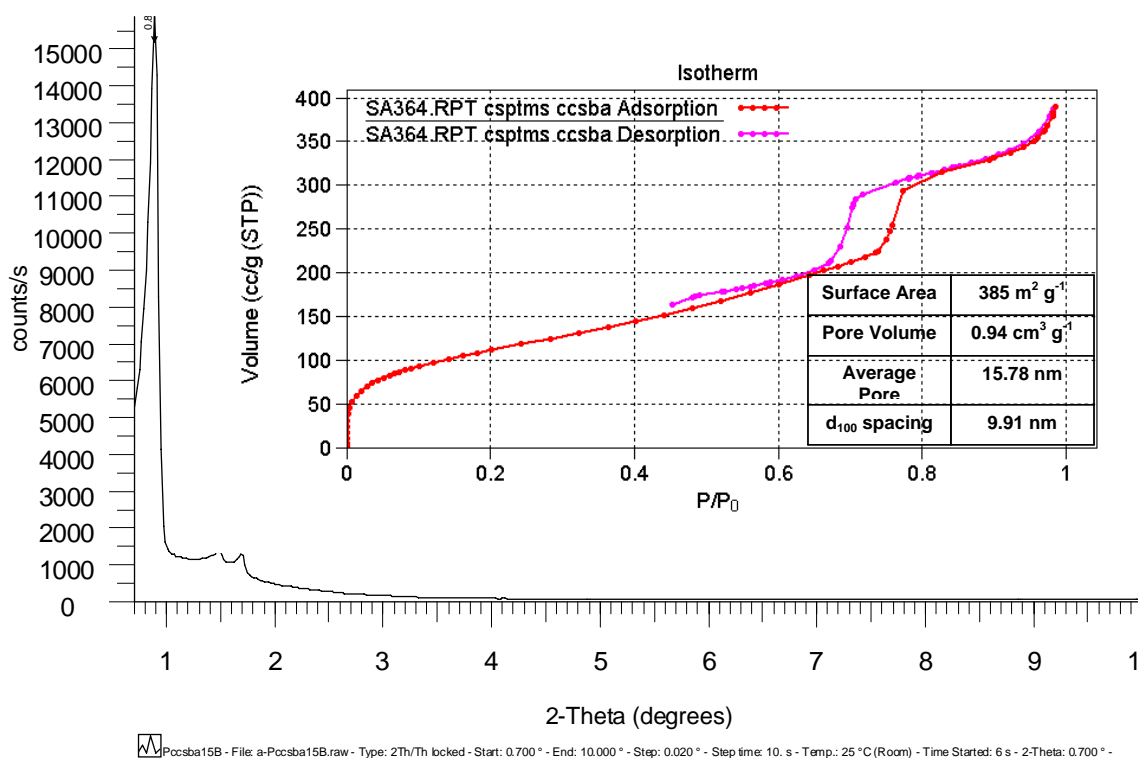


Figure 3.15 X-Ray diffraction pattern and Nitrogen adsorption/desorption isotherms for SBA-PhenylSO<sub>3</sub>H

The N<sub>2</sub> adsorption/desorption isotherm shows a smaller step corresponding to adsorption in/desorption from mesopores. This SBA-15-phenylSO<sub>3</sub>H has a surface area of 385 m<sup>2</sup> g<sup>-1</sup>, a pore volume of 0.94 cm<sup>3</sup> g<sup>-1</sup>, and a pore size distribution with a maximum at pore diameter of 15.78 nm. This is consistent with an SBA-15 silica structure in which pore volume and pore size is reduced by the presence of functional sulfonic acid groups, tethered to the surface by alkyl chains.

### 3.5 Summary

The solid acid catalysts were characterised in terms of physical properties using the following techniques;

- I. Nitrogen adsorption.** Gives information on surface areas, pore sizes and distributions.
- II. Powder X-Ray Diffraction.** Provides information on the three dimensional structure and long range order of the samples.
- III. Elemental analysis.** Provides information on mass percentage of carbon, hydrogen and sulfur, in order to determine if the synthesised materials have been successfully functionalised. **XPS** analyses the environment of the sulfur atom in order to determine if it has been successfully acidified.
- IV. Base Adsorption Calorimetry in the liquid phase.** Measures the concentration of acid sites via heats of adsorption measurements from the neutralization reaction of base to solid material in varying solvents.
- V. Base Adsorption Calorimetry in the gas phase.** Measures the concentration of acid sites via heats of adsorption measurements of the base gas to the solid material in the absence of solvents.
- VI. Catalytic Activity Reaction; Isomerization of  $\alpha$ -pinene using GC.** Measures the activity of the solid material in a sample reaction.

From the structural data obtained for the synthesised samples, with both grafted **sulfonated silica gels** and the co-condensed **sulfonated mesoporous silicas**, each support type has been successfully functionalised with the propylSO<sub>3</sub>H MPTMS, and phenylSO<sub>3</sub>H CSPTMS and the additional non acidic phenyl PTES tethers, and furthermore successfully oxidised and acidified to give sulfonic acid loadings in the region of 0.36-1.09 mmolg<sup>-1</sup>. Both synthesis routes produced materials within the mesoporous range and with structural order. The accompanying adsorption/desorption isotherms are very distinctive of a mesoporous material with a type IV 'S' shape loop. This data is in accordance with that found in the literature for these materials.<sup>[1-5]</sup>

The results reported here show that the derived sulfonic acid loadings of the silica supports are similar despite the use of grafting and co-condensation for synthesis. However the commercially available polystyrene and Nafion resins loadings are significantly higher.

Pore size determination does verify that after functionalization in both synthesised types of support (compared to the pure unfunctionalised material) the pore size does indeed decrease along with the surface area, which is consistent with the idea that a bulky functional group reduces pore size upon inclusion.

Elemental analysis and XPS show both grafted and co-condensed supports to possess sulfonic acid in both the bulk and the majority on the surface of the materials. Both grafted and co-condensed materials demonstrated comparable amounts of sulfonic acid. It was notably unusual that the co-condensed materials contained a higher percentage of sulfur in the sulfuric acid form on the surface compared to its bulk which would have been expected due to the nature of its synthesis.

In both synthesis routes a reasonable percentage of the silane groups remained resistant to conversion, indicating not all groups were accessible to oxidation/acidification.

Altering the functional group tether from propyl to phenyl sulfonic acid or the addition of the extra phenyl group made no discernable difference between the synthesised samples, with the exception of the highest observed sulfonic acid loading on the propylSO<sub>3</sub>H MCM-41 in comparison to the other synthesised materials.

However in comparison the commercially available polystyrene resins are still more viable as solid acid catalysts due to their high sulfonic acid loadings (4.9 mmol g<sup>-1</sup> compared to 1.08 mmol g<sup>-1</sup> at highest).

After comparing the three types of support structurally, the next objective was to compare their acidity and catalytic activity using techniques IV-VI summarised above.

**References:****[1] Solid acid catalysts,**

A. Corma, *Current Opinion in Solid State and Materials Science*, 2, 1, (Feb 1997), 63-75.

**[2] From Microporous to Mesoporous Molecular Sieve Materials and Their Use in Catalysis.**

Avelino Coma. *Chem. Rev.* 97, (1997), 2373-2419.

**[3] Inorganic Solid Acids and Their Use in Acid-Catalysed Hydrocarbon Reactions.**

A. Corma. *Chem. Rev.* 95, (1995), 559-614.

**[4] What do we know about the acidity of solid acids?**

R. J. Gorte. *Cat. Lett.* 62, (1999), 1-13.

**[5] Solid Acids and bases as catalysts**

I. Arends, R. Sheldon, U. Hanefeld. *Green chemistry and catalysis*, Wiley-VCH, (2007), 49-90.

**[6] SA3100 Nitrogen adsorption technical information.**

[www.beckmancoulter.com](http://www.beckmancoulter.com)

**[7] SA3100 Nitrogen adsorption principles of operation.**

[www.beckmancoulter.com](http://www.beckmancoulter.com)

**[8] SA3100 Nitrogen adsorption calculations.**

[www.beckmancoulter.com](http://www.beckmancoulter.com)

**[9] Physical Chemistry, Atkins, 7<sup>th</sup> edition, 240-266.****[10] Physical Chemistry, Laidler, Meiser, 3<sup>rd</sup> edition, 456-459.****[11] Physical Organic Chemistry, Neil Isaacs, 2<sup>nd</sup> edition.****[12] CRC Rubber Handbook of Physics and Chemistry**

80<sup>th</sup> Edition, D. R. Lide, (1999-2000).

**[13] Basics of X-ray diffraction.**

H. Stanjek, W. Hausler. *Hyperfine interactions*. 15, (2004), 107-119.

**[14] Surfaces**

G. Attard and C. Barnes. *Oxford Chemistry Primers*, 59, (1998).

# ***Chapter Four***

## ***Acidity Measurements: Results and Discussion***

---

## Chapter 4 Acidity Measurements

### 4.1 General Overview

This chapter aims to introduce the theory behind surface acidity and the techniques used to measure it. In the second section, as the primary technique used in this research, Base Adsorption Calorimetry will be discussed in detail including the experimental routes followed and the results of the characterised supports discussed. A complete summary table of all results obtained is shown in the appendix of this thesis.

### 4.2 Introduction and Background to Surface Acidity

With the extensive use of solid acid catalysts in industry today, the concentration, strength, nature and accessibility of the acid sites are crucial in controlling catalyst properties, in order to specifically tailor the physical properties of a catalyst to the individual reactions requirements. Before the acidity of the solid acid catalyst can be related to its catalytic performance, the relative strength of the surface acid sites present must be determined and characterised. There are several known techniques that have been used and reviewed in various literatures <sup>[1-5]</sup> that will be further discussed in this chapter.

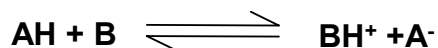
The catalytic properties of a solid acid catalyst also need to be considered: its lifetime, thermal stability, regeneration capabilities, and possible leaching and poisoning tendencies.

#### 4.2.1 Surface Acidity

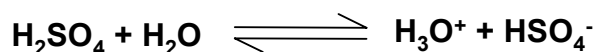
Solid acid catalysts are characterised in terms of acidity by the presence of both Brønsted and Lewis acid sites on their surfaces.

##### ❖ Brønsted Acidity

A Brønsted acid is a substance which has the ability to donate a proton <sup>[6-7]</sup>. As represented in the equation below, the Brønsted acid **AH** is the proton donor, the Brønsted base **B** is the proton acceptor. **BH<sup>+</sup>** is the conjugate acid of base **B** (the species formed when a proton has been gained). And **A<sup>-</sup>** is the conjugate base of acid **AH** (the species formed after a proton is lost).



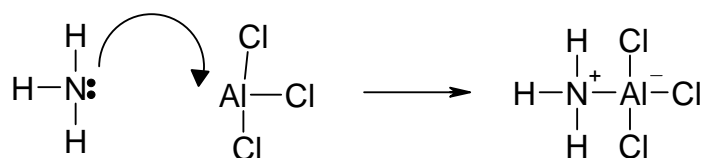
Sulfuric acid  $\text{H}_2\text{SO}_4$  is an example of a Brønsted acid, and in the following example reaction, water is acting as the Brønsted base.



Brønsted acidity in solid acids typically arises from the exchange of  $\text{H}^+$  ions associated with anionic sites on the solid, which in this project are the most relevant.

### ❖ Lewis Acidity

A Lewis acid is a substance which has the ability to accept an electron pair<sup>[6-7]</sup>. As represented in the schematic below using the most commonly used Lewis acid in industry, aluminium chloride  $\text{AlCl}_3$ , the Lewis base  $:\text{NH}_3$  is the electron donor, and the Lewis acid  $\text{AlCl}_3$  is the electron pair acceptor. Aluminium chloride acts as a good Lewis acid, because it contains only 6 electrons in the outermost shell of the Al atom, and can therefore readily accept an electron pair.



Lewis acidity typically arises in zeolites and clays when they have been ion exchanged with high charge to radius metal cations which, in the absence of water, may be powerful electron acceptors. Many other sites on typical solid acids behave as Lewis acids but it is worth mentioning that Lewis acids tend to react with water when present to become a Brønsted acid site. Thus in the characterization of solid acid catalysts in this particular project, Lewis acidity is not the most relevant.

### 4.3 Methods of characterization of surface acidity <sup>[1-5]</sup>

#### 4.3.1 Titration Methods

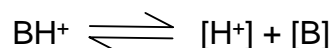
The quantitative measurement of all the acidic properties of a solid acid catalyst is difficult. The simplest and most commonly used method of acid site determination for solid acid catalysts involves the use of a suitable colour indicator adsorbed onto its surface.

In dilute aqueous media, the relative strength of an acid can be measured using the **pH scale**. This scale assumes the strength of individual  $\text{H}_3\text{O}^+$  ions to be fixed. The pH of a solution is expressed below, where  $[\text{H}_3\text{O}^+]$  is the concentration, and  $a_{\text{H}^+}$  is the activity of the hydronium ions. The acid/base pH scale varies from 0 (pure 1.0 M HCl) to 14 (1.0 M NaOH).

$$\text{pH} = -\log [\text{H}_3\text{O}^+]$$

or strictly:  $\text{pH} = -\log a_{[\text{H}_3\text{O}^+]}$

However in strong acid media the colour indicator driven pH scale is extrapolated to cover the assumption that the strength of  $\text{H}_3\text{O}^+$  ions are not fixed. This extended scale is called the **Hammett Acidity scale ( $H_0$ )**. The Hammett acidity function  $H_0$  is related to the degree of transformation of a weakly basic indicator **B** into its conjugate acid **BH<sup>+</sup>**.



$$K_a = \frac{a_{\text{H}^+} \times a_{\text{B}}}{a_{\text{BH}^+}}$$

$$\text{p}K_a = -\log \frac{a_{\text{H}^+} \times a_{\text{B}}}{a_{\text{BH}^+}}$$

Hammett defined the acidity function  $H_0$  as  $\text{p}K_a - \log \frac{[\text{BH}^+]}{[\text{B}]}$

In dilute solutions the concentration of conjugate acid  $[BH^+]$  is equal to the activity of the conjugate acid  $a_{BH^+}$ , and the concentration of base  $[B]$  is equal to the activity of the base  $a_B$ . Therefore the Hammett acidity function is equal to the pH.

$$H_0 = -\log a_{H^+} = pH$$

However, in concentrated solutions this is not the case. In heterogeneous systems, **Hammett acidity indicators** can be used to ascertain the pKa value of a solid acid ( $BH^+$ ) in the system, by adsorbing onto the surface of the solid, and the solid adopting its colour. Each Hammett indicator has a known pKa value, and exhibits different colours when in the protonated and unprotonated forms, as demonstrated in Table 4.1 below. In a typical experiment each Hammett indicator in a dilute benzene solution is added to the surface of the solid acid catalyst. The indicator is adsorbed onto the surface of the solid and adopts the colour of the conjugate acid if the acid sites  $H_0$  is lower than that of the indicators. Titration of the solution with a suitable strong base to its endpoint allows the determination of the concentration of acid sites with a lower pKa/ $H_0$  than the indicator.

Indicators	Colour in Basic Form	Colour in Acidic Form	pKa	Equivalent (H <sub>2</sub> SO <sub>4</sub> %)
Natural Red	Yellow	Red	+6.8	8*10 <sup>-8</sup>
Methyl Red	Yellow	Red	+4.8	
Phenylazonaphthylamine	Yellow	Red	+4.0	5*10 <sup>-5</sup>
p-(dimethylamino)azobenzene	Yellow	Red	+3.3	3*10 <sup>-4</sup>
2-amino-5-azotoluene	Yellow	Red	+2.0	5*10 <sup>-3</sup>
Benzeneazodiphenylamine	Yellow	Purple	+1.5	2*10 <sup>-2</sup>
Crystal Violet	Blue	Yellow	+0.8	0.1
p-nitrobenzeneazo(p-nitrodiphenylamine)	Orange	Purple	+0.43	
Dicinnamalacetone	Yellow	Red	-3.0	48
Benzalacetophenone	Colourless	Yellow	-5.6	71
Anthraquinone	Colourless	Yellow	-8.2	90
2,4,6-trinitroaniline	Colourless	Yellow	-10.10	90

Table 4.1 Commonly used Hammett Indicators

Despite the relative ease of use of this system, it is not without its limitations. Detecting the colour change of the Hammett indicator is not always easy. The solid surface itself may hide any colour changes, and in addition the indicators may not be able to access all the acid sites present thereby providing inaccurate values.

### 4.3.2 Thermal Characterization Methods <sup>[1-5]</sup>

#### ❖ Calorimetric Titration

The base adsorption calorimetry technique is widely regarded as the most reproducible thermochemical method for the measurement of the concentration of acid sites on a solid acid and their relative strengths <sup>[8-13]</sup>, from the direct determination of the heats of adsorption of basic probe molecules. This technique has proven successful with acidic zeolites and ammonia, leading to extensive experimentation by Auroux et al to use calorimetry to distinguish between the physisorbed and chemisorbed sites <sup>[10-13]</sup>.

Ammonia and pyridine vapour have been successfully used to determine the number of acid sites and their relative strength on zeolites and on other solid acids <sup>[13/14]</sup>, as reported by Gorte et al the thermochemical cycle below was used to justify the relationship between the molar heat of adsorption of ammonia and acid strength <sup>[17]</sup>. It is also possible to titrate acid sites with a probe base compound in solution. Typically, a liquid base probe solution at an equilibrated temperature is dosed into the system in aliquots. Any heat changes as a direct result of the addition of base is measured in the form of a pulse, and integrated. Once the reaction is complete, the dosing ceases. The calorimetric data is represented via plots of molar enthalpy of adsorption against extent of reaction. This technique offers the direct evaluation of the abundance and relative strength of acid sites. It cannot however be used to distinguish between the different types of acid site. The heat measured on the addition of base is also not the precise action of a proton transfer, but a combination of proton transfer from the base to the acid site, and the proton affinity of the base, and the heat of interaction of the resulting ion-pair. Relating the data to catalytic activity is also complicated, as there is no guarantee that the acid sites to which the base is adsorbed are catalytically active.

However this technique is the primary technique used in the course of the research documented here, and is discussed further in this chapter.

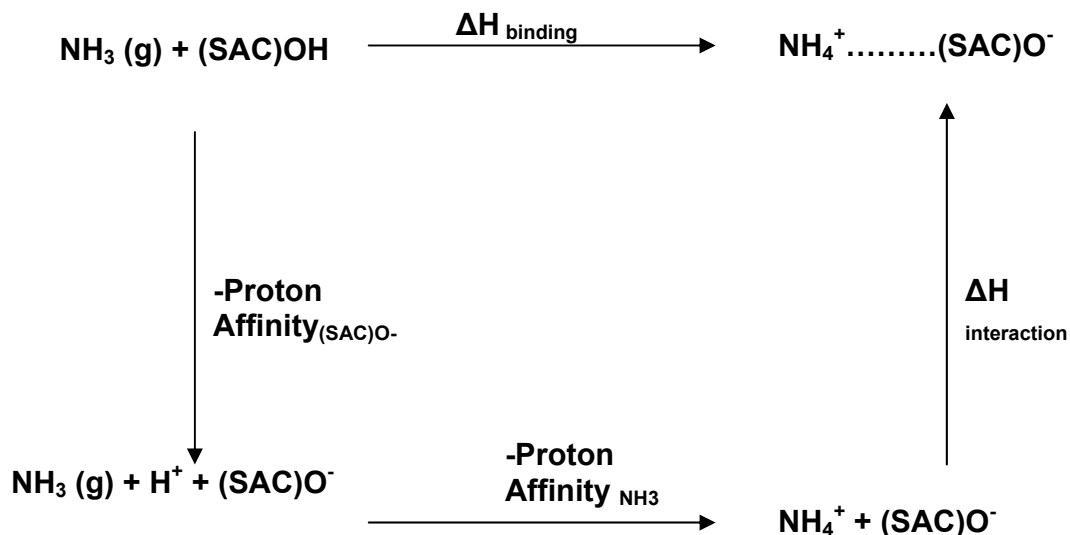


Figure 4.1 Thermochemical cycle for the adsorption of ammonia by a solid acid catalyst.

### ❖ Temperature Programmed Desorption

Temperature programmed desorption is a method which studies the kinetics and thermodynamics of the desorption of gaseous molecules from a solids surface. When molecules adsorb to a solid surface, they decrease their energy in forming chemical/physical bonds. When heat is applied to the sample molecules will desorb at different rates depending on the strength of their binding energies to the surface. The higher the temperature required to desorb the molecule; the stronger its binding energy.

It is a technique widely used (particularly with zeolites and clays) to determine the number of acid sites on solid catalysts, using volatile bases, such as ammonia, pyridine and n-butylamine. This technique is a direct measure of the heats of adsorption of the pre-adsorbed base at different temperatures. Typically, an excess of base is adsorbed onto the solid catalyst. What is considered physically adsorbed is removed by evacuation. After evacuation, what is left is regarded as chemically adsorbed, and can be used to measure the total amount/concentration of acid sites. Despite its wide reported use with zeolitic catalysts, its use with thermally sensitive solids i.e. ion exchange resins is limited, as the desorption temperatures may cycle higher than the

temperatures at which the solid becomes structurally unstable. This technique also does not distinguish between the Bronsted and Lewis acid sites, but measures the total amount of both. Identical conditions are required for comparison, these may be complicated to reproduce, and certain heat transfer effects may affect the analysis <sup>[15]</sup>.

### 4.3.3 Vibration Spectroscopic Methods

#### ❖ Infra-red and Raman Spectroscopy

Both of these techniques are widely used and reported in literature <sup>[1-5/9]</sup> to determine the concentration of acid sites, and indeed the type of acid sites present in the solid catalysts. Due to the unique characteristic bands which both Bronsted and Lewis acid sites exhibit. Generally, the most effective base probe molecules used are pyridine and ammonia. The protonated pyridine or ammonium molecules exhibit IR bands separate to those of the co-ordinately bonded pyridine and ammonia molecules. Therefore enabling the distinction between the protonated Brønsted acid sites, and the co-ordinately bonded Lewis acid sites. However Raman spectroscopy has been found to be relatively insensitive to Brønsted acid sites, and so infra-red adsorption spectroscopy is the more useful technique.<sup>[1-5]</sup> Infra-red identifies the environments of the hydroxyl groups present on the solid acid catalyst surface, and which interact with the base probe molecules. The intensity of the IR band generated gives an indication of the concentration of acid sites. With the use of pyridine as a basic probe molecule, both protons on the acid sites vibrate at particular individual wavelengths, thereby enabling the distinction between their environments. Pyridine protonated at a Brønsted acid site characteristically vibrates at around 1540 and 1640  $\text{cm}^{-1}$ , whereas the pyridine bound to the co-ordinately bonded Lewis acid sites characteristically vibrate at 1450 and 1620  $\text{cm}^{-1}$ . In comparison hydrogen atoms bonded to the surface vibrate at 1400-1600  $\text{cm}^{-1}$ . Quantitative expression of the data is difficult though, after measuring the intensity of the bands, and using the values of the extinction coefficients, it has been found possible to calculate the total number of Brønsted and Lewis acid sites that are capable of absorbing and retaining the Pyridine base molecules.

### 4.3.4 Nuclear Magnetic Resonance (NMR) Methods

#### ❖ $^1\text{H}$ NMR and $^{13}\text{C}$ NMR

Nuclear Magnetic Resonance is a technique used to determine the structure of samples. It studies the magnetic moments of atoms within a sample. A strong magnetic field splits the nuclear energy levels of the sample. At certain resonating frequencies, particular energy levels are split and recorded. The resonance frequencies of a particular element are influenced by the electronic environment in which the atom is situated. The resonance frequencies that are recorded are displayed as a spectrum, the extent and nature of the nuclei coupling can be ascertained giving further information on the molecular structure of the element from chemical shifts and coupling constants compared to known standards.  $^1\text{H}$  NMR detects the environment of the hydrogen protons within a sample, and  $^{13}\text{C}$  detects the environment of the carbon atom.

In various publications <sup>[1-5/16/17]</sup>,  $^{13}\text{C}$  NMR methods have been used to study the acidity of solid acid catalysts, the most notable results having been performed with acidic zeolites. Using advanced techniques such as cross polarization (CP) and magic-angle spinning (MAS) NMR it has been possible to determine the total number of acid sites and their relative strength, based on the intensity and  $^{13}\text{C}$  chemical shift signals due to the environment of the OH acidic groups studied, using both strong and weak base probe molecules. However it is not possible to distinguish between the two types of acid sites using this technique.

#### 4.3.5 Conclusion

All of the methods mentioned above have been found to be successful in part determining the relative concentration of acid sites on solid acid catalysts (in particular zeolites) and indeed distinguishing between the two types of acid sites. Quantitative analysis of the acids sites has proven more complex, and therefore directly relating the results of one particular technique to the predictions of catalytic activity is sometime difficult, and in some cases giving contradictory results. However with the use of dual techniques such as IR and NMR combined with TPD, it is possible to determine the relative abundance of both Brønsted and Lewis acid sites, and their relative strengths,

and thus predict its relationship to catalyst performance, all of which is of course dependant on the nature of the base probe molecules used.

#### **4.4 Base Adsorption Calorimetry (Acid Site Concentration Characterization Technique)**

Adsorption calorimetry is a direct technique that enables the measurement of the heats of adsorption of a reference base at the solid acid sites. The specific use of base adsorption calorimetry as a dual technique to characterise solid acid catalysts is well documented in the literature [18-22]. This involves the injection of set amounts of reference base onto the solid acid catalyst at a given temperature (isothermal) until saturation of the solid is complete. The resulting heat outputs are measured for each addition and integrated. The cumulative heat is plotted against the amount of base added, the gradient calculated and expressed as the molar enthalpy of neutralization in  $\text{kJ mol}^{-1}$  [23].

There are limitations to this technique however that mean it cannot be used alone as a measure of acid strength, but acts as a measure of the concentration of acid sites. The nature of the binding sites cannot be known through calorimetry. Adsorption may occur at both Bronsted and Lewis acid sites, or as a result of surface/vapour attractive forces. The heat of adsorption is not a direct measure of the proton affinity of the acid sites, but of a combination of proton affinity of the acid sites on the solid, the proton affinity of the reference base and the acid sites, and the heat of interaction of the resulting ion pair formation.

##### **4.4.1 Surface Acidity**

The concentration of acid sites on a solid's surface is termed its surface acidity and is commonly expressed as the number of mmol of acid sites per unit weight or surface area of the solid. Solid acid catalysts are characterised in terms of acidity by the presence of both Brønsted and Lewis acid sites on their surfaces. Brønsted acidity dominates in the case of this research.

### 4.4.2 Thermodynamics of Calorimetry <sup>[24/27]</sup>

A Calorimeter is an instrument that measures the thermal production of heat from a reaction. The First Law of Thermodynamics states “The energy of an isolated system is constant”. This law considers the internal energy (U) of a system and how it is affected by the work done on it (w) and the heat energy added to it (q). The change in internal energy of a system ( $\Delta U$ ) is determined using the equation below.

$$\Delta U = q + w$$

If the system is maintained at constant volume, and the system is only affected by pressure/volume work, then

$$\Delta U = q$$

However, most changes occur not at constant volume, so w is generally zero. Measuring  $\Delta U$  is very complicated, measuring the change in enthalpy ( $\Delta H$ ) is easier, and can be directly related to  $\Delta U$ . Where P is the pressure of the system.

$$H = U + PV$$

$$\Delta H = \Delta U + \Delta(PV)$$

$$\Delta H = \Delta U + P\Delta V + V\Delta P$$

If change takes place at constant pressure, then  $V\Delta P = 0$

$$\Delta H = \Delta U + P\Delta V$$

When replacing equation 1 with the equation above

$$\Delta H = q + w + P\Delta V$$

If work done on the system is only pressure or volume related, then  $w = -P\Delta V$

$$\Delta H = q - P\Delta V + P\Delta V$$

Therefore

$$\Delta H = q$$

The calorimeter used in this research operates at a constant pressure, therefore the *measurement of heat is equal to the enthalpy change of the system.*

Evolution of heat at constant pressure is regarded as exothermic, the enthalpy of the system decreases and the  $\Delta H$  is negative. When heat is taken from the surroundings of the system, the reaction is endothermic and the  $\Delta H$  is positive.

For a given reaction to be spontaneous according to the second law of thermodynamics, the entropy (S) of the universe must increase. It is possible to predict the spontaneity based only on the entropy of a system using the state function Gibbs free energy (G). Gibbs free energy combines enthalpy and entropy and allows the combination of their effects on the system only. Where T is the temperature of the system.

$$G = H - TS$$

$$\Delta G = \Delta H - T\Delta S$$

Free energy change  $\Delta G$  serves as an indicator for the potential of a reaction to take place, and if change is thermodynamically favourable  $\Delta G$  is negative. Table 4.1 below demonstrates the relationships between  $\Delta G$ ,  $\Delta H$  and  $\Delta S$  and their effect on the spontaneity of the reaction.

$\Delta H$	$\Delta S$	$\Delta G = \Delta H - T \Delta S$
-ve	+ve	-ve spontaneous at all temperatures
-ve	-ve	-ve spontaneous at low temperatures where $\Delta H$ outweighs $T \Delta S$ OR +ve non spontaneous at all temperatures
+ve	-ve	+ve non spontaneous at all temperatures
+ve	+ve	-ve spontaneous at high temperatures where $T \Delta S$ outweighs $H$ OR +ve non spontaneous at low temperatures where $\Delta H$ outweighs $T \Delta S$

Table 4.2 Thermodynamics of a spontaneous system

$\Delta G$  can be further related to the equilibrium constant (K) using the following equation

$$\Delta G^\theta = -RT \ln K$$

$\Delta G^\theta$  is the Gibbs free energy change under standard conditions. Where R is the universal gas constant and T is the temperature of the reaction.

#### 4.4.3 Types of Calorimeter

There are two main types of calorimeter, (i) heat accumulation, (ii) heat exchange/heat conduction. Both are composed of an inner vessel/s whereby the thermal production of heat from a reaction is measured. The intensity of the heat exchange from the reaction in the inner vessel and its surroundings is measured but varies with each kind of calorimeter<sup>[25-26]</sup>.

### ❖ Heat Accumulation Calorimeter

Also known as an adiabatic calorimeter, this allows the temperature to increase for exothermic reactions, and decrease for endothermic reactions. There is no heat exchange between the inner vessel and its surroundings, the temperature of the vessel varies when heat is generated or adsorbed.

### ❖ Heat Conduction Calorimeter

Otherwise known as an isothermal/heat flow calorimeter, operates at a constant temperature, the heat produced or adsorbed within the inner vessel which then flows or is “conducted” to or from the surrounding heat sink is measured.

In the case of this research a *Seteram (Tian-Calvet) Titrys Heat Flow Microcalorimeter* was used, a diagram of which is shown in Figure 4.1 below. The calorimeter consists of two cells (sample and reference) situated within the same calorimetric block (heat sink). The cells are surrounded by thermoelectric piles (made up of a number of thermocouples arranged in a series), which conduct any heat generated in the reaction away from the cell, converting it into an electrical signal. The heat conducted by each injection is measured by thermocouples and calculated. The use of both the sample and reference cells simultaneously allows the calorimeter to function in a differential mode, whereby voltage is only detected if the heat flow in the sample cell is different to that in the reference cell. This mode compensates for any temperature fluctuations (when isothermally set) of the calorimeter, thereby minimising any potential error, resulting in a high stability.

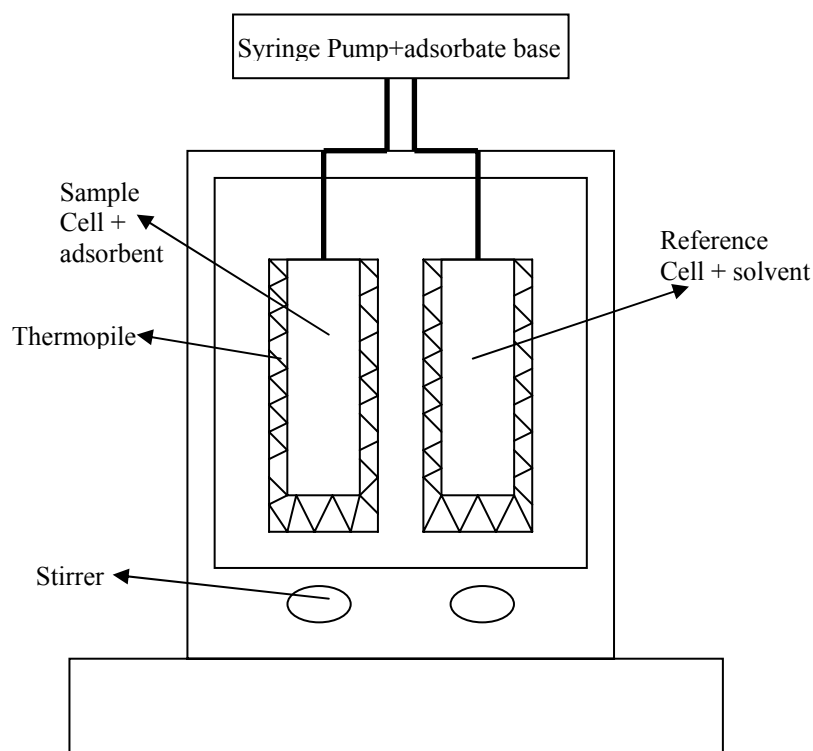


Figure 4.2 Diagram of a Seteram Titrys Tain-Calvet Heat Flow Calorimeter.

#### 4.4.5 Base Adsorption Calorimetry in the Liquid Phase

##### ❖ Calibration of the Seteram Titrys microcalorimeter <sup>[28]</sup>

As described later in the experimental section of this chapter, the calorimeter was initially electrically and chemically calibrated. Electrical calibration was primarily used for the calculation of the sensitivity coefficient ( $A^0$ ) via an automated programme which cycled through a series of pre-set sensitivity coefficient values and temperatures. The resultant curve was integrated, and the sensitivity coefficient calculated. Once the sensitivity coefficient value had been established, the Titrys was calibrated chemically using standardised reactions. In this case the neutralization reaction between 0.1M hydrochloric acid and 0.1M sodium hydroxide. These acid base titrations were designed to establish confidence with the equipment, and to verify data in the literature. The microcalorimeter was also chemically calibrated using a standard barium chloride/crown ether reaction.

### ❖ Corrections for heats of addition/dilution

In practice, Titrations were planned in which a standardised solution of base would be titrated with a solid acid suspended in the same solvent in the cell. Blank experiments were conducted in order to establish if any overriding effect of the interaction of base with solvent or solvent with the solid acid catalyst would cause any extra heats to be generated, that would mask the true heats of neutralization.

The established methods for determining and correcting for the heat of base dilution, and the interaction between the solvent and catalyst are summarised in Tables 4.2 and 4.3 for both systems respectively.

Sample Cell	Reference Cell
2ml 0.1M NaOH/H <sub>2</sub> O into 2ml H <sub>2</sub> O	2ml H <sub>2</sub> O into 2ml H <sub>2</sub> O
2ml 0.1M NaOH/MeOH into 2ml MeOH	2ml MeOH into 2ml MeOH
2ml 0.1M NBA (n-butylamine)/MeOH into 2ml MeOH	2ml MeOH into 2ml MeOH
2ml 0.05M NBA/CH (cyclohexane) into 2ml CH	2ml CH into 2ml CH

*Table 4.3: Method of correcting for the heat of base dilution as a blank run, for all the calorimetric systems investigated.*

Sample Cell	Reference Cell
2ml H <sub>2</sub> O into 2ml H <sub>2</sub> O + 100mg solid acid catalyst	2ml H <sub>2</sub> O into 2ml H <sub>2</sub> O
2ml MeOH into 2ml MeOH + 100mg solid acid catalyst	2ml MeOH into 2ml MeOH
2ml MeOH into 2ml MeOH + 100mg solid acid catalyst	2ml MeOH into 2ml MeOH
2ml CH into 2ml CH + 100mg solid acid catalyst	2ml CH into 2ml CH

*Table 4.4: Method of correcting for the heat of interaction between solvent and catalyst as a blank run, for all the calorimetric systems investigated.*

### ❖ Treatment of data

A Seteram Titrys microcalorimeter conducted isothermally at 30° C was used for all experiments. In a typical experiment, 2 cm<sup>3</sup> of titrant was added in 0.20 cm<sup>3</sup> aliquots at one hour intervals until neutralization of the solid acid catalyst suspended in 2 cm<sup>3</sup> of the appropriate solvent was complete. The resulting heat output (peak) for each addition of titrant into the solvent containing the solid acid, was measured and displayed as seen in Figure 4.2. This sketch shows the gradual decline of each peak, and the abrupt change in peak size at the end, indicating complete neutralization of the solid acid. After integration of the peaks, the cumulative heat was plotted against the volume of base added producing a straight line graph, the gradient of which was expressed as a molar enthalpy of neutralization in kJ mol<sup>-1</sup>, an example of which can be seen in Figure 4.3. It is assumed that (after the first addition is discounted due to possible injection error.) each aliquot of added base reacts completely with the solid acid. This was verified by conducting parallel titrations outside the calorimeter, utilizing the appropriate base and solid acids. Results showed a negligible excess of unreacted base remaining after titration from pH monitoring. The line of best fit shown in Figure 4.3 does not go through the origin because the first injection could not be fully controlled and almost certainly involved less than 0.2 ml being injected, resulting in a positive intercept.

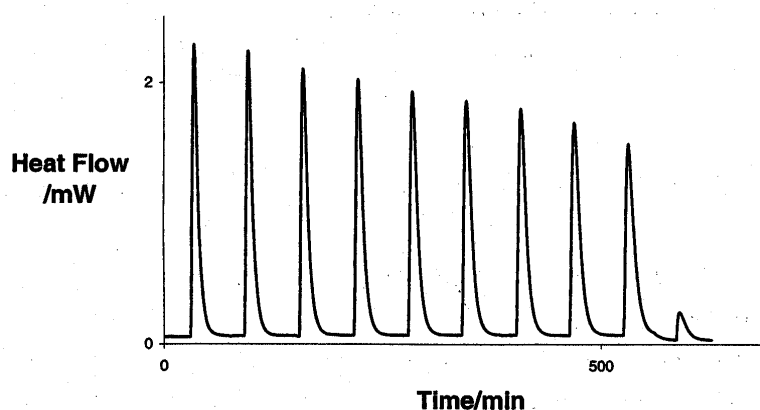


Figure 4.3 Sample heat output from the ITC

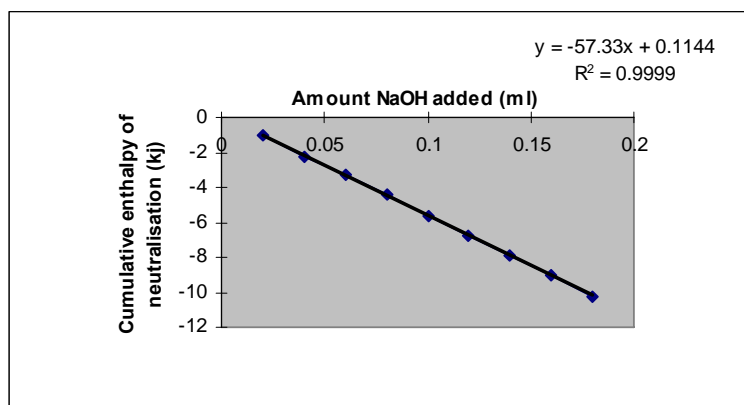


Figure 4.4: Typical plot of cumulative enthalpy versus amount of base added, for a titration of aqueous 0.1M NaOH solution against 0.1M HCl solution. This gradient gives  $\Delta H_{neut}^{\circ} : -57.33 \text{kJ mol}^{-1}$ .

Figure 4.2 shows a sample heat output from the Titrys, resulting in a series of peaks or addition of titrant into the system. This calorimetric output varies with each solid acid catalyst analysed. Figure 4.3 above demonstrates an ideal output from an acid base calibration reaction (a homogenous system). It is worth noting the flat baseline between the peaks, and the gradual decrease in peak height and an increase in width as the reaction comes to neutralization. For each and every Titrys heat output sequence, the peaks are integrated in precisely the same manner. The software allows the drawing of a baseline under and between each peak. In this work it was drawn from the point where the calorimeter signal starts to rise at the beginning of each peak through to the same point on the next peak. Once tabulated, the remaining cumulative heat outputs in the reaction are plotted against the volume of base added producing a straight line graph (each analysis possessing the same number of data points to enable a direct comparison), the slope of which is the molar enthalpy of neutralization for that reaction. Analysis in this way minimises possible errors.

Three different types of support for the solid acid catalyst were used, and two main base/solvent systems were used. Firstly, mainly for the poly(styrene-co-divinylbenzene) resins, an aqueous system involving a strong base was used. Some of the resins required a swelling solvent to allow the base to access their intrinsic acid sites. In this case the 0.1M NaOH/H<sub>2</sub>O system was appropriate. The synthesised inorganic solid acid catalysts however require no swelling in order to access their acid sites, so an appropriate non swelling solvent was used, in this case cyclohexane. Due to

the change in solvent, it was necessary to alter the base used, in this case n-butylamine, as it is a simple alkylamine that dissolves in most solvents. It is also bulkier than NaOH and should therefore be more selective with accessing acid sites due to steric hindrance. A 0.05M n-butylamine/cyclohexane system was used.

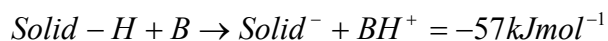
As a source of comparison, the polymer resins were also tested using the n-butylamine/cyclohexane, n-butylamine/methanol and NaOH/methanol systems, and the sulfonated inorganic silicas (both mesoporous and amorphous) were tested using the NaOH/H<sub>2</sub>O system.

The relative concentration of acid sites measured by base adsorption liquid calorimetry is a measure of the relative proton donating ability of the solid acid catalyst to the reference base within the solvent medium.

Three types of solvent medium were used, the highly polar water, the semi polar methanol and the non polar cyclohexane. A polar molecule possesses a separation of charge over the bond between atoms resulting in a dipole moment (non equal charge distribution). The greater the dipole moment, the more polar the solvent.

The stronger the acid, the greater its acid dissociation constant  $K_a$  and the smaller its  $pK_a$ . The type of solvent used will effect the dissociation of the acid in solution, more specifically in terms of solvation and polar interactions. Every molecule possesses a dipole moment; that is a distribution of electrical charge over the bond between atoms. The greater the dipole moment (non equal charge distribution) the more easily solvated the molecule is. A polar solvent has a good solvating power as it has a greater dipole moment and is able to solvate molecules more readily. In reactions whereby the activation step is accompanied by an increase in electrical charges on the reactants, a more polar solvent will cause an increase in the rate. Solvents have been known to have a levelling effect on the strength of the acids in solution due to the subsequent charge neutralization during equilibrium of the reaction.

Titration calorimetry provides the molar enthalpy of neutralization of the acid sites ( $\Delta H_{\text{neut}}^{\theta}$ ). It was hoped that the values of  $\Delta H_{\text{neut}}^{\theta}$  could be used as a relative indicator of the strength of acid sites on the catalyst, on the basis that it reflects the facilities of the reaction:



In water, this was not going to be the case because water behaves as a base itself with the result that titration will involve neutralization of  $\text{H}_3\text{O}^+$  if acid is strong enough to react with water. This is the reported “levelling effect” of water as a solvent which suggests that any acids stronger than  $\text{H}_3\text{O}^+$  will show the same  $\Delta H_{\text{neut}}^\theta$  of  $-57 \text{kJmol}^{-1}$ .

In methanol the possibility of levelling exists as  $\text{MeOH}_3^+$  can form. Methanol is regarded as a weaker base than water according to its established  $K_a$  value and therefore will not level as many acid sites. However in Cyclohexane it is reasonable to expect neutralization reaction to be between the solid acid and its base and so  $\Delta H_{\text{neut}}^\theta$  could reasonable be expected to reflect the strength of the acid sites.

However the highly polar water solvent has been found to have a levelling effect on the absolute strength of the solid acid catalyst (its strong basicity deprotonates the acid groups) and therefore measurements in water should not be used as a direct indicator of acid strength. But it is required for use as a solvent with the polymeric resin catalysts as its high polar properties enable it to swell the resin in order for to access the intrinsic acid sites. The use of the solvent with the other solid acids is as a comparison.

The non polar cyclohexane behaves as a non swelling solvent, it has no specific interactions with solute molecules and only ion pair formation is expected with strong bronsted acid sites. The enthalpy of reaction of a base with an acid in cyclohexane reflects the heat required to break the H-X bond. And therefore the heats of neutralization could be related to acid strength.

The semi polar methanol would be expected to behave in the region between water and cyclohexane, thereby acting as a comparative solvent system with the appropriate reference bases.

#### 4.4.6 Base Adsorption Calorimetry in the Gas Phase

Acid sites can be characterised using calorimetry by base adsorption in the absence of solvent, typically  $\text{NH}_3$  is used <sup>[29]</sup>. Samples are activated and held under vacuum and  $\text{NH}_3$  is introduced in small pulses to the sample and allowed to equilibrate after each addition. The amount adsorbed is determined from pressure measurements in the gas handling system and enthalpies from the calculations. After each pulse the ammonia that is adsorbed weakly and reversibly onto the catalyst surface desorbs back into the carrier after each pulse has passed. This ensures that the ammonia which remains bound, and the enthalpies of adsorption, are associated only with irreversibly and strongly adsorbed ammonia – presumably that which is chemisorbed onto the acid sites.

It is assumed that the binding enthalpy is measured when the strong base  $\text{NH}_3$  is adsorbed at an acid site forming  $\text{NH}_4^+$  which is ion paired to the deprotonated acid site. The binding enthalpy reflects the acid strength but cannot be measured by this type of calorimetry. However it is assumed that the proton affinity of  $\text{NH}_3$  and the enthalpy change associated with the ion pair formation between the  $\text{NH}_4^+$  and the solid surface is the same for all solid acids of this type. Therefore the heats measured by gas adsorption calorimetry reflect the variations in the proton affinity of the solid acid and therefore its acid strength. The number of adsorbed base molecules is assumed to provide the number of acid sites, while the heats of adsorption can be considered a measure of acid strength. The subsequent plot of enthalpy of adsorption vs coverage gives an indication of the distribution of acid site strength.

## 4.5 Base Adsorption Calorimetry: Experimental

### 4.5.1 In the liquid phase; Base adsorption microcalorimetry

A SETERAM “TITRYS” differential heat flow microcalorimeter with continuous stirring mode was used for all experiments. All experiments were conducted isothermally at 303 K. The 0.10 M standardised NaOH (ampules provided by Aldrich) and the methanol and cyclohexane solvents were obtained from Aldrich chemicals. The solvents were dried for 48 hours using molecular sieves. The 0.10 M HCl solution was standardised using acid-base titration with the standard NaOH solution, and subsequently the aqueous 0.10 M and 0.05 M n-butylamine solutions were standardised by acid-base titration with the HCl solution.

Blank experiments and heats of dilution experiments were conducted with every base/solvent system to ascertain the effect if any of the addition of the titrant into the solvent containing the solid. In all cases any heats observed were negligible, therefore no corrections were necessary.

In a typical experiment 80 mg of catalyst was suspended in 2.0 cm<sup>3</sup> of solvent in the sample cell, with only solvent in the reference cell. A 3 hour equilibration time was used to maintain the titrant at the desired temperature to ensure no adverse effects when added to the solution. The preheated titrant was added simultaneously to both sample and reference cells using a programmable twin syringe pump. Titrant was added in 0.2 cm<sup>3</sup> aliquots at one hour intervals until neutralisation was complete, usually after 15 hours. Titrant was added to the reference cell in the same manner.

Various solvents and titrants were used when characterising the different solid acid catalysts, and are detailed below in the following text and Table 4.5

Sample Cell	Reference Cell
2ml 0.1M NaOH/H <sub>2</sub> O into 2ml H <sub>2</sub> O+ 100mg solid catalyst	2ml H <sub>2</sub> O into 2ml H <sub>2</sub> O
2ml 0.1M NaOH/MeOH into 2ml MeOH + 100mg solid catalyst	2ml MeOH into 2ml MeOH
2ml 0.1M NBA/MeOH into 2ml MeOH + 100mg solid catalyst	2ml MeOH into 2ml MeOH
2ml 0.1M NBA/CH into 2ml CH + 100mg solid catalyst	2ml CH into 2ml CH
2ml 0.05M NBA/CH into 2ml CH + 100mg solid catalyst	2ml CH into 2ml CH

*Table 4.5: Experimental base adsorption calorimetry systems with varying solvents and titrants for use with the characterization of the solid acid catalysts in the liquid phase.*

The sulfonated polystyrene resin catalysts used were C10OH, SP 21/15, CT175, and CT275. The solvents investigated were deionised H<sub>2</sub>O, MeOH and cyclohexane (denoted CH). The titrants investigated were, 0.1 M NaOH and 0.1 M n-butylamine in each of the solvents.

The resins were prepared by drying at 373 K for two hours, weighing, and then solvating in the appropriate solvent for 12 hours or more.

The synthesised sulfonated mesoporous molecular sieve silicas and the functionalised silica gels were tested in the same manner, with the use of water and and pre-dried cyclohexane as solvents. The titrants investigated were 0.1 M NaOH/H<sub>2</sub>O and 0.1 M/0.05 M n-butylamine/Cyclohexane.

The resulting heat output (peak) was measured for each addition of base probe molecule and integrated using the SETSOFT software package. The cumulative heat was plotted against the amount of base added, the gradient calculated and expressed as the molar enthalpy of neutralization in kJ mol<sup>-1</sup>.

Identical titration experiments using the same concentrations and solid acids were conducted outside the cell to ensure complete reaction of the titrant base after each

injection had occurred. Approximately 100 mg solid acid catalyst was solvated in 2.0 ml solvent with stirring, after 3 hours, 2.5 ml of base (NaOH or NBA) was injected (to correspond with 0.2 ml aliquots injected every hour for 15 hours). The solution was then separated from the solid, if the solvent used was non aqueous then water was added to the liquid to extract any un-reacted base. This was then back titrated with standard 0.10 M HCl solution while monitoring the pH.

#### 4.5.2 Gas phase; Flow adsorption calorimetric studies

The calorimetric studies were performed in house by Dr. Prem Siril , using a SETARAM DSC111 DIFFERENTIAL SCANNING CALORIMETER connected to a HIDEN HPR 20 MASS SPECTROMETER GAS ANALYSER. Dried helium and 1 % ammonia in helium mixture were obtained from BOC ltd.

“In a typical experiment, the catalyst (5-30 mg) was activated at 423 K under dried helium flow at 5 ml min<sup>-1</sup>. Following activation, and maintaining the sample temperature at 423 K, small (typically 1.0 ml but from 0.2 to 5.0 ml) pulses of the probe gas (1 % ammonia in helium) at atmospheric pressure were injected at regular intervals (every 30 minutes) into the carrier gas stream from a gas-sampling valve. The concentration of ammonia downstream of the sample was monitored continuously with the mass spectrometer. The interval between pulses was chosen to ensure that the ammonia concentration in the carrier gas (including that adsorbed and then desorbed after the pulse has passed) returned to zero, and to allow the DSC baseline to re-establish itself. The net amount of ammonia irreversibly adsorbed from each pulse was determined by comparing the MS signal during each pulse with a signal recorded during a control experiment through a blank sample tube. Net heat released for each pulse, corresponding to irreversible adsorption of ammonia, was calculated from the DSC output curve. From this molar enthalpy of adsorption of ammonia ( $\Delta H_{\text{ads}}^{\circ}$ ) was obtained for the ammonia adsorbed from each successive pulse. The  $\Delta H_{\text{ads}}^{\circ}$  values were then plotted against the amount of (irreversibly) adsorbed ammonia per gram of the catalyst, to give a  $\Delta H_{\text{ads}}^{\circ}$  / coverage profile for each catalyst.”<sup>[31]</sup>

## 4.6 Base Adsorption Calorimetry: Results and Discussion

### 4.6.1 General Overview

This section shows the results from the acidity characterization of the synthesised materials using: base adsorption calorimetry using water, methanol and cyclohexane solvents, and base adsorption calorimetry in the absence of solvent using ammonia.

It was the aim of this work to answer the following hypotheses of the synthesised sulfonated materials.

- ❖ In water all strong acids behave similarly giving an enthalpy of neutralization of  $-57 \text{ kJ mol}^{-1}$ . Due to the internal solution concentration, the commercially available polystyrene resins behave as strong acids in accordance with results published in the literature, demonstrating enthalpies of neutralization greater than  $-57 \text{ kJ mol}^{-1}$ . Do the synthesised solid acid supports with no internal solution (non swelling) behave like strong acids, or more like the sulfonated polystyrene resins in water?
  
- ❖ Do the solid acid supports behave as strong acids in different solvent systems?
  
- ❖ Does altering the propyl / phenyl sulfonic acid tether group or the additional phenyl group make any difference to the observed concentration of acid groups of the samples?

The acidity of the supports was measured in the presence of liquid using base adsorption calorimetry, and in the absence of solvent using flow base adsorption calorimetry. Measurements in the liquid phase were conducted isothermally using a Seteram Titrys differential heat flow titration calorimeter, with sodium hydroxide/water and n-butylamine/cyclohexane systems. Measurements in the gas phase were conducted using a Seteram DSC111 differential scanning calorimeter connected to a Hiden HPR 20 mass spectrometer, with a 1% ammonia in helium gas flow mixture.

## 4.6.2 In the liquid phase; Isothermal Titration Microcalorimetry (Base adsorption calorimetry)

### ❖ 4.6.2.1 Calibration of the Seteram Titrys microcalorimeter

Electrical calibration was primarily used for the calculation of the sensitivity coefficient ( $A^0$ ) which converts the electrical signal from the thermopile to power generated in the calorimeter in watts and milliwatts. The resultant curve was integrated, and the sensitivity coefficient calculated. The Titrys was then checked chemically using a standardised reaction, in this case the neutralization reaction between 0.100 M hydrochloric acid and 0.100 M sodium hydroxide. 0.100 M Standardised NaOH(aq) was titrated into 2.00 cm<sup>3</sup> 0.100 M HCl. Deionised water was the solvent used and this was simultaneously titrated in aliquots of 0.200 cm<sup>3</sup> into 2.00 cm<sup>3</sup> water in the reference cell. The resultant heats of neutralization were calculated and cross referenced against the literature value of -57.1 kJ mol<sup>-1</sup> as shown in Table 4.6 below.

Sample Cell	Enthalpy of neutralization kJ mol <sup>-1</sup>
Acid Base: 0.1M NaOH (aq) : 2ml 0.1M HCl :	-53.9 ± 0.28
ΔH neutralization before electrical calibration	
Literature Value of ΔH Neutralization HCl	-57.1 <sup>[32]</sup>
ΔH neutralization after electrical calibration	-57.39 ± 0.36

*Table 4.6: Average experimental enthalpy of neutralization HCl values compared to literature value before and after electrical calibration. The values are expressed as an average from triplicate data sources.*

The microcalorimeter was also checked using a standard barium chloride/18-crown-6 reaction giving consistent results with the literature <sup>[18]</sup> as shown in Table 4.7. 0.01 M barium chloride solution was titrated into 2.00 cm<sup>3</sup> 0.100 M 18 crown 6 in the sample cell. Deionised water was simultaneously titrated into 2.00 cm<sup>3</sup> water in the reference cell. The results for  $\Delta H_{\text{react}}^0$  were within experimental error of the literature value therefore concluding that calibration of the equipment was successful.

Sample Cell	Enthalpy of neutralization $\text{kJ mol}^{-1}$
0.100 M $\text{BaCl}_2$ into 2.00 ml 0.100 M 18-Crown-6	Literature Value $-31.42 \pm 0.2$
$\Delta H^0_{\text{experimental}}$	$-31.29 \pm 0.73$

*Table 4.7: Chemical calibration of the calorimeter titrating 2ml 0.100M barium chloride into 2ml 0.01M 18 crown 6. The values are expressed as an average from triplicate data sources.*

#### ❖ 4.6.2.2 Corrections for heats of addition/dilution

With both the sodium hydroxide/water, and the n-butylamine/cyclohexane Titrys systems, blank experiments were conducted to investigate possible heats of dilution that might affect the overall results.

The established methods for determining the heats of base dilution, and any heat effects associated with solvent addition to solid catalysts are summarised in Tables 4.8 and 4.9 for both systems respectively.

Sample Cell	Reference Cell
0.100 M NaOH/ $\text{H}_2\text{O}$ into 2.00 ml $\text{H}_2\text{O}$	$\text{H}_2\text{O}$ into 2.00 ml $\text{H}_2\text{O}$
0.100 M NaOH/MeOH into 2.00 ml MeOH	MeOH into 2.00 ml MeOH
0.100 M NBA/MeOH into 2.00 ml MeOH	MeOH into 2.00 ml MeOH
0.05 M NBA/CH into 2.00 ml CH	CH into 2.00 ml CH

*Table 4.8: Experiments to detect heats of dilution during the planned titrations.*

Sample Cell	Reference Cell
H <sub>2</sub> O into 2.00 ml H <sub>2</sub> O + 100 mg solid acid catalyst	H <sub>2</sub> O into 2.00 ml H <sub>2</sub> O
MeOH into 2.00 ml MeOH + 100 mg solid acid catalyst	MeOH into 2.00 ml MeOH
MeOH into 2.00 ml MeOH + 100 mg solid acid catalyst	MeOH into 2.00 ml MeOH
CH into 2.00 ml CH + 100 mg solid acid catalyst	CH into 2.00 ml CH

Table 4.9: Experiments to detect heats due to interaction between solvent and solid acid catalysts.

In all of these blank experiments, no significant additional heats were detected therefore no further correction was required to subsequent data.

For the three different types of solid acid catalyst, two main base/solvent systems were used. Firstly, mainly for the sulfonated poly(styrene-co-divinylbenzene) resins, an aqueous NaOH solution was used. Some of the resins required a swelling solvent to allow the base to access their intrinsic acid sites. The synthesised inorganic solid acid catalysts however require no swelling to access their acid sites, so an appropriate non swelling solvent was used, in this case cyclohexane with n-butylamine at a 0.05 M concentration. As a source of comparison, the polymer resins were also tested using n-butylamine/cyclohexane, n-butylamine/methanol and NaOH/methanol, and the sulfonated inorganic silicas were tested using NaOH/H<sub>2</sub>O. The results for both systems with the relevant solid acid catalysts were as follows.

### 4.6.3 In the liquid phase; Isothermal Titration Microcalorimetry (Base adsorption calorimetry) Solvent Systems

In a typical experiment 80 mg of catalyst was suspended in 2.00 cm<sup>3</sup> of solvent in the sample cell. Titrant was added in 0.20 cm<sup>3</sup> aliquots at one hour intervals until neutralization was complete. The reference cells contained the solvent, and solvent was titrated into the reference cell in the same manner. The solid catalysts were prepared by drying at 60°C for two hours, weighing, and then solvating in the appropriate solvent for 12 hours or more before analysis. The enthalpy of neutralization of paratoluenesulfonic acid (abbreviated to p-TSA) solution was determined. In homogeneous solution p-TSA is an analogue of the supported sulfonic acids used here. The experimental method was unaltered. This  $\Delta H_{\text{Neut}}^0$  value was found to be -52.3 kJ mol<sup>-1</sup>. This therefore offers a good comparison of strength along side the benchmark HCl data. In the case of the methanol solvent system, the NaOH (s) was dried in the same way as the solid catalysts before preparing the solvent solution. All concentrations of base solutions used were standardised using standard 0.1 M HCl purchased commercially.

All the experiments were performed in triplicate from which the average values stated in the following tables were obtained.

A series of sulfonated resins were examined covering a range of acid loadings, from an “under-sulfonated” macroporous resin SP 21/15 through to the conventional stoichiometrically sulfonated C100H gel resin and CT175 macroporous resin, to the persulfonated CT275 macroporous resin. Also including the fluorinated Nafion and Nafion-silica composite resins. The synthesised sulfonated silicas and sulfonated mesoporous silicas were also examined and compared.

#### 4.6.3.1 Water solvent system.

##### *0.1M NaOH/H<sub>2</sub>O system*

The highly polar water solvent has been found to have a levelling effect on the absolute strength of the solid acid catalyst (its strong basicity deprotonates the acid groups) and therefore measurements in water should not be used as a direct indicator of acid strength. However with careful interpretation it can be a useful insight into the

enthalpies of neutralization of solid acid catalysts when compared to other solvent systems.

Water is required for use as a solvent with the polymeric resin catalysts as its high polar properties enable it to swell the resin in order for to access the intrinsic acid sites. The use of the solvent with the other solid acids acts as a comparison.

The reported “levelling effect” of water as a solvent suggests that any acids stronger than  $\text{H}_3\text{O}^+$  will show the same  $\Delta H_{\text{neut}}^0$  value of  $-57 \text{ kJmol}^{-1}$  as the strong acid HCl.

In homogeneous solution p-TSA is an analogue of the supported sulfonic acids used here, and a useful comparison to the enthalpy values derived.

The results of the three types of solid acid support are as follows.

### ❖ Sulfonated Polymer Supported Sulfonic Resins

#### Sulfonated Poly(styrene-co-divinylbenzene) Resins

After drying and re-solvation and subsequent analysis, the results from the 0.1M NaOH/H<sub>2</sub>O (aq) titration system are shown in Table 4.10 below (also indicating the benchmark values for the two acids as a comparison).

Resin	Sulfonic Acid Loading (mmolg <sup>-1</sup> )	$\Delta H$ Neutralization value (kJ mol <sup>-1</sup> )
0.1 M HCl	-	$-57.4 \pm 2$
0.1 M p-TSA	-	$-52.5 \pm 2$
SP21/15	2.97	$-55.3 \pm 2$
C100H	4.9	$-61.0 \pm 2$
AMB 15	4.9	$-64.7 \pm 2$
CT175	4.9	$-61.5 \pm 2$
CT275	5.3	$-64.5 \pm 2$

Table 4.10  $\Delta H_{\text{Neut}}^0$  value (kJ mol<sup>-1</sup>) from the 0.1M NaOH/H<sub>2</sub>O system for the Sulfonated Poly(styrene-co-divinylbenzene) Resins. (average triplicate values).

In this system the persulfonated CT275 resin demonstrates the most exothermic molar enthalpy of neutralization value of  $-64.5 \text{ kJ mol}^{-1}$ . It appears that as the sulfonic acid loading of the resins decreases, so do the observed molar enthalpies of neutralization. It is worth noting that all observed values are higher than those of the two homogeneous

acid solution systems, proving that the water solvent has not completely levelled all the acid sites on the resins. The trend of increasing enthalpies of neutralization with increasing sulfonic acid loading is in accordance with previous results in the literature. The lowest enthalpy of neutralization value is observed by the lowest sulfonated SP21/15 resin. The stoichiometrically sulfonated resins (equivalent to roughly one sulfonic acid group per styrene unit) Amberlyst 15 and CT175 have very similar values, higher than that of the SP 21/15 resin. The C100H gel resin gave a lower value than its macroporous stoichiometrically sulfonated counterparts, yet still higher than that of the low sulfonated sp21/15 resin. The persulfonated CT275 resin demonstrates the highest enthalpy value of the resins.

However in a stark contrast, the fluorinated Nafion resin which would have been expected to demonstrate the highest enthalpy of neutralization of the polymer resin group due to the presence of the electronegative fluorine groups giving rise to what was predicted to be a stronger solid acid (yet in water should demonstrate the same enthalpy of neutralization as the strong acid HCl), gave values lower than that of the resins in water as shown in Table 4.11 below. It appears the water solvent has indeed levelled the strength of the acid sites on these fluorinated materials.

### Fluorinated Sulfonated Polymer Resins

Resin	Sulfonic Acid Loading (mmolg <sup>-1</sup> )	$\Delta H$ Neutralization value (kJ mol <sup>-1</sup> )
0.1 M HCl	-	-57.4 ± 2
0.1 M p-TSA	-	-52.5 ± 2
NAFION	0.8	-51.1 ± 2
NAFION SiO <sub>2</sub>	0.1	-39.9 ± 2

Table 4.11  $\Delta H_{Neut}^0$  value (kJ mol<sup>-1</sup>) from the 0.1M NaOH/H<sub>2</sub>O system for the fluorinated sulfonated polymer resins. (average triplicate values).

The fluorinated polymer resin Nafion with its perceived high acid strength demonstrates a molar enthalpy of neutralization very similar to that of two homogeneous strong acid solutions, but less than that observed by the sulfonated resins. The silica supported

Nafion composite however demonstrates the lowest enthalpy of neutralization values of all the polymer supported resins.

This is highly unexpected, the low value for Nafion resin suggests that the use of water as a solvent for enthalpy of neutralization experiments is not a useful indicator of acid strength in this case, either the solvent is unable to access some of the intrinsic acid sites, or has successfully levelled the acidity of these sites.

The persulfonated CT275 resin demonstrates a higher enthalpy of neutralization than its CT175 stiochiometrically sulfonated counterpart, yet the stronger acid Nafion resin demonstrates a lower enthalpy value.

As a comparison to the polymer supported sulfonic acid resin supports, the synthesised silica and mesoporous silica supports were also tested in this solvent. As they require no swelling in order to access the intrinsic acid sites on the silica support, it is thought that water would not demonstrate as much of a levelling effect (its ability to access the intrinsic acid sites may be complicated by their smaller pore sizes).

### ❖ Sulfonated Silica Gels. Grafting route

In Table 4.12 below, the three types of functionalised silica gel are shown, functionalised with propyl, phenyl and the additional hydrophobic phenyl group.

Sample	Sulfonic Acid Loading (mmol g <sup>-1</sup> )	$\Delta H$ Neutralization value (kJ mol <sup>-1</sup> )
0.1 M HCl	-	-57.4 ± 2
0.1 M p-TSA	-	-52.5 ± 2
SiO <sub>2</sub> -PropylSO <sub>3</sub> H	0.36 ± 0.02	-32.5 ± 2
SiO <sub>2</sub> -PhenylSO <sub>3</sub> H	0.72 ± 0.02	-55.8 ± 2
Phenyl-SiO <sub>2</sub> -PropylSO <sub>3</sub> H	0.52 ± 0.03	-43.8 ± 2

Table 4.12  $\Delta H_{Neut}^0$  value (kJ mol<sup>-1</sup>) from the 0.1M NaOH/H<sub>2</sub>O system for the Sulfonated Silica Gels (average of triplicate values).

From the data shown in Table 4.12, the phenyl silica gel demonstrates the largest value of -55.8 kJ mol<sup>-1</sup> which is comparable to the enthalpy of neutralization of the strong acid

HCl in aqueous solution. The other molar enthalpies of neutralization observed from the sulfonated silica gels are less than that of the homogenous acid solutions and the commercially available polymer supported resins. There is again a trend between increasing sulfonic acid loading and increasing enthalpies of neutralization.

### ❖ Sulfonated mesoporous molecular sieve silicas. Co-condensed route

From the data shown in Table 4.13 below, the benchmark acid systems produced higher enthalpy of neutralization values, with the exception of the propyl MCM-41SO<sub>3</sub>H material. All the remaining samples demonstrate no reasonable correlation between increased sulfonic acid loading and enthalpy of neutralization values.

Sample	Sulfonic Acid Loading (mmolg <sup>-1</sup> )	ΔH Neutralization value (kJ mol <sup>-1</sup> )
0.1 M HCl	-	-57.4 ± 2
0.1 M p-TSA	-	-52.5 ± 2
MCM41-PropylSO <sub>3</sub> H	1.09 ± 0.05	-60.6 ± 2
MCM41-PhenylSO <sub>3</sub> H	0.40 ± 0.03	-34.0 ± 2
Phenyl-MCM41-PropylSO <sub>3</sub> H	0.12 ± 0.01	-24.5 ± 2
SBA-Propyl-SO <sub>3</sub> H	0.53 ± 0.01	-40.1 ± 2
SBA-Phenyl-SO <sub>3</sub> H	0.67 ± 0.01	-50.3 ± 2
Phenyl-SBA-PropylSO <sub>3</sub> H	0.41 ± 0.03	-55.5 ± 2
Phenyl-SBA-PhenylSO <sub>3</sub> H	0.39 ± 0.01	-44.4 ± 2
HMS-Propyl-SO <sub>3</sub> H	0.48 ± 0.01	-35.4 ± 2

Table 4.13  $\Delta H_{Neut}^0$  value (kJ mol<sup>-1</sup>) from the 0.1M NaOH/H<sub>2</sub>O system for the Sulfonated Mesoporous Silicas (average of triplicate values).

Despite their lack of trend, the molar enthalpies of neutralization demonstrated by the sulfonated mesoporous silicas are very similar to those of the sulfonated silica gels.

However, in this acid/base system, it is the sulfonated polymer supported resins that demonstrate the highest molar enthalpies of neutralization values and the most comparable data, possibly due to their much higher levels of sulfonation compared to

the two types of silica support. It is therefore evident that the role of the solvent with each support is crucial. A swelling solvent such as water offers complications when characterising the synthesised solid acid catalyst's concentration of acid sites, be it through problems with accessibility to the acid sites due to pore size of the solid acid or due to the subsequent levelling action of the water decreasing the observed enthalpies. It was assumed the sulfonic acid groups within the silica supported materials would completely dissociate when in contact with water, from the enthalpies of neutralization observed, this appears to not be the case.

Therefore the following results in methanol and cyclohexane solvent systems will prove vital in the determination of the acid strength of the synthesised solid acid catalysts.

#### **4.6.3.2 Methanol solvent system**

##### ***0.1M NaOH/MeOH system***

In the semi polar methanol the possibility of levelling exists as  $\text{MeOH}_3^+$  can form. Methanol is regarded as a weaker base than water according to its established  $K_a$  value and therefore should not level as many acid sites in comparison.

The results are as follows.

##### **❖ Sulfonated Poly(styrene-co-divinylbenzene) Resins**

After drying, re-solvation and subsequent analysis the results from the 0.1M NaOH/MeOH system were as shown in Table 4.14 below (also indicating the benchmark values for the p-TSA acid as a comparison).

Resin	Sulfonic Acid Loading (mmolg <sup>-1</sup> )	$\Delta H$ Neutralization value (kJ mol <sup>-1</sup> )
0.1 M p-TSA	-	-36.59 $\pm$ 2
SP 21/15	2.97	-33.4 $\pm$ 2
C100H	4.9	-35.8 $\pm$ 2
CT175	4.9	-34.3 $\pm$ 2
CT275	5.3	-39.49 $\pm$ 2

Table 4.14  $\Delta H_{Neut}^0$  value (kJ mol<sup>-1</sup>) from the 0.1M NaOH/MeOH system for the Sulfonated Poly(styrene-co-divinylbenzene) Resins. (average of triplicate values).

It appears in this system that as the sulfonic acid loading of the resins increases, so do the observed molar enthalpies of neutralization albeit by small amounts. It is worth noting, that all observed values are comparable to the p-TSA homogeneous acid solution systems within experimental error, and all very similar. As with the water solvent system, the lowest sulfonated resin SP 21/15 demonstrates the lowest enthalpy value, and the persulfonated CT275 resin demonstrating the highest enthalpy value. The stoichiometrically sulfonated resins (equivalent to roughly one sulfonic acid group per styrene unit) have very similar values higher than the lower sulfonated resin.

However due to solvation complications entailed with the preparation of the base solution using solid sodium hydroxide in methanol, no further experiments were conducted with this particular system. Poor reproducibility with uneven heat output signals were observed. The alternative n-butylamine base probe molecule was used, it was decided upon as it is a simple alkylamine that dissolves in most solvents, and is considerably more bulky than the NaOH molecules thereby offering more selectivity towards acid sites.

### 0.1M n-butylamine/MeOH system

The observed enthalpies of neutralization of the sulfonated polymeric resins in the n-butylamine/MeOH system are shown below in Table 4.15 and 4.16 respectively.

#### ❖ Sulfonated Poly(styrene-co-divinylbenzene) Resins

Resin	Sulfonic Acid Loading (mmolg <sup>-1</sup> )	$\Delta H$ Neutralization value (kJ mol <sup>-1</sup> )
0.1 M p-TSA	-	-62.13 $\pm$ 2
SP 21/15	2.97	-76.3 $\pm$ 2
C100H	4.9	-60.28 $\pm$ 2
CT175	4.9	-61.9 $\pm$ 2
CT275	5.3	-76.8 $\pm$ 2

Table 4.15  $\Delta H_{Neut}^0$  value (kJ mol<sup>-1</sup>) from the 0.1M NBA/MeOH system for the Sulfonated Poly(styrene-co-divinylbenzene) Resins. (average of triplicate values).

With the exception of the under-sulfonated SP 21/15 resin, the other resins again follow the trend that as sulfonation increases, the enthalpy of neutralization also increases with the persulfonated CT275 resin demonstrating higher enthalpy of neutralization value compared to its stoichiometrically sulfonated counterparts. The gel type C100H resin demonstrates the lowest enthalpy in this system. The values determined for the stoichiometrically sulfonated resins are equivalent to the benchmark acid, the persulfonated resins' enthalpy value is higher. [It is important to note here that the observed enthalpy of neutralization value from the under sulfonated SP21/15 resin is abnormally high and unexpected based on the observed trends].

Yet as with the sodium hydroxide/methanol system, there was poor reproducibility in this solvent with uneven heat output signals observed. This lead to poor linearity and the observed enthalpies of neutralization possibly giving rise to the odd trends.

It is worth noting that these particular MeOH systems were attempted with the Nafion type resin and sulfonated Nafion material and the synthesised silica materials, however all peaks produced upon the addition of base to solid acid were inconsistent, and did not resemble the sample output demonstrated earlier in this chapter, in most cases the peaks

were indistinguishable and very complicated to interpret. Therefore the use of this particular methanol solvent system was discontinued.

The third and final solvent used was the non swelling cyclohexane. The three types of sulfonic acid supports were tested with this solvent system, a lower concentration of base was used in order to facilitate the solvation of the base within the solvent.

#### **4.6.3.3 Cyclohexane solvent system**

The non polar cyclohexane behaves as a non swelling solvent, it has no specific interactions with solute molecules and only ion pair formation is expected with strong bronsted acid sites. The enthalpy of reaction of a base with an acid in cyclohexane reflects the heat required to break the H-X bond. Therefore it is reasonable to expect the heats of neutralization could reflect the strength of the acid sites.

##### ***0.05M n-butylamine/cyclohexane system***

This system was utilized for comparison of the polymer supported resins to the sulfonated silicas. The non aqueous, non swelling organic solvent cyclohexane, would not be able to swell the resins to enable the base probe molecule to access the intrinsic acid sites, therefore the values produced would not have followed the same trend as with the aqueous swelling water solvent. However the system may offer a comparison of the resins to the other sulfonic acid supports, and thus is included as results of this research.

#### **❖ Sulfonated Polymer Supported Sulfonic Resins**

Table 4.15 below shows the enthalpies of neutralization obtained for the sulfonated polystyrene co divinylbenzene resins in the n-butylamine/cyclohexane system.

### Sulfonated Poly(styrene-co-divinylbenzene) Resins

Sample	Sulfonic Acid Loading (mmolg <sup>-1</sup> )	$\Delta H$ Neutralization value (kJ mol <sup>-1</sup> )
0.05 M p-TSA	-	-60.3 ± 2
SP21/15	2.97	-99.2 ± 2
C100H	4.9	-110.4 ± 2
AMB 15	4.9	-107.6 ± 2
CT175	4.9	-100.9 ± 2
CT275	5.3	-90.45 ± 2

Table 4.16  $\Delta H_{Neut}^0$  value (kJ mol<sup>-1</sup>) from the 0.05M NBA/CH system for the resins (average of triplicate values).

As demonstrated in Table 4.16, unlike the NaOH/H<sub>2</sub>O system, the trend of increasing sulfonic acid loading with increasing enthalpies of neutralization is not followed. The resins with the higher acid loading values have not produced molar enthalpies of neutralization values of the same calibre. The results are varied. It is also worth noting that the enthalpy of neutralization values derived from the resins in this system are much higher than that observed from the homogenous paratoluenesulfonic acid solution system, thereby verifying the lack of trend in this solvent. Unexpectedly the resin with the highest enthalpy of neutralization is the gel type C100H, the one resin that requires the solvent to swell its matrix in order to access the intrinsic acid sites, and in this case the non swelling cyclohexane should not have.

### Fluorinated Sulfonated Polymer Resins

The same absence of trend is observed with the sulfonated polystyrene resins as seen in Table 4.16 below, the molar enthalpies of neutralization obtained are much higher than that observed by the benchmark paratoluenesulfonic acid system. Yet in this instance the solid acid catalyst with the higher sulfonic acid loading value, does demonstrate the higher molar enthalpy of neutralization.

Sample	Sulfonic Acid Loading (mmolg <sup>-1</sup> )	$\Delta H$ Neutralization value (kJ mol <sup>-1</sup> )
0.05 M p-TSA	-	-60.3 ± 0.23
NAFION	0.8	-103.2 ± 2.61
NAFION SiO <sub>2</sub>	0.1	-77.17 ± 2.86

Table 4.17  $\Delta H_{Neut}^0$  value (kJ mol<sup>-1</sup>) from the 0.05M NBA/CH system for the resins (average triplicate values).

It can therefore be concluded that the cyclohexane solvent is not appropriate for measuring the polymer supported sulfonic acid resins with respect to their enthalpies of neutralization

#### ❖ Sulfonated Silica Gels. Grafting route

Table 4.18 below demonstrates the enthalpies of neutralization obtained for the sulfonated silica gels in the n-butylamine/cyclohexane system.

Sample	Sulfonic Acid Loading (mmolg <sup>-1</sup> )	$\Delta H$ Neutralization value (kJ mol <sup>-1</sup> )
0.05 M p-TSA	-	-60.2 ± 2
SiO <sub>2</sub> -PropylSO <sub>3</sub> H	0.36 ± 0.01	-94.2 ± 2
SiO <sub>2</sub> -PhenylSO <sub>3</sub> H	0.71 ± 0.03	-97.1 ± 2
Phenyl-SiO <sub>2</sub> -PropylSO <sub>3</sub> H	0.52 ± 0.02	-81.4 ± 2

Table 4.18  $\Delta H_{Neut}^0$  value (kJ mol<sup>-1</sup>) from the 0.05M NBA/CH system for the Sulfonated Silica Gels (average triplicate values).

Again, unexpectedly, the synthesised silica gels in this system show no obvious trend with increasing acid loading. All enthalpies of neutralization are much larger than that of the homogenous p-TSA acid solution.

### ❖ Sulfonated Mesoporous Molecular Sieve Silicas (Co-condensed)

Table 4.19 below demonstrates the enthalpies of neutralization obtained for the sulfonated mesoporous silicas in the n-butylamine/cyclohexane system.

Sample	Sulfonic Acid Loading (mmolg <sup>-1</sup> )	$\Delta H$ Neutralization value (kJ mol <sup>-1</sup> )
0.05 M p-TSA	-	-60.3 ± 2
MCM41-PropylSO <sub>3</sub> H	1.09 ± 0.05	-98.2 ± 2
MCM41-PhenylSO <sub>3</sub> H	0.40 ± 0.03	-91.2 ± 2
Phenyl-MCM41-PropylSO <sub>3</sub> H	0.13 ± 0.01	-79.3 ± 2
SBA-PropylSO <sub>3</sub> H	0.53 ± 0.01	-96.4 ± 2
SBA-PhenylSO <sub>3</sub> H	0.68 ± 0.01	-85.2 ± 2
Phenyl-SBA-PropylSO <sub>3</sub> H	0.41 ± 0.03	-81.6 ± 2
Phenyl-SBA-PhenylSO <sub>3</sub> H	0.39 ± 0.01	-75.4 ± 2
HMS-Propyl-SO <sub>3</sub> H	0.48 ± 0.01	-73.9 ± 2

Table 4.19  $\Delta H_{Neut}^0$  value (kJ mol<sup>-1</sup>) from the 0.05M NBA/CH system for the Sulfonated Mesoporous Silicas (average triplicate values).

As shown in Table 4.18 in this case all the synthesised samples gave higher molar enthalpy of neutralization values compared to the benchmark acid p-TSA, with propyl MCM-41SO<sub>3</sub>H demonstrating the highest value of -98.2 kJ mol<sup>-1</sup>. The other materials show no trend with regards increasing sulfonic acid loading and the enthalpies of neutralizations derived. The enthalpies derived for the sulfonated mesoporous materials are similar to that of the sulfonated silicas, yet lower than that of the sulfonated polymeric resins despite the complete lack of trend observed. The non swelling solvent has been proven inappropriate in this instance.

#### 4.6.3.4 Summary

It is apparent from the results obtained using the three systems, that the solvent required for allowing the base probe molecule to access the acid sites is vital in its outcome, and the materials effectiveness varies in the solvents used. With the synthesised sulfonated materials demonstrating comparable molar enthalpies of neutralization to the commercially available and readily used acid solutions, it can be concluded that the use

of base adsorption calorimetry to assess the concentration of acid sites on a solid catalyst is sketchy at best without the correct solvent. This method is not a direct measure of the acidity of the solid acid catalyst, but an idea of concentration of acid sites within the designated sample at the time of reaction. However the accessibility of these sites to the base probe molecule is the key for future thoughts with regards to the materials ability to act as a solid acid catalyst in both aqueous and non aqueous solvent environments for use in specific reactions.

It is assumed that the higher the sulfonic acid loading of the sample, the stronger the acid, i.e. the more  $H^+$  ions it would be able to dissociate. Yet in the water solvent system, despite demonstrating the trend of increasing sulfonic acid loading giving rise to increased enthalpies of neutralization, the synthesised supports did not demonstrate enthalpies of neutralization higher than that of the commercially available homogenous acid solutions, thereby not acting as a strong acid in this aqueous solvent. The sulfonated polystyrene resins did behave as strong acids in water giving enthalpies of neutralization over that of the benchmark homogenous acid solutions. The unexpected result was of the fluorinated Nafion resin not demonstrating the highest enthalpy of neutralization in water when it has been classed as a strong acid in literature.

The use of the non polar methanol solvent system produced results lacking in reproducibility and trend.

The use of the semi polar cyclohexane solvent system demonstrated the sulfonated polymeric resins and the sulfonated silica samples to behave as strong acids compared to the benchmark homogenous acid solution, but with no discernable trend between sulfonic acid loading and enthalpy of neutralization. Unexpectedly the sulfonated polymeric resins demonstrated the higher enthalpies of neutralization in this non aqueous solvent as well as in the aqueous water solvent system.

This may well be attributed to their much higher levels of sulfonation compared to the synthesised samples. The matrices of the polymeric resins allow for grouping of sulfonic acid groups through strong hydrogen bonding, enhanced acid strength could be facilitated by disulfonated phenyl groups, and through possible sulfone bridges between neighbouring phenyl groups. In comparison to the isolated groups on the silica

supports, whereby increased sulfonation was attempted by altering the hydrophobicity of the support in order to facilitate a more regular grouping of sulfonic acid groups, and the altering of the functional group tether used during synthesis in order to facilitate a larger pore size in which to incorporate increased levels of sulfonic acid groups[cite]. Yet despite efforts it seems the distribution of sulfonic acid groups is not uniform over the surface or within the bulk of the material (as discussed previously in Chapter 3), and is most likely the cause of the decreased levels of sulfonation observed and therefore also decreased values of enthalpies of neutralization.

It appeared overall that the type of tether involved with the synthesised materials had no effect on the resulting enthalpy of neutralization despite the assumption that the more electronegative phenyl group would allow the material to behave more readily as a Bronsted acid. The commercially available sulfonated resins proved to behave as the strongest acids compared to the synthesised materials.

The use of base adsorption calorimetry in the liquid phase has been proven not to be a direct measure of the acidity of the solid acid catalyst, but an idea of concentration of acid sites within the designated sample at the time of reaction.

In contrast the use of base adsorption calorimetry in the absence of solvent has proven more successful in the determination of enthalpies of adsorption that are more of a reflection of the acid strength of the material due to the lack of any solvation effects. Thus the samples were characterised with ammonia in the absence of solvent.

#### **4.6.4 In the gas phase; Flow Adsorption Calorimetry**

Measurements of gaseous ammonia adsorption were conducted using a Seteram DSC111 differential scanning calorimeter connected to a Hiden HPR 20 mass spectrometer, with a 1% ammonia in helium gas flow mixture. All measurements/analysis and material pre-treatments were conducted in house by Dr. Prem Siril. The results are shown in Figures 4.6-4.9 below.

In these experiments, the sample is exposed to a series of pulses of ammonia at 150°C and the amount of each pulse adsorbed irreversibly is measured along with the molar

enthalpy of adsorption for each pulse. This is converted to molar enthalpy of adsorption. It is assumed that the value of the molar enthalpy of adsorption of ammonia reflects the relative strength of the acid sites on each catalyst and the point at which the enthalpy of adsorption falls below  $-80 \text{ kJ mol}^{-1}$  is taken as the point at which acid sites are saturated. On the basis that the strongest sites are populated first, the profile shown can be regarded as an acid site strength distribution profile for each catalyst.

#### 4.6.4.1 Polymer Supported Sulfonic Acid Resins

##### ❖ Sulfonated poly(styrene-co-divinylbenzene) resins

Figure 4.5 below shows the enthalpy of adsorption vs surface coverage profile adsorbed at  $150^\circ\text{C}$  for the polystyrene sulfonic acid resin catalysts, all analysed in powder form. These data are similar to those reported previously for the same catalysts where ammonia adsorption was carried out in a static system and allowed to reach equilibrium after each pulse.

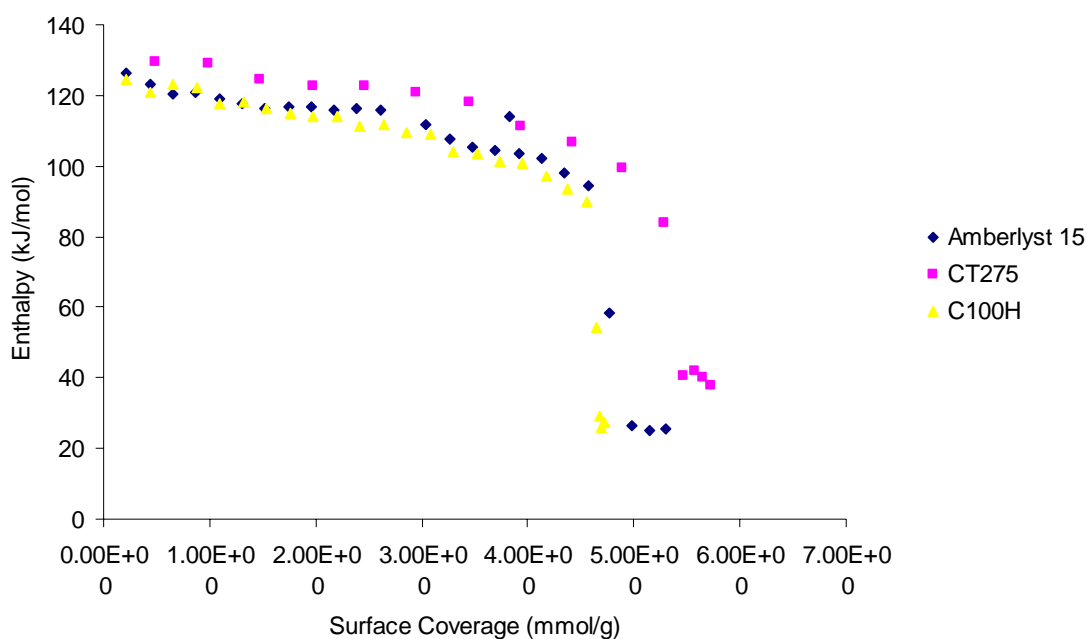


Figure 4.5: Molar enthalpy of ammonia (irreversible) adsorption vs. surface coverage for the polystyrene sulfonic acid resins, Amberlyst 15, persulfonated CT275 (Amb 35) and the gel type C100H resin.

It is assumed the point at which the molar enthalpy of adsorption steeply drops corresponds directly to the complete saturation of acid sites on the material, which closely corresponds to the cation exchange capacity for each catalyst, or its known concentration of acid sites. This suggests a) ammonia can access every acid site on each resin and there is one ammonia molecule per acid site. b) There is no irreversible adsorption on non acidic sites. It is also assumed that the strength of each catalyst is relatively uniform.

When ammonia adsorption occurs at enthalpies numerically higher than  $-80 \text{ kJ mol}^{-1}$ , these values correspond to acid sites with significant strength, at which point stoichiometric adsorption of one ammonia molecule to one acid site group occurs.

The specific polystyrene sulfonic acid resin samples analysed, were the stoichiometrically sulfonated amberlyst 15, and the persulfonated Amberlyst 35 macroporous resins. (The amberlyst 35 resin is equivalent to the CT275 resin), and the gel C100H resin.

As seen in Figure 4.5 the persulfonated Amberlyst 35 resin demonstrates higher enthalpies of adsorption at  $-130 \text{ kJ mol}^{-1}$  compared to the normal sulfonated Amberlyst 15 and the gel C100H resins at  $-125 \text{ kJ mol}^{-1}$ . This increased acid strength is assumed due to the presence of a second sulfonic acid group situated on the phenyl rings of the polymer backbone, the first acid group activates the sites increasing acid strength compared to the action of a single acid group. The normally sulfonated macroporous Amberlyst 15 and the gel C100H resins demonstrate enthalpies of adsorption at similar levels, generating a nearly identical coverage profile. The ammonia should access the macroporous resin's acid sites with ease, due to their degree of permanent porosity that ensures a high proportion of acid sites, which are distributed throughout the resin. The gel resin however has no permanent porosity, and access to acid sites requires diffusion through the gel. Yet ammonia appears to be very effective at diffusing through the unswollen polymer matrix when in powder form. The polystyrene resins are known to be sulfonated to specific levels, the C100H and the Amberlyst 15 at approximately  $4.9 \text{ mmol g}^{-1}$ , the Amberlyst 35 at  $5.2 \text{ mmol g}^{-1}$ . The surface coverage data obtained from ammonia adsorption analysis confirms these levels of sulfonation, as the profiles produced tail off at their respective sulfonic acid loadings. The molar enthalpies of adsorption increase with the increasing level of sulfonation of the resins, implying that

the strength of the acid sites increases with the increasing sulfonation. This is believed to be due to the presence of the highly electronegative phenyl groups and their interactions on the persulfonated resins.

### ❖ Fluorinated Sulfonated Polymer Resins

Figure 4.6 below shows the enthalpy of adsorption of ammonia vs amount adsorbed at 150°C for the Nafion and the Nafion silica composite material SAC-13, both in analysed in powder form.

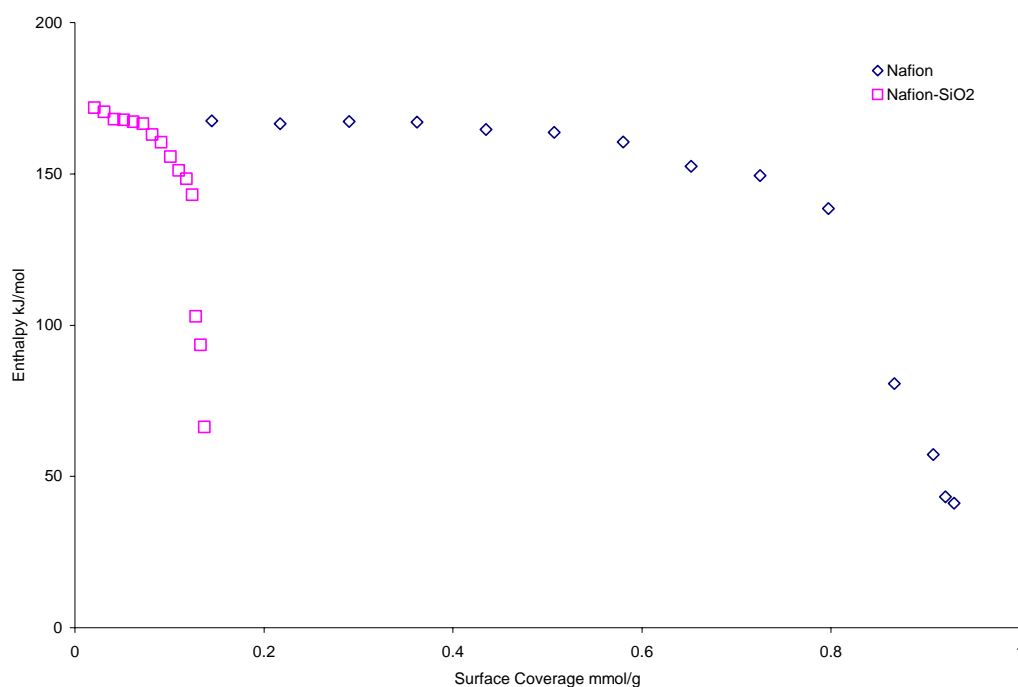


Figure 4.6: Molar enthalpy of ammonia (irreversible) adsorption vs. surface coverage for the fluorinated sulfonated polymer resins, Nafion and the Nafion silica composite (SAC-13).

Nafion is known to be highly permeable to ammonia, so despite its absence of permanent porosity, the acid sites were expected to be freely accessible to ammonia. As seen in Figure 4.6, ammonia saturation for both of these Nafion materials occurs at a surface coverage close to their known concentration of acid sites. As their enthalpies of adsorption are greater than  $-80 \text{ kJ mol}^{-1}$ , (approx  $-170 \text{ kJ mol}^{-1}$  for both) it can be assumed these are acid sites of significant strength. Both Nafion materials demonstrate enthalpies of adsorption much higher than those of the polymer sulfonic acid resins, yet the surface coverage of acid sites are a lot lower. Nafion in its silica composite does not

demonstrate such a broad surface coverage profile, yet compared to Nafion this is expected due to the presence of the porous silica support. Again the surface coverage of the material corresponds to its sulfonic acid loading as previously indicated by the manufacturers (Nafion sulfonated to  $0.8 \text{ mmol g}^{-1}$ , and the Nafion silica composite to  $0.12 \text{ mmol g}^{-1}$ ). The surface coverage of the Nafion silica composite was not as high as the polymer sulfonic acid resins, but its enthalpies of adsorption were greatly higher. Both show 100% coverage of acid sites by ammonia, and crucially, much stronger sites than the Amberlyst and gel resins. It is also worth noting the strength of Nafion is the same when supported on silica. The shape of the profiles produced also suggest a uniform distribution of acid sites.

#### 4.6.4.2 Sulfonated Silica Gels (Grafted route)

Figure 4.7 below shows the enthalpy of adsorption of ammonia vs amount adsorbed at  $150^\circ\text{C}$  for the propyl (MPTMS) and phenyl (CSPTMS) functionalised silica gels, both in analysed in powder form.

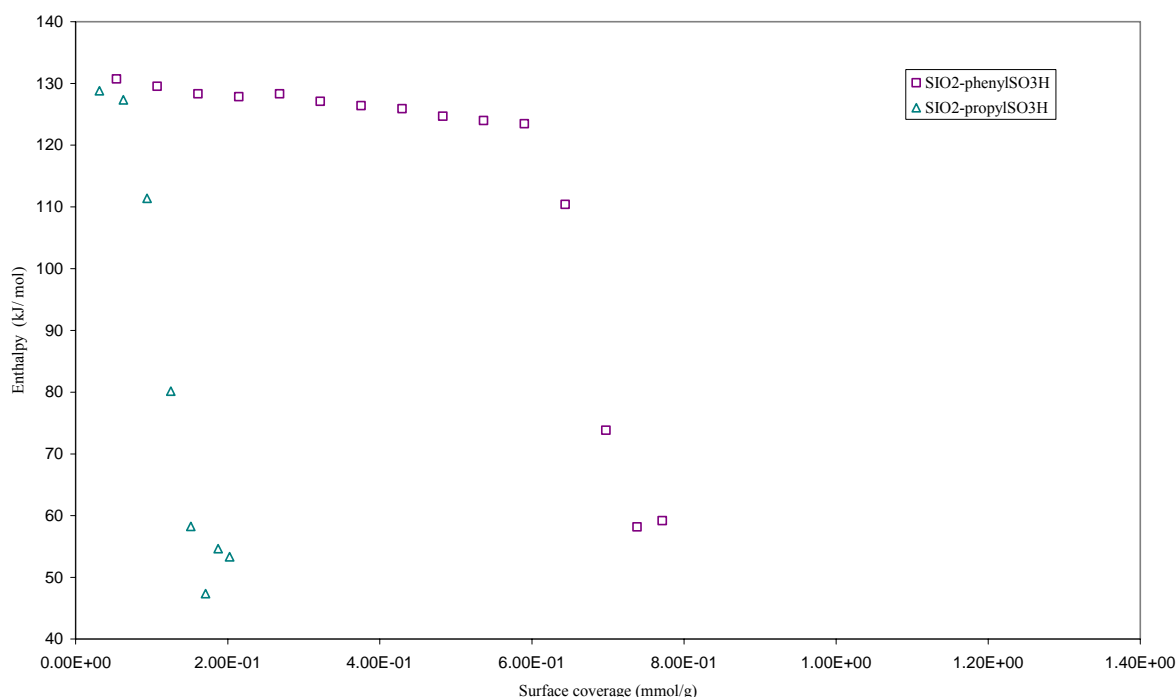


Figure 4.7: Molar enthalpy of ammonia (irreversible) adsorption vs. surface coverage for the sulfonated silica gels, propyl and phenyl functionalised grafted silica materials.

As seen in Figure 4.7, ammonia saturation for both of these silica materials occurs at a surface coverage close to their known concentration of acid sites. As their enthalpies of

adsorption are greater than  $-80 \text{ kJ mol}^{-1}$ , (approx  $-130 \text{ kJ mol}^{-1}$  for both) it can be assumed these are acid sites of significant strength. Both silica materials demonstrate enthalpies of adsorption lower than those of the Nafion materials but comparable and slightly higher than the polymer sulfonic acid resins, yet the surface coverage of acid sites are a lot lower. The propyl functionalised material does not demonstrate such a broad surface coverage profile compared to its phenyl functionalised counterpart. Again the surface coverage of the material corresponds to its sulfonic acid loading as previously characterised, with the phenyl functionalised material having a loading of  $0.72 \text{ mmol g}^{-1}$ , and the propyl functionalised material possessing a  $0.32 \text{ mmol g}^{-1}$  sulfonic acid loading. From this it can be assumed that a significant percentage of the precursor resists conversion to the acid form, possibly due to the thiol group remaining inaccessible during the synthesis procedure. The coverage profiles confirms a correlation between the type of tether and increase in sulfonic acid loading and an increase the enthalpies of neutralization of the materials.

#### 4.6.4.3 Sulfonated Mesoporous Silicas (Co-condensed)

Figure 4.8 below shows the enthalpy of adsorption of ammonia vs amount adsorbed at  $150 \text{ }^\circ\text{C}$  for the propyl (MPTMS) and phenyl (CSPTMS) and bi-functionalised sulfonated co-condensed mesoporous materials, all analysed in powder form.

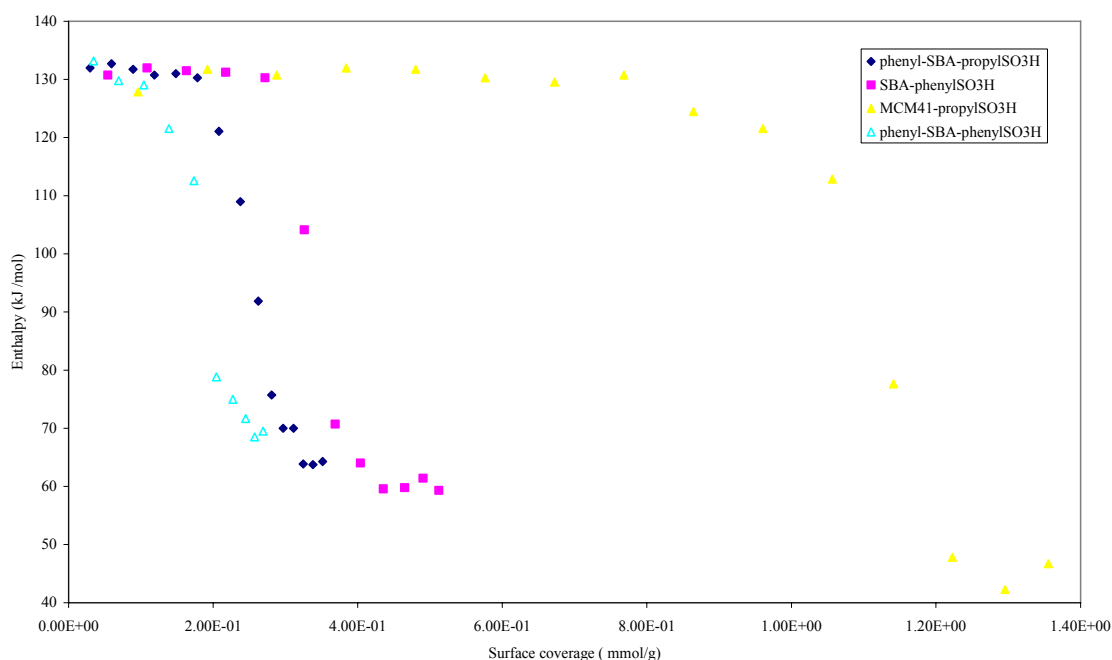


*Figure 4.8: Molar enthalpy of ammonia (irreversible) adsorption vs. surface coverage for the selected sulfonated mesoporous silicas.*

As seen in Figure 4.8, ammonia saturation for all of these silica materials occurs at a surface coverage close to their known concentration of acid sites. As their enthalpies of adsorption are greater than  $-80 \text{ kJ mol}^{-1}$ , (approx  $-130 \text{ kJ mol}^{-1}$  for all) it can be assumed these are acid sites of significant strength. All these materials demonstrate enthalpies of adsorption lower than those of the Nafion materials but comparable with the polymer sulfonic acid resins and the sulfonated silica gels, yet the surface coverage of acid sites are comparable with the sulfonated silica gels but lower than the sulfonated polymeric resins. From the shape of the surface coverage profiles, it appears the propyl functionalised MCM-41 material possesses the higher acid strength of the group. The surface coverage profiles correspond to the sulfonic acid loading of the samples, with the propyl functionalised MCM-41 material having a loading of  $1.00 \text{ mmol g}^{-1}$ . There appears to be no other correlation between increased acid strength and type of tether or indeed type of silica support used (SBA-15 or MCM-41), as all acid strengths are not significantly different, but well below that of the fluorinated Nafion catalysts. This is despite the previous expectation that the presence of the electron withdrawing aryl group of the CSPTMS tether might have increased the acid strength when compared to its propyl MPTMS counterpart.

#### **4.6.4.4 Summary**

It is assumed the point at which the molar enthalpy of adsorption steeply drops corresponds directly to the complete saturation of acid sites on the material, which closely corresponds to the cation exchange capacity for each catalyst. This suggests that ammonia can access every acid site on each support and there is one ammonia molecule per acid site. From the difference between the profiles, it is evident that irreversible and reversible adsorption is occurring on both acidic and non acidic sites. From the shapes of the profiles it is also assumed that despite this, the strength of each catalyst is relatively uniform.

The calorimetric data obtained by ammonia adsorption at  $150^\circ\text{C}$ , suggests that the ammonia can access essentially all the acid sites on the functionalised silicas (both

grafted and co-condensed, and the sulfonated polymer resins alike), perhaps unsurprisingly due to their relatively large pores and high surface areas. The concentrations of acid sites on these synthesised catalysts are, however, relatively low compared to the sulfonated polymer resins. The acid strengths are relatively uniform and are slightly higher than that of the polystyrene resins, but well below that of the fluorinated Nafion catalysts. Enthalpies of adsorption with propyl and phenyl tethers for the acid groups are not significantly different, despite the expectation that the electron withdrawing aryl might have increased the sulfonic acid strength compared to the propyl tether. From the shapes of the profiles it can also be assumed that a significant percentage of the precursor in the functionalised mesoporous supports resists conversion to the acid form.

The reason for the difference in apparent acid strengths between polystyrene and silica supported sulfonic acids is not clear. The tether on polystyrene is a phenyl group, so is essentially similar to that of the tethers on the silica materials. It is thought the persulfonated resins would have shown higher acid strengths than the nominally sulfonated silica materials. The fact that the reverse is actually observed may be linked to the possibility that the removal of water from the sulfonated polystyrene resins (when in powder form) is difficult, meaning the measured acidity is in fact that of the  $\text{H}_3\text{O}^+$  ion. Another alternative factor which may influence the difference between the enthalpies of adsorption of ammonia on sulfonated silica and sulfonated polystyrene is the enthalpies associated with adsorption and chelation of ammonia molecules in silica pores: The “confinement” effect<sup>[31]</sup>.

**References****[1] Solid acid catalysts,**

Avelino Corma, *Current Opinion in Solid State and Materials Science*, 2, 1, (Feb 1997), 63-75.

**[2] From Microporous to Mesoporous Molecular Sieve Materials and Their Use in Catalysis.**

Avelino Coma. *Chem. Rev*, 97, (1997), 2373-2419.

**[3] Inorganic Solid Acids and Their Use in Acid-Catalysed Hydrocarbon Reactions.**

A. Corma. *Chem. Rev*. 95, (1995), 559-614.

**[4] What do we know about the acidity of solid acids?**

R. J. Gorte. *Cat. Lett.* 62, (1999), 1-13.

**[5] Solid Acids and bases as catalysts**

I. Arends, R. Sheldon, U. Hanefeld. *Green chemistry and catalysis*, Wiley-VCH, (2007), 49-90.

**[6] Physical Chemistry**

*Atkins*, 7<sup>th</sup> edition, (2002), 240-266.

**[7] Physical Chemistry**

Laidler, Meiser, 3<sup>rd</sup> edition, (1999), 456-459.

**[8] The influence of solvent on the acidity and activity of supported sulfonic acid catalysts.**

S. Koujout, D. R. Brown, *Cat lett*, 98, (Dec 2004), 195-202.

**[9] Calorimetric base adsorption and neutralization studies of supported sulfonic acids.**

S. Koujout, D. R. Brown, *Thermochimica acta*, 434, (2005), 158-164.

**[10] Calorimetric study of the acidity of a new family of mesoporous catalysts.**

S. D'Arbonneau, A. Tuel, A. Auroux. *J. Therm. Anal. Calorim.* 56, (1999), 287-296.

**[11] Acidity characterisation by microcalorimetry and relationship with reactivity.**

A. Auroux. *Topics in catalysis* 4, (1997), 71-89

**[12] Microcalorimetry methods to study the acidity and reactivity of zeolites, pillared clays and mesoporous materials.**

Aline. Auroux. *Topics in Catalysis*, 19, (2002), 3-4.

**[13] Supported sulfonic acid catalysts in aqueous reactions.**

S. Koujout, D. R. Brown. *Centre for applied catalysis, university of Huddersfield paper.*

**[14] A new technique for measuring surface acidity by ammonia adsorption**

D. R. Brown, C. N. Rhodes. *Thermochimica Acta*, 294, (1997), 33-37.

**[15] Mesoporous solid acid catalysts: relationship between amine TPD data and catalytic activities.**

H. H. P. Yiu, D. R. Brown, and P. A. Barnes, *Catal lett*, 59, (1999), 207-211.

**[16] Acid measurement for solid acids by  $^{13}\text{C}$  solid state NMR.**

*Rohm and Haas Ion exchange resin technical info. www.rohmhaas.com*

**[17] Relationship between differential heats of adsorption and bronsted acid strengths of acidic zeolites: H-ZSM-5 and H-Mordenite.**

C. Lee, D. J. Parrillo, R. J. Gorte, W. E. Farneth. *J. Am. Chem. Soc*, 118, (1996), 3262-3268.

**[18] Solid acid catalysts,**

Avelino Corma, *Current Opinion in Solid State and Materials Science*, 2, 1, (1997), 63-75.

**[19] From Microporous to Mesoporous Molecular Sieve Materials and Their Use in Catalysis.**

Avelino Corma. *Chem. Rev.* 97, (1997), 2373-2419.

**[20] Inorganic Solid Acids and Their Use in Acid-Catalysed Hydrocarbon Reactions.**

B. Corma. *Chem. Rev.* 95, (1995), 559-614.

**[21] What do we know about the acidity of solid acids?**

R. J. Gorte. *Cat. Lett.* 62, (1999), 1-13.

**[22] Solid acids and bases as catalysts**

I. Arends, R. Sheldon, U. Hanefeld. *Green chemistry and catalysis*, Wiley-VCH, (2007), 49-90.

**[23] CRC Rubber Handbook**

*80th Edition, D. R. Lide, (1999-2000).*

**[24] Concise chemical thermodynamics 2<sup>nd</sup> edition**

*J. R. W. Warn, A. P. H. Peters, Routledge, (1996).*

**[25] Principles of thermal analysis and calorimetry**

*P. J. Haines, RSC paperback, (2002).*

**[26] Titrys : Tian-Calvet type microcalorimeter.**

Seteram paper. [www.seteram.com](http://www.seteram.com)

**[27] Thermodynamic background to isothermal titration calorimetry.**

M. J. Blandamer. *Chapter 1, Biocalorimetry applications of calorimetry in the biological sciences. John Wiley and Sons, (1998).*

**[28] Isothermal Calibration of a C-80 Calorimeter.**

K. Ardhaoul, A. Ben Cherifa, and M. Jemal. *Seteram newsletter, (Dec 03).*

**[29] A new technique for measuring surface acidity by ammonia adsorption**

D. R. Brown, C. N. Rhodes. *Thermochimica Acta, 294, (1997), 33-37.*

**[30] The influence of solvent on the acidity and activity of supported sulfonic acid catalysts.** S. Koujout, D. R. Brown, *Cat lett, 98, 4, (2004), 195-202.***[31] Acid strengths and catalytic activities of sulfonic acid on polymeric and silica supports.** P. F. Siril, A. D. Davison, J. K. Randhawa, D. R. Brown, *J. Molec Cat. A, 267, (2007), 72-78.***[32] Test and calibration processes for microcalorimeters, with special reference to heat conduction instruments used with aqueous systems.** L. Briggner, I. Wadso, J. *Biochem and Biophys methods, 22, 2, (1991), 101-118.*

# *Chapter Five*

## *Catalytic Activity: Results and Discussion*

---

## Chapter 5 Catalytic Activity

### 5.1 General Overview

This Chapter aims to show the results obtained from the catalytic activity characterization of the synthesised materials. The solid acid catalysts were assessed in terms of catalytic activity using the  $\alpha$ -pinene isomerization reaction. A complete summary table of all results obtained is shown in the appendix of this thesis.

### 5.2 Catalytic Activity Characterization: Introduction and Background

The catalytic activity of the sulfonated materials was tested using a typical liquid phase reaction, the isomerization of  $\alpha$ -pinene, the mechanism of which is shown in Figure 5.1 below. This particular reaction was chosen due to its ease of use, readiness of chemicals and facilitation within the in house set-up. This particular reaction reacts in the presence of Bronsted acids, which in the case of this research was ideal. Both the reactants and products are non-polar, therefore the reaction only probes the acid sites that are accessible in the unswollen state for catalysts that are prone to swell in the presence of polar solvents.

If the solvent used is pinene, salvation of the acid sites is minimised and it is felt that the environment of the acid sites is not discriminated against when under vacuum and when in the presence of cyclohexane.

The first step of the reaction is the protonation of the double bond. The resulting carbocation rearranges to alleviate the ring strain associated with the four membered ring. The resulting product is camphene with additional small amount of limonenes formed.<sup>[6]</sup>

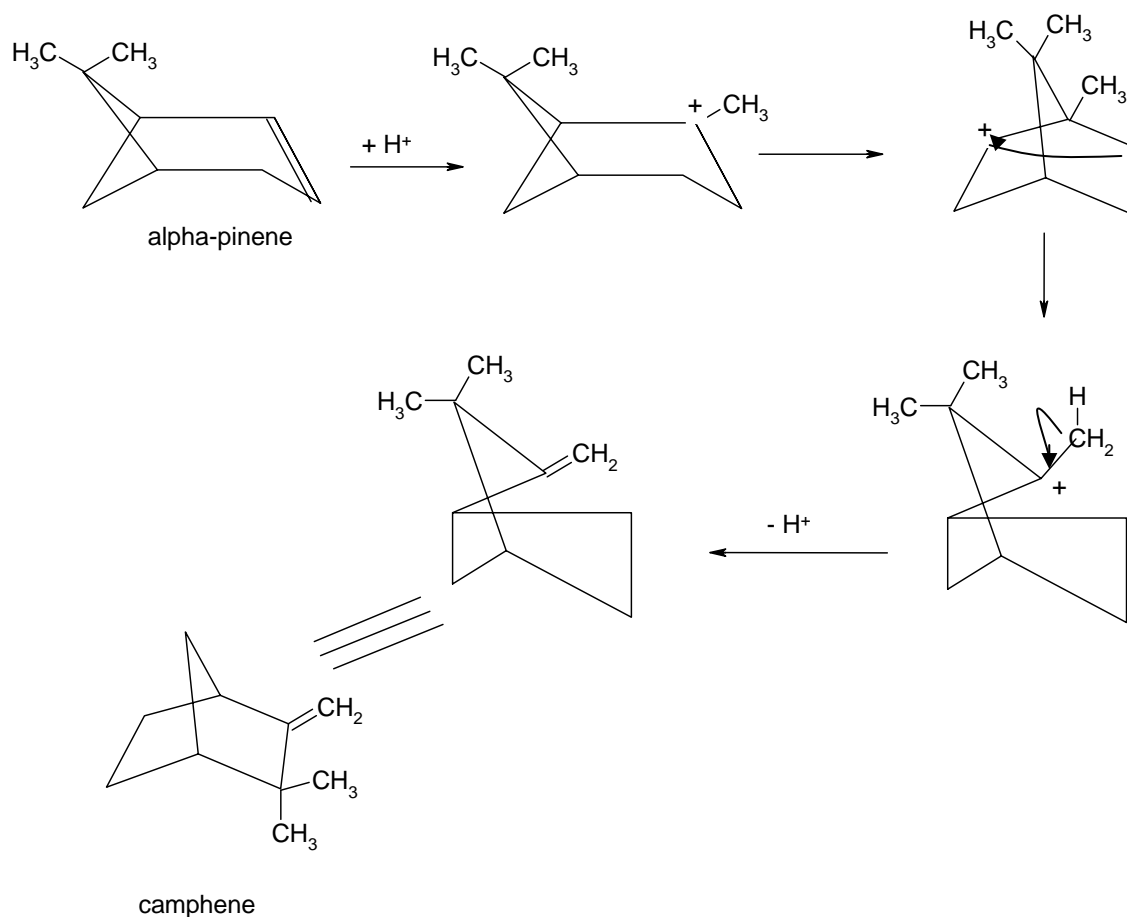


Figure 5.1 Mechanism of formation of alpha pinene.

The use of liquid phase reactions in determining the catalytic activity of solid acid catalysts is widespread in the literature, with various model reactions such as the hydrolysis of ethyl acetate, the acetalization of cyclohexanone, and acylation of anisole. The choice of liquid phase reaction is dependant on the temperature of thermal degradation of the solid catalyst used.<sup>[1-5 / 7-10]</sup> Gas chromatography is used to measure the decline of the reagents within the reaction in order to ascertain the catalytic activity of the samples.

### 5.2.1 Gas Chromatography

Gas Chromatography is a technique that separates volatile organic compounds distributed between two phases, stationary and mobile. In this case, Gas-Liquid Chromatography is the separation of an analyte between a gaseous mobile phase and a liquid phase immobilised on a surface of an inert solid. The sample is vapourised and injected onto the head of a chromatographic packed column. It is transported through the column by an inert carrier gas (mobile phase), the column itself contains the liquid

stationary phase which is adsorbed onto an inert solid. Once separated inside the column, the components are detected using a Flame Ionization Detector (FID).

The FID is a mass sensitive detector which works by mixing air and hydrogen and the effluent from the column and igniting it. The organic compounds burning in the flame produce electrons and ions which produce an electrical signal. Above the flame is a collector electrode which collects and records the ions produced. Chromatograms are produced based on the retention time of the analyte by the column, and the intensity of the concentration of ions detected.

### 5.3 Experimental

The catalytic activity of all the catalysts was tested in the absence of solvent using the  $\alpha$ -pinene isomerization reaction. The reactions were performed in a stirred batch glass reactor, under air using a pre-programmed hotplate and overhead stirrer to maintain temperature and stirring rates, with samples taken every hour and analysed using a PERKIN ELMER CLARUS 500 gas chromatograph, with an SGE fused silica 25 m BP1 capillary column with a  $5 \text{ ml min}^{-1}$  helium flow and a constant oven temperature of 348K. The reactions were conducted at 373 K using 75 mg of dry ground up ( $<125 \mu\text{m}$ ) catalyst (pre-activated for 3 hours at 373 K under nitrogen and introduced after reaction had equilibrated to the appropriate temperature), 5.0 ml of  $\alpha$ -pinene, and 1.0 ml of decane as an internal GC standard. Reactions were run for 4 hours with 0.01 ml samples taken, filtered and injected manually into the GC before the reaction was initiated and then at every hour. The initial rates of reaction (as a rate of loss of reactant) were determined from the subsequent pinene to decane ratio calculations. The reaction mixture was stirred at the maximum stirrer speed as this has been previously demonstrated as being effective in preventing the reaction progressing under external diffusion control. The small amount of solution removed for GC analysis was removed in such a way that no solid catalyst was present in the liquid injected, and was assumed not to have any unnecessary effects on the volume of the reaction mixture that was remaining during experimentation.

#### ❖ Thermal Activation

Prior to reaction, the solid materials were activated at  $100^\circ\text{C}$  for three hours. The solid material was ground up into a fine powder, placed into a quick-fit boiling tube, and

lowered into the furnace by a clamp. A digital Eurotherm 818 P programmer was connected to the furnace in order to control the temperature. A diagram of this setup is shown in Figure 5.2 below. The activation vessel had dry air flowing through by the use of a “Hy-Flo” air piston pump passing the air through a tube of dehydrated silica gel before entering the vessel. After activation, the sample was cooled to the reaction temperature, the reaction mixture of 5.0 ml of  $\alpha$ -pinene, and 1.0 ml of decane as an internal GC standard was quickly poured over the catalyst, transferred into the catalytic activity reaction vessel and the reaction started.

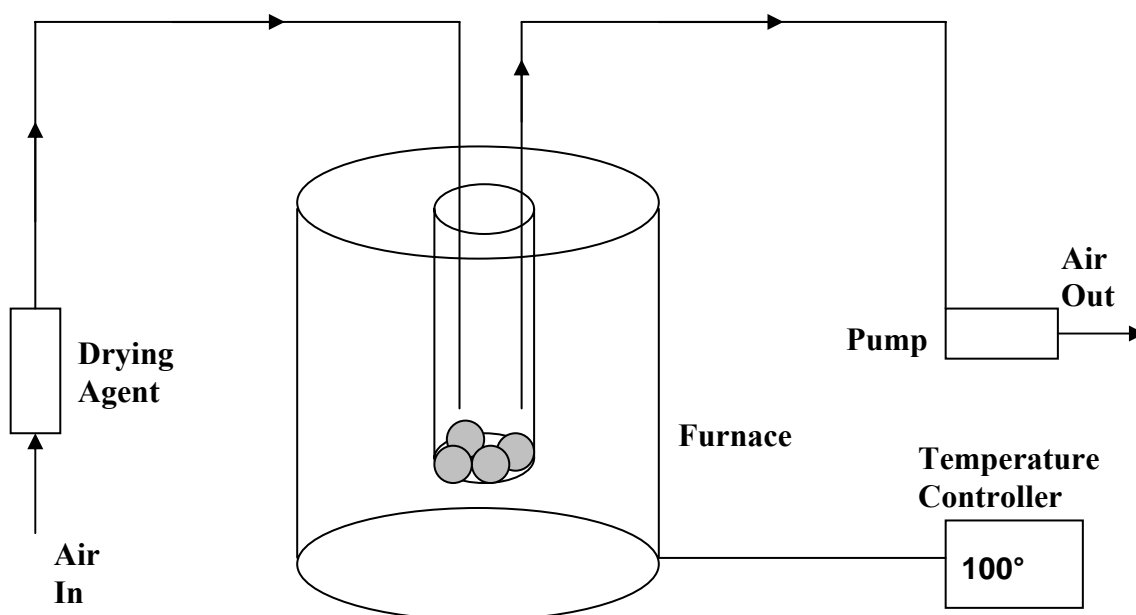


Figure 5.2 Catalytic Activity activation setup.

### ❖ Reaction Vessel

The reactions were performed in a stirred batch glass reactor (as shown in Figure 5.3 below), under air using a pre-programmed hotplate and overhead stirrer to maintain temperature and stirring rates, with samples taken every hour and analysed using a PERKIN ELMER CLARUS 500 gas chromatograph, with an SGE fused silica 25 m BP1 capillary column with a  $5 \text{ ml min}^{-1}$  helium flow.

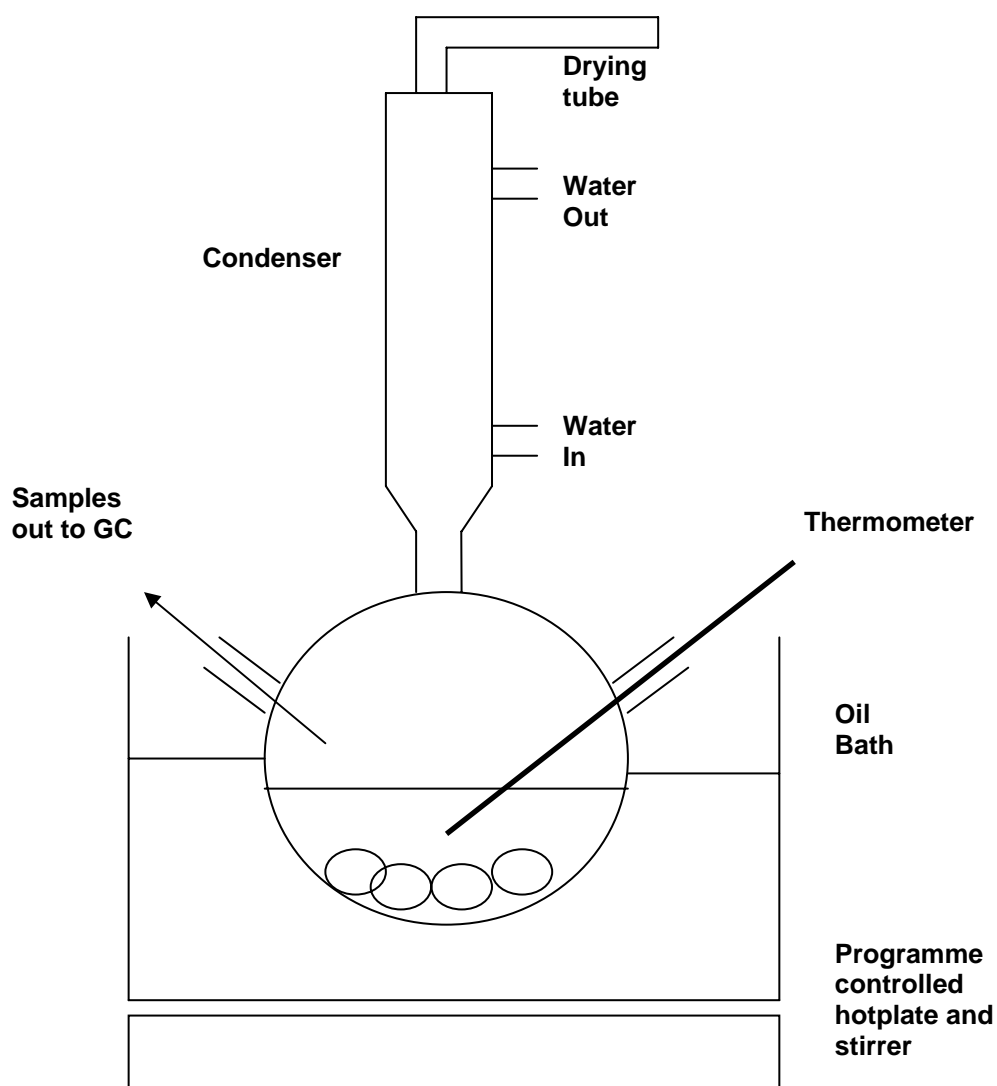


Figure 5.3 Catalytic Activity Reaction Setup.

## 5.4 Summary

The experimental methods discussed in this chapter were the actual routes used for the synthesis, functionalization and characterization of the solid acid catalysts, the results of which are detailed below.

## 5.5 Catalytic Activity Results and Discussion

### 5.5.1 Polymer supported sulfonic acid resins

#### ❖ Sulfonated poly(styrene-co-divinylbenzene) resins and Fluorinated sulfonated polymer resins

The catalytic activities of the sulfonated poly(styrene-co-divinylbenzene) resins and the fluorinated sulfonated resins are shown as reactant conversion over four hour reaction periods in Figure 5.4 below. The kinetic data is shown in Table 5.1 below as turnover numbers per hour (TONs) and the percentage conversion of Pinene after 4 hours. Note that the macroporous Amberlyst 35 resin was analysed as it was equivalent to the CT275, and the Amberlyst 15 resin is equivalent to CT175.

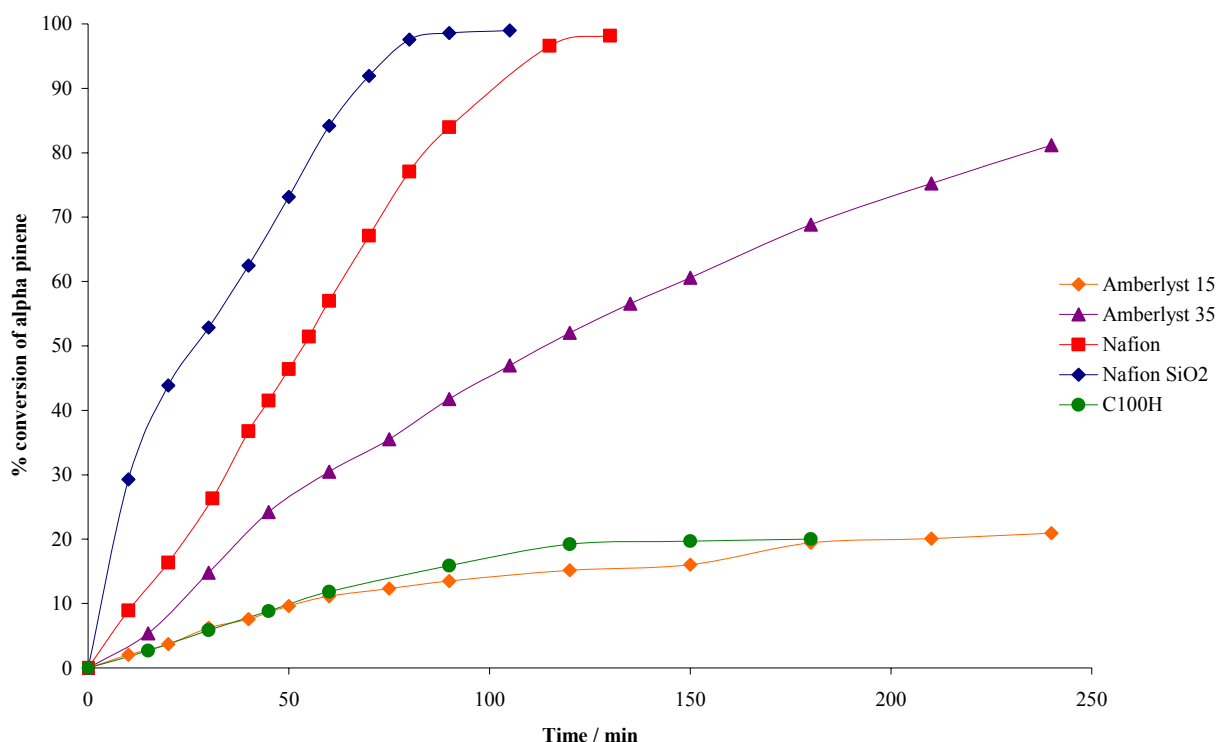


Figure 5.4 Catalytic activity data for the macroporous, stochiometrically sulfonated Amberlyst 15, the persulfonated Amberlyst 35, the gel C100H poly(styrene-co-divinyl)benzene resins and the Fluorinated Nafion type resins. Conversion of  $\alpha$ -pinene as a function of time.

Sample	Sulfonic Acid Loading (mmol g <sup>-1</sup> acid sites)	Turn Over Number (h <sup>-1</sup> )
C100H	4.9	9
AMB 15	4.9	47
AMB 35	5.3	112
Nafion	0.8	1325
Nafion-SiO <sub>2</sub>	0.10	1709

*Table 5.1 Catalytic activity in terms of percentage conversion of  $\alpha$ -pinene over a period of 4 hours, rate of conversion in mol min<sup>-1</sup> g<sup>-1</sup>, and reaction turn over number in h<sup>-1</sup> of the sulfonated poly(styrene-co-divinylbenzene) resins and the fluorinated sulfonated polymer resins.*

Of the polystyrene supported sulfonic acid resins, the non porous C100H resin showed a very low activity. The stoichiometrically sulfonated macroporous resins Amberlyst 15 and the persulfonated Amberlyst 35 demonstrating the highest catalytic activities. The higher TON for Amberlyst 35 over Amberlyst 15 reflects the higher acid site strength on this resin. Of the fluorinated sulfonated polymer resins, Nafion powder and Nafion SAC-13 both exhibited TONs ten times higher than the Amberlyst sulfonic acids.

It is evident that the acid sites present in the C100H gel resin are deep within the polymer matrix and are un-accessible to a bulky, non-swelling reactant such as  $\alpha$ -pinene. The high TONs of sulfonic acid in powdered Nafion and Nafion SAC-13 catalysts reflect the high acid strengths of Nafion. As the measured strengths of the acid sites are similar for Nafion powder and SAC-13, it seems likely that the higher activity and TON of Nafion SAC-13 is due to the better accessibility of acid sites. This is most likely due to its dispersion “on a nanometre scale” during synthesis.

### 5.5.2 Sulfonated Silica Gels. grafting route and Sulfonated Mesoporous Silicas (Co-condensed)

The catalytic activities of the sulfonated silica gels and the sulfonated mesoporous molecular sieves are shown as reactant conversion over four hour reaction periods in Figure 5.4 below. The kinetic data is shown in Table 5.2 below as turnover numbers per hour (TONs) and the percentage conversion of Pinene after 4 hours.

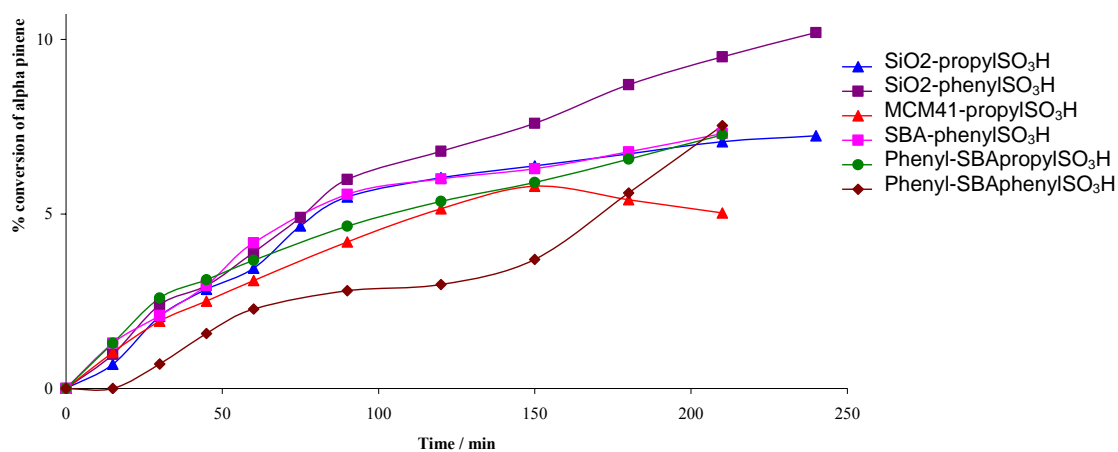


Figure 5.5 Catalytic activity data for the propyl and phenyl grafted silica gels, and the mesoporous sulfonated sulfonic acid materials. Conversion of  $\alpha$ -pinene as a function of time

Sample	Sulfonic Acid Loading (mmolg <sup>-1</sup> acid sites)	Turn Over Number (h <sup>-1</sup> )
SiO <sub>2</sub> -PropylSO <sub>3</sub> H	0.36 ± 0.01	11
SiO <sub>2</sub> -PhenylSO <sub>3</sub> H	0.72 ± 0.04	13
MCM41-PropylSO <sub>3</sub> H	1.09 ± 0.05	17
SBA-PhenylSO <sub>3</sub> H	0.68 ± 0.01	48
Phenyl-SBA- PropylSO <sub>3</sub> H	0.41 ± 0.03	81
Phenyl-SBA- PhenylSO <sub>3</sub> H	0.39 ± 0.01	93

*Table 5.2 Catalytic activity in terms of percentage conversion of  $\alpha$ -Pinene over a period of 4 hours, and rate of conversion in mol min<sup>-1</sup> g<sup>-1</sup> and reaction turn over number in h<sup>-1</sup> of the sulfonated silica gels and the sulfonated mesoporous materials.*

Silica supported sulfonic acids show comparatively low activities with low TONs, yet slightly higher than that of the sulfonated mesoporous materials. As all exhibit low activities, it is not possible to determine if altering the tether from propyl to phenyl has any discernable effect on these materials with respect to their catalytic activities. The accessibility of the acid sites was expected to be good as the porosity data indicates that neither the pores are blocked nor are the surface areas reduced after functionalization of the materials.

## 5.6 Summary

Overall, both the sulfonated silica gels and sulfonated mesoporous silicas show comparatively low activities when compared to the polymer supported resin catalysts. With these low activities, it is not possible to determine with any certainty if changing the tether from propyl to phenyl or indeed the presence of the additional non acid bearing phenyl group, has any effect on the activity of the material. It is assumed from nitrogen adsorption data that these sulfonated materials have a reasonable accessibility to their acid sites, therefore this low activity is unexpected.

The supported sulfonic acid catalysts showed varied catalytic activities, the Nafion and Nafion SAC-13 materials demonstrated the highest activities and turn over numbers.

The polystyrene sulfonated resins were the next highly active catalysts in this reaction, with Amberlyst 35 showing the highest percentage conversion of Pinene. The sulfonated silica/mesoporous supported catalysts demonstrated the lowest activity in comparison, despite varying functional groups on the surface of the materials.

Given that previous experimentation with ammonia demonstrates the comparable strengths of the silica supported and sulfonated mesoporous sulfonic acid groups to those of sulfonic acid on polystyrene, the low activity is surprising. A possible explanation is that the hydrophilicity of the support hinders the surface reaction with the hydrophobic reactant  $\alpha$ -pinene. As demonstrated in other reactions involving more polar reactants, silica supported sulfonic acid has been reported to be as active as polystyrene sulfonic acid, and even in the very polar methanol/ethanoic acid esterification reaction medium, more active than Nafion.

It is clear that the relative activities of the supported sulfonic acids are extremely sensitive to the nature of the reaction, and the compatibility of the catalyst surface with the reaction medium. It is well documented that the activity of silica supported sulfonic acid towards non-polar reactants can be enhanced by tuning the surface hydrophobicity of the silica supported acids with additional grafted alkyl or aryl groups [1-8], it has been shown however in this particular reaction, this was not the case. It is possible the majority of the alkyl and aryl tethers remained incorporated within the bulk of material, thus not providing a sufficient charge difference on the surface of the materials. Or the attempt to stagger the thiol group tethers with intermittent aryl groups did not facilitate a uniform distribution, it therefore seems impossible to specifically tailor the surface in this way without in-situ manipulation, and careful consideration given to the materials and solvents used in synthesis.

Therefore it is evident in the use of the sulfonated silica supported catalysts, the nature of the catalytic reaction, and the surface properties of the support, and the type of support should be seriously considered.

There seems to be no correlation between the sulfonic acid loadings (acidity) and the catalytic activities of the samples, the accessibility of the acid sites to the reaction medium is paramount in the sulfonic acids catalytic activity.

The type of support required for the appropriate reaction should also be seriously considered, it is evident here that the structure of the polymeric macroporous resins

allows the accessibility of acid sites to a far greater extent than the mesoporous sulfonated silica supports despite varying functionalization of their surfaces.

## References

### [1] Solid acid catalysts,

Avelino Corma, *Current Opinion in Solid State and Materials Science*, 2, 1, (Feb 1997), 63-75.

### [2] From Microporous to Mesoporous Molecular Sieve Materials and Their Use in Catalysis.

Avelino Coma. *Chem. Rev.* 1997, 97, 2373-2419.

### [3] Inorganic Solid Acids and Their Use in Acid-Catalysed Hydrocarbon Reactions.

A. Corma. *Chem. Rev.* 1995, 95, 559-614.

### [4] What do we know about the acidity of solid acids?

R. J. Gorte. *Cat. Lett.* 62, (1999), 1-13.

### [5] Solid Acids and bases as catalysts

I. Arends, R. Sheldon, U. Hanefeld. *Green chemistry and catalysis*, Wiley-VCH, (2007), 49-90.

### [6] Acid-Activated Organoclays: Preparation, Characterization and Catalytic Activity of Acid-Treated Tetraalkylammonium-Exchanged Smectites

C. Breen, R. Watson, J. Madejava, P. Komadel, Z. Klapyta, *Langmuir* (1997) 13, 6473.

### [7] M. Hart PhD Thesis:

*The University of Huddersfield*, (2002).

### [8] S. Koujout PhD Thesis:

*The University of Huddersfield*, (2003).

### [9] High activity, templated mesoporous SO<sub>4</sub>/ZrO<sub>2</sub>/HMS catalysts controlled acid site density for $\alpha$ -pinene isomerization. M. A. Ecomier, A. F. Lee, K. Wilson. *Microporous and mesoporous materials* 80, (2005), 301-310.

### [10] Isomerization of $\alpha$ -pinene using modified montmorillonite clays

M. Kr. Yadav, C. D. Chudasama, R. V. Jasra. *Journ Molec Cat A, Chem* 216, (2004), 51-59.

# *Chapter Six*

## *Conclusions and Future Work*

## Chapter 6 Conclusions and Future Work

### 6.1 General Overview

This chapter aims to summarise and bring about conclusions for the research conducted throughout this project.

### 6.2 Overall Aim and Specific Objectives

The overall aim of this project was to determine the role of the support in imparting acidity and catalytic activity in the liquid phase of three different types of supported solid acid catalysts.

As mentioned in previously in Chapter One, section 1.6, the specific objectives of this project were as follows.

- ❖ To determine the role of the support in controlling acidity and activity of the catalysts based on chemically supported sulfonic acid, and the optimization of these materials in liquid phase reactions.
- ❖ To determine the influence of the nature of the support and the sulfonic acid tether on the resultant properties of the supported acid catalyst.
- ❖ To evaluate the effect of the solvent on the accessibilities and strengths of surface acid sites in the differing supports.
- ❖ To investigate the relationship between acidity measured by base adsorption calorimetry in the liquid phase and catalytic activity.

The main objective of this research was to compare the observed structural characteristics, acidities / catalytic activities of sulfonic acid functionalised on 3 differing supports. For comparison the synthesis/preparation methods were varied utilising different functionalised tether chain lengths and additional hydrophobic groups. Those catalysts were:

- ❖ **Polymer supported sulfonic acid resins.** These consisted of two types, the *sulfonated poly(styrene-co-divinylbenzene) ion exchange resins* with varying levels of sulfonation, and the *sulfonated fluorinated polymer resins*.
- ❖ **Sulfonated silica gels.** Synthesised in house with both propyl and phenyl organic tethers, and the inclusion of a hydrophobic phenyl group.
- ❖ **Sulfonated co-condensed mesoporous silicas.** Functionalised in house with both propyl and phenyl organic tethers, and the inclusion of a hydrophobic phenyl group. Three types were synthesised, *MCM-41*, *SBA-15* and *HMS*.

All resulting materials were characterised in terms of structure, acid site concentration and catalytic activity.

This chapter is detailed in order to represent the data reported in three particular sections, structural, acidity and catalytic activity measurements. A complete summary Table is shown in the appendix, detailing the complete physical characteristics, acidity and catalytic activity data obtained of the synthesised catalyst supports.

### 6.3 Structural Analysis Conclusions

#### ❖ **Sulfonated polymer supported sulfonic acid resins**

These materials did not require structural characterization.

#### ❖ **Sulfonated silica gels**

From the variations in the synthesis routes, neither pre-treatment; nor variations in the oxidation/acidification steps produced materials with increased sulfonic acid loadings. Thus the syntheses progressed as reported in chapter 3 with no deviations. From the nitrogen adsorption data of these samples, it is evident that functionalization of the material decreases the overall surface areas and pore volumes as expected. From elemental analysis it was deduced that both tethers were bound by at least two points on their structure, and from XPS measurements 48% and 69% of the sulfur was in sulfonic acid form.

### ❖ Sulfonated Mesoporous Molecular Sieve silicas

From the nitrogen adsorption data of these samples, it is evident that functionalization of the material decreases the overall surface areas and pore volumes as expected, the materials produced were mesoporous in nature. From elemental analysis it was deduced that both tethers were bound by at least two points on their structure, and from XPS measurements 75% and 54% of the sulfur was in sulfonic acid form. Between the three different supports of MCM/SBA and HMS none was better than the other. The pure unfunctionalised MCM material produced samples of the highest long range order followed by the functionalised SBA materials. The propyl functionalised MCM material produced the highest sulfonic acid loading of  $1.09 \text{ mmol g}^{-1}$ .

## 6.4 Base Adsorption Calorimetry Conclusions

In general, the acid strength of sulfonic acid supported on silica are similar but much less than that of sulfonic acid supported on polymeric and Nafion® materials. The type of solvent used is crucial in accessing the acid sites of the materials. There is no simple correlation between acid strength and catalytic activity as measured by calorimetry in the liquid phase. However in the gas phase from the reliable results obtained, there is a correlation with increasing acid strength showing a greater catalytic activity to the conversion of pinene reaction used, indicating either a presence of abundant bronsted acid groups accessible for reaction.

### 6.4.1 In the Liquid Phase

#### ❖ 0.1M NaOH/MeOH

##### *Sulfonated poly(styrene-co-divinylbenzene) resins*

The enthalpy of neutralization values obtained are comparable to that of the p-TSA homogenous acid system. As the level of sulfonation increases, the enthalpy of neutralization also increases.

### ❖ 0.1M NBA/MeOH

#### *Sulfonated poly(styrene-co-divinylbenzene) resins*

The enthalpy of neutralization values obtained are comparable and higher than that of the p-TSA homogenous acid system. Again, as the level of sulfonation increases, so does the enthalpy of neutralization.

The methanol solvent system was not utilised on the other materials.

### ❖ 0.1M NaOH/H<sub>2</sub>O

The enthalpy of neutralization values obtained are comparable and higher than that of the p-TSA and HCl homogenous acid systems. Again, as the level of sulfonation increases, so does the enthalpy of neutralization. The relative orders of enthalpies of neutralization in this system are summarised below:

**Fluorinated Nafion Resin > Poly(styrene-co-divinylbenzene) resins > Sulfonated Mesoporous silicas = Sulfonated Amorphous silicas = Nafion SiO<sub>2</sub>**

### ❖ 0.05M NBA/CH

The enthalpy of neutralization values obtained are comparable and higher than that of the p-TSA homogenous acid system. Again, as the level of sulfonation increases, so does the enthalpy of neutralization. The relative orders of enthalpies of neutralization in this system are summarised below:

**Fluorinated Nafion Resin > Poly(styrene-co-divinylbenzene) resins > Sulfonated Mesoporous silicas = Sulfonated Amorphous silicas = Nafion SiO<sub>2</sub>**

## 6.4.2 In the Gas Phase

All of the solid acid catalysts characterised in this research demonstrated enthalpies of adsorption of ammonia at values numerically higher than  $-80 \text{ kJ mol}^{-1}$  which corresponds to acid sites regarding as having significant strength. All absorption coverage profiles indicate a relatively strong adsorption occurs up to a coverage close to one ammonia molecule per acid site, followed by a fall in enthalpy after this is exceeded. As the enthalpies vary very little, this suggests the acid sites on each solid

acid catalyst are uniform in strength. In general increasing the sulfonation increases the enthalpies of adsorption, the relative orders of which are summarised below:

**Fluorinated Nafion Resin > Nafion SiO<sub>2</sub> > Poly(styrene-co-divinylbenzene) resins > Sulfonated Mesoporous silicas = Sulfonated Amorphous silicas**

### 6.5 Catalytic Activity Conclusions

From the general trend observed that as the sulfonation of the material increases, the enthalpy of neutralization increases, thus indicating a high concentration of acid sites, and therefore possibly a higher resultant acid strength. It was hoped that through this greater acid strength, the material will behave as a stronger solid acid catalyst in the appropriate test reaction. In the materials characterised in this research, this trend is confirmed. Nafion catalysts show much higher specific activities of pinene conversion than the other supported acids. The relative orders of catalytic activity are shown below.

**Fluorinated Nafion Resin > Nafion SiO<sub>2</sub> = Poly(styrene-co-divinylbenzene) resins > Sulfonated Mesoporous silicas = Sulfonated Amorphous silicas**

### 6.6 Overall Conclusions

The specific objectives of this project were met, resulting in the major conclusions below.

- ❖ Solid acid catalysts were successfully synthesised, functionalised and acidified to a high degree, both in the bulk of the material and on the surface.
- ❖ The fluorinated Nafion resin demonstrated the highest acidity and catalytic activity, followed by the poly(styrene-co-divinylbenzene) resins, and then the synthesised silicas. Indicating the resin materials to be the better type of support for this particular acid catalysed reaction.

- ❖ As the sulfonation of each solid acid catalyst increases, the relative acidity and catalytic activity also increases.
- ❖ There appears to be no discernable difference between the mesoporous ordered materials and the amorphous materials in terms of acidity and catalytic activity.
- ❖ There also appears to be no discernable difference between the nature of the propyl or phenyl tether imparting a better acidity or catalytic activity, despite the assumption of the phenyl electron withdrawing group behaving more like a bronsted acid compared to its propyl counterpart.
- ❖ The use of the additional hydrophobic phenyl group appeared to have no added effect on the hydrophilicity of the support as was hoped.
- ❖ Relative acid strength varies depending upon the medium in which the acidity is measured, ammonia adsorption offering the most reliable and confirmable results, with sensitivity to both the strength of the sulfonic acid groups and their environment.
- ❖ The nature of the solvent for liquid phase titrations can have a dramatic effect on the measured acid strength.
- ❖ Relating acid strength to catalytic activity requires the solvent system to be identical.
- ❖ The relative strength of the acid sites is dependant on the nature of the environment of the sulfonic acid group.
- ❖ The catalytic activity of the solid acid catalysts is dependant on the type of reaction and solvent system used.

Despite the incorrect choice of solvent system this work demonstrates the usefulness of base adsorption studies (in both the liquid and gaseous phases) for characterising surface acidity in terms of acid site abundance, strength and distribution. And in the gas

phase, the ability to distinguish between reversibly and irreversibly adsorbed compounds.

Both techniques have however highlighted the vital fact that differences between the ways a base probe molecule and the solvent system might interact with the catalyst and its acid sites and the catalyst surface in general must be taken into account before choosing a suitable reaction system.

These acidity characterization techniques that rely on calorimetric measurements of adsorption of probe compounds can only be safely used to predict catalytic activities in closely related catalysts.

## **6.7 Future Work**

### **6.7.1 Improvements of equipment**

Using a more sensitive isothermal titration microcalorimeter would be desirable, with the addition of titrant directly into the solvent containing the solid with an in-situ stirrer thereby minimising any possible errors.

Placing the microcalorimeter in a simple fume hood would allow for the use of more industrially viable and stronger base compounds such as pyridine, making the research more applicable in the field.

The use of a direct in-situ measurement to enable the determination of the exact amount of base neutralised at the point of addition would remove any errors made from assumptions of complete neutralization after each addition.

### **6.7.2 Materials**

Interesting and novel work with the use of protecting groups in order to facilitate the production of a material that contains both acidic and basic groups for use in particular reactions. The use of groups in order to protect the active functional group before the desired reaction period is a positive step forward. This would enable the use of (as shown) often antagonistic groups in order to obtain materials that are able to function as a multiple catalyst/reactant for any synthetic reactions.

More research into the use of a materials hydrophobic/hydrophilic nature in order to ascertain its impact on the resultant acidity/catalytic activity of the material.

### **6.7.3 Further Experimentation**

Further research into alternative catalytic reactions in which to assess the solid acid catalysts viability is certainly required. In this case a wider investigation of the solvent system specific to the catalytic reaction is needed.

Once an appropriate solvent system and catalytic reaction have been ascertained, it would be vitally important to assess the reusability and longevity of the catalysts, i.e. would they maintain their acidity after reaction? Would a simple re-acidification step be required to renew the acidity, or would a complete re-functionalization step be required?

# *Appendix*

It is important to note that throughout this thesis in certain sections, the results shown are summarily formatted to demonstrate the best results obtained based on triplicate readings. Below for reference are the complete summary tables for all materials tested during this research with regards to structural, acidity and catalytic activity characterisation respectively. All relative discussion and conclusions drawn are mentioned in the previous appropriate chapters of this thesis.

Catalyst	Nitrogen adsorption data			Sulfonic Acid Loading (mmol g <sup>-1</sup> )
	Surface Area (m <sup>2</sup> g <sup>-1</sup> )	Pore Volume (cm <sup>3</sup> g <sup>-1</sup> )	Av Pore Diam (nm)	
SP 21/15	-	-	-	2.97
C100H	-	-	-	4.9
AMB 15	53 <sup>a</sup>	0.4	30	4.9
CT175	-	-	-	4.9
CT275	50 <sup>a</sup>	0.35	30	5.3
Nafion	-	-	-	0.8
Nafion-SiO <sub>2</sub>	196 <sup>a</sup>	0.6	10	0.1
Pure SiO <sub>2</sub>	324	2.01	19.9	0
SiO <sub>2</sub> -propylSO <sub>3</sub> H	271	1.39	16.8	0.36 ± 0.02
SiO <sub>2</sub> -phenylSO <sub>3</sub> H	191	0.95	15.4	0.72 ± 0.02
Phenyl-SiO <sub>2</sub> -propylSO <sub>3</sub> H	232	1.19	17.6	0.52 ± 0.03
Pure MCM-41	638	0.69	3.42	0
MCM41-propylSO <sub>3</sub> H	301	0.03	20.9	1.09 ± 0.05
MCM41-phenylSO <sub>3</sub> H	301.7	0.176	3.63	0.40 ± 0.03
Phenyl-MCM41-propylSO <sub>3</sub> H	340	0.17	18.4	0.12 ± 0.01

Pure SBA-15	612	0.38	4.39	0
SBA15-propylSO <sub>3</sub> H	438.5	0.56	10.38	0.53 ± 0.01
SBA15-phenylSO <sub>3</sub> H	385	0.94	15.78	0.67 ± 0.01
Phenyl-SBA15-propylSO <sub>3</sub> H	453	0.19	4.24	0.41 ± 0.03
Phenyl-SBA15-phenylSO <sub>3</sub> H	676	0.37	4.19	0.39 ± 0.01
HMS-propylSO <sub>3</sub> H	410	0.25	28.3	0.48 ± 0.01

Tables 7.1 Structural characterization for the supported sulfonic acid catalysts.

<sup>a</sup> Value supplied by the manufactures.

Catalyst	Av ΔH adsorption (kJ mol <sup>-1</sup> )				Sulfonic Acid Loading (mmolg <sup>-1</sup> )	Av ΔHads NH <sub>3</sub> <sup>b</sup> (kJ mol <sup>-1</sup> )	Saturation NH <sub>3</sub> <sup>c</sup> coverage (mmolg <sup>-1</sup> )
	NaOH / MeOH	NBA / MeOH	0.1 M NaOH / H <sub>2</sub> O	0.05 M NBA / CH			
SP 21/15	-33.4 ± 2	-76.30 ± 2	-55.3 ± 2	-99.2 ± 2	2.97	-	-
C100H	-35.8 ± 2	-60.28 ± 2	-61.0 ± 2	-110.4 ± 2	4.9	-110 ± 4	4.6
AMB 15			-64.7 ± 2	-107.6 ± 2	4.9	-110 ± 4	4.7
CT175	-34.3 ± 2	-61.9 ± 2	-61.5 ± 2	-100.9 ± 2	4.9	-110 ± 4	4.7
CT275	-39.49 ± 2	-76.8 ± 2	-64.5 ± 2	-90.45 ± 2	5.3	-116 ± 4	5.3
Nafion			-51.1 ± 2	-103.2 ± 2	0.8	-161 ± 5	0.85
Nafion-SiO <sub>2</sub>			-39.9 ± 2	-77.17 ± 2	0.1	-162 ± 5	0.12
Pure SiO <sub>2</sub>					0		
SiO <sub>2</sub> -propylSO <sub>3</sub> H			-32.5 ± 2	-94.2 ± 2	0.36 ± 0.02	-128 ± 5	1.10

SiO <sub>2</sub> -phenylSO <sub>3</sub> H			-55.8 ± 2	-97.1 ± 2	0.72 ± 0.02	-126 ± 5	0.68
Phenyl-SiO <sub>2</sub> -propylSO <sub>3</sub> H			-43.8 ± 2	-81.4 ± 2	0.52 ± 0.03	-	0.52
Pure MCM-41			-	-	0	-	-
MCM41-propylSO <sub>3</sub> H			-60.6 ± 2	-98 ± 2	1.09 ± 0.05	-127 ± 4	1.14
MCM41-phenylSO <sub>3</sub> H			-34.0 ± 2	-91.2 ± 2	0.40 ± 0.03	-	0.42
Phenyl-MCM41-propylSO <sub>3</sub> H			-24.5 ± 2	-79.3 ± 2	0.12 ± 0.01	-	0.15
Pure SBA-15			-	-	0	-	-
SBA15-propylSO <sub>3</sub> H			-40.1 ± 2	-96.4 ± 2	0.53 ± 0.01	-	0.55
SBA15-phenylSO <sub>3</sub> H			-50.3 ± 2	-85.2 ± 2	0.67 ± 0.01	-126 ± 4	0.37
Phenyl-SBA15-propylSO <sub>3</sub> H			-55.5 ± 2	-81.6 ± 2	0.41 ± 0.03	-125 ± 4	0.28
Phenyl-SBA15-phenylSO <sub>3</sub> H			-44.4 ± 2	-75.4 ± 2	0.39 ± 0.01	-	0.21
HMS-propylSO <sub>3</sub> H			-35.4 ± 2	-73.9 ± 2	0.48 ± 0.01	-118 ± 4	0.32

Tables 7.2 Acidity data for the supported sulfonic acid catalysts.

<sup>b</sup> Average value of  $\Delta H_{ads} NH_3$  up to saturation coverage

<sup>c</sup> Saturation  $NH_3$  coverage defined as total  $NH_3$  uptake with  $\Delta H_{ads}$  numerically greater than  $-80 \text{ kJ mol}^{-1}$

Catalyst	Sulfonic Acid Loading (mmolg <sup>-1</sup> )	TON (h <sup>-1</sup> )	Molar select to camphene (%)
SP 21/15	2.97	5	8
C100H	4.9	9	20
AMB 15	4.9	47	22
CT175	4.9	54	10
CT275	5.3	112	40
Nafion	0.8	1325	55
Nafion-SiO <sub>2</sub>	0.1	1709	50
Pure SiO <sub>2</sub>	0	-	-
SiO <sub>2</sub> -propylSO <sub>3</sub> H	0.36 ± 0.02	11	8
SiO <sub>2</sub> -phenylSO <sub>3</sub> H	0.72 ± 0.02	13	10
Phenyl-SiO <sub>2</sub> -propylSO <sub>3</sub> H	0.52 ± 0.03	48	8
Pure MCM-41	0	-	-
MCM41-propylSO <sub>3</sub> H	1.09 ± 0.05	17	7
MCM41-phenylSO <sub>3</sub> H	0.40 ± 0.03	12	6
Phenyl-MCM41-propylSO <sub>3</sub> H	0.12 ± 0.01	48	9
Pure SBA-15	0	-	-
SBA15-propylSO <sub>3</sub> H	0.53 ± 0.01	51	8
SBA15-phenylSO <sub>3</sub> H	0.67 ± 0.01	48	9
Phenyl-SBA15-propylSO <sub>3</sub> H	0.41 ± 0.03	81	9
Phenyl-SBA15-phenylSO <sub>3</sub> H	0.39 ± 0.01	93	9
HMS-propylSO <sub>3</sub> H	0.48 ± 0.01	8	4

Tables 7.3 Catalytic activity data for the supported sulfonic acid catalysts.